Interleukin-6 as a Potential Mediator of Breast Cancer Progression and Non-Melanoma Skin Carcinogenesis

Dissertation

Presented in Partial Fulfillment of the Requirements for the Degree Doctor of Philosophy in the Graduate School of The Ohio State University

By

Nicholas James Sullivan

Integrated Biomedical Science Graduate Program

The Ohio State University

2009

Dissertation Committee:

Tatiana M. Oberyszyn, Ph.D., Advisor

Xue-Feng Bai, M.D., Ph.D.

Traci A. Wilgus, Ph.D.

Lisa D. Yee, M.D.

ABSTRACT

Breast cancer is the second leading malignancy in women behind only non-melanoma skin cancer. Likewise, it is the second leading cause of cancer-specific female mortality behind only lung cancer. Breast tumor interleukin-6 (IL-6) expression increases with tumor grade, and elevated serum IL-6 levels are associated with poor breast cancer patient survival. However, the mechanisms driving these clinical anomalies are currently undefined. Whereas IL-6 is better known as an inflammatory cytokine which mediates hematopoiesis and lymphocyte activation, it is becoming increasingly appreciated as a mediator of cancer progression. Our previous studies demonstrated that IL-6 is necessary for breast, bone, and lung fibroblast-induced breast cancer cell growth enhancement and furthermore, showed that IL-6 alone is a potent growth factor for breast cancer cells. Thus, we set out to further characterize the molecular consequences of IL-6 signaling in breast cancer, focusing on those associated with poor clinical outcome.

In Chapter 2, we highlight IL-6 as one of only few factors capable of inducing a carcinoma-associated epithelial-mesenchymal transition (EMT) phenotype. Such EMT phenotypes correlate with decreased breast cancer patient survival. In particular, we demonstrated E-cadherin repression among multiple estrogen receptor-alpha (ERα)-positive human breast cancer cell lines following IL-6 exposure. Ectopic IL-6 expressing MCF-7 cells (MCF-$7^{IL\text{-}6}$) exhibited a gene expression profile and phenotype consistent

with EMT including down-regulated E-cadherin and aberrant induction of N-cadherin, Vimentin, Twist, and Snail. Furthermore, ectopic autocrine IL-6 signaling promoted breast cancer cell invasiveness. Intriguingly, Twist, a transcriptional repressor of E-cadherin, was shown to promote IL-6 production and constitutive STAT3 phophorylation. Ectopic IL-6 expression maintained an EMT phenotype in an orthotopic xenograft model, which exhibited increased tumor cell proliferative index, advanced histologic grade, and poor tumor cell differentiation.

Chapter 3 exposes E-cadherin as a suppressor of breast cancer cell growth and IL-6 production. The objective of these studies was to characterize the mechanisms by which IL-6 promotes breast cancer cell growth. As shown in Chapter 2, IL-6 induces repression of E-cadherin, a putative regulator of epithelial cell adhesion, phenotype, and consequent homeostasis. Hence, we hypothesized that IL-6-induced E-cadherin repression may promote breast cancer cell growth and moreover, that E-cadherin expression may inhibit breast cancer cell growth. IL-6 enhanced ERα-positive breast cancer cell growth in a 3-dimensional (3D) tumor growth assay (TGA) and promoted E-cadherin repression in a dose-dependent manner. Additionally, E-cadherin expression status was inversely associated with breast cancer cell growth rates. Likewise, cells which lack E-cadherin due to ectopic Twist expression showed unaffected growth following IL-6 exposure. These findings are corroborated by our results in Chapter 2, which showed that Twist stimulated autocrine IL-6 production, which may negate the effects of additional IL-6 supplementation. To determine if E-cadherin inhibits breast cancer cell growth, we expressed either full-length E-cadherin or truncated E-cadherin lacking a β-catenin binding domain (mutant E-cadherin) in MDA-MB-231 cells, a

commonly used aggressive E-cadherin-negative breast cancer cell line. Full-length E-cadherin completely abrogated IL-6 production, and mutant E-cadherin induced an intermediate impairment of IL-6 production, suggesting that β-catenin and to a lesser extent, E-cadherin adhesive activity, may mediate IL-6 expression. Full-length E-cadherin also inhibited MDA-MB-231 cell growth. Furthermore, mutant E-cadherin sustained slightly increased growth rates compared to full-length E-cadherin, suggesting that β-catenin may regulate MDA-MB-231 growth as well as IL-6 production.

Non-melanoma skin cancer (NMSC) incidence rates far exceed any other type of human cancer and continue to increase annually. Ultraviolet light B (UVB) is considered a predominant risk factor for NMSC. Whereas higher incidence rates in men have been attributed to increased chronic male sun exposure, work from our laboratory has revealed inherent gender differences in the well-established Skh-1 mouse model of UVB-induced skin carcinogenesis. In particular, we have previously shown that male mice exhibit less inflammation, more oxidative DNA damage, and increased tumorigenesis upon UVB exposure compared to female mice.

Myeloid-derived suppressor cells (MDSC) represent a heterogeneous population of immature myeloid cells with potent immunosuppressive properties and were the focus of Chapter 4. Although peripheral MDSC induction has been described in various mouse tumor models and in patients with a wide range of cancers, this is not the case for UVB-induced NMSC. IL-6, which has been shown to be up-regulated following UVB irradiation, also promotes MDSC expansion *in vivo*. Therefore, we conducted a pilot study to evaluate the presence of peripheral MDSC in Skh-1 tumor-bearing mice following chronic UVB exposure. We hypothesized that tumor-bearing mice would have

relatively elevated MDSC levels compared to tumor-free control mice. Additionally, we hypothesized that male mice may be more susceptible to peripheral MDSC expansion due to their relatively low inflammatory response compared to females following UVB exposure.

Our preliminary results confirmed our previous report of higher UVB-induced skin tumor burden in male mice. An expanded MDSC population of splenocytes was detected in UVB-induced skin tumor-bearing mice and moreover, our findings suggest a gender discrepancy in which male mice appear more susceptible to skin tumor-induced MDSC expansion. Furthermore, relatively high compared to relatively low tumor burden mice showed more MDSC, particularly in males. We evaluated splenocyte interferon (IFN)-induced STAT1 phophorylation as a measure of systemic immune function in tumor-free and tumor-bearing mice. Whereas we did not detect a gender difference in IFN responsiveness in tumor-free mice, male high tumor burden mice showed an apparent decrease in IFN responsiveness compared to female high tumor burden mice. In fact, IFN-stimulated STAT1 phosphorylation was completely abrogated in male high tumor burden mice when compared to male tumor-free control mice.

Collectively, the following body of research emphasizes the potential impact of IL-6 on breast cancer progression and non-melanoma skin carcinogenesis. Although our results strengthen the notion that IL-6 promotes carcinoma progression and contest that which considers IL-6 a mere consequence of cancer-associated inflammation, future clinical studies will be needed to validate these conclusions.

DEDICATION

I dedicate this effort to my grandfather. The tragic memory of his physical demise during his swift battle with cancer was undoubtedly an early critical inspiration for me to study cancer and will always be so.

ACKNOWLEDGEMENTS

Due to the seemingly impossible task of prioritizing my many acknowledgements, I will do my best to thank those who helped me along this journey in chronological order. Therefore, I start with Dr. Jim Waldman. I suspect that he played a significant role as my advocate in getting me accepted into IBGP. He served as my mentor through my tenure in the OSU Pathology Master's Program, and without his direction, I would have been lost. Dr. Gerard Lozanski gave me nothing but support when I let him know that I would be leaving his clinical flow cytometry lab to pursue my Ph.D., and for that, I cannot thank him enough. As I approach the end of my time in IBGP, I realize even more now what an exceptional program it is, and I thank all those who have made IBGP what it is today.

Likewise, I don't know if I would be where I am today, either in Columbus or in IBGP, if it wasn't for the unconditional support of my incredible wife, Jenn, who was by my side throughout my entire graduate school experience. Not only does she bring home the bacon, but she also supported my crazy decision to take a huge pay cut to pursue a goal that would take years to achieve. That may mean more to me than anything. Furthermore, she was an unwavering source of encouragement through my tough times of repeated DOD rejections, high western blot background, pipetting difficulty without part of an index finger, and of course, my forced transition into a new world of skin

cancer. Last but far from least, I have watched Jenn take motherhood in stride, and how could I not thank her for making me the happiest father in the world? Our son, Carter, is the best distraction to work that I could imagine, and he has unknowingly kept life in perspective for me.

Although my time with Dr. Brett Hall (pronounced "BreTT") didn't end the way I was anticipating, our time together was unforgettable. From suggesting that Terrie watch Carter daily during his early months to going green and occasionally carpooling to paying for lunches at CBC, Brett was a great mentor. In all seriousness, he is responsible for my respect of the tumor microenvironment and my knowledge of breast cancer biology and for that, I will be forever grateful. He taught me to think independently (even if it means *going against dogma*; Massague, anyone?), and to this day, makes me think about the homeless in a different light, particularly homeless Jewish comedians. Although he left me for Belgium in a stressful state of being, he was instrumental in connecting me with my current mentor. My wounds have since healed and no hard feelings remain except toward Herbert Auer, the S.O.B. who started all of that. Brett's first student, Dr. Kate Sasser, has to be recognized as the pioneer of all IL-6 and subsequent EMT studies, and therefore, I thank her for paving the way for my success.

Dr. Tatiana Oberyszyn deserves immense credit for her heroic deed of agreeing to let me finish my dissertation research in her lab and for that simple act, I am forever indebted. Jenn and I can't thank her enough for preventing an imminent ulcer and alleviating unhealthy levels of stress. It became quickly apparent that I had landed in a productive lab headed by a successful scientist with a proven track record. I knew Tania was a great mentor from several accounts inside and outside her lab, but my experience

as her student has emphasized this exceptional quality. Beyond being an extraordinary mentor, Tania is also the leader of an amazing collaborative research team that deserves recognition. I would like to first thank the members of the Oberyszyn Lab for their hospitality. Some labs would have ignored a sudden refugee taking up their space and resources, but they were nothing but fantastic. Each one of them did their part to facilitate my productiveness and this was never unnoticed or taken for granted. I thank them for their time and patience with me as I stumbled around my new setting.

I would also like to acknowledge my Dissertation Committee members, Dr. Xue-Feng Bai, Dr. Traci Wilgus, and Dr. Lisa Yee. First, thank you for agreeing to take part in my dissertation research, and second, thank you for your time and supportive feedback at meetings. Each one of you offers distinct expertise that lends support to my project, and I hope you see that in my dissertation.

VITA

November 14, 1978..... Born – Kettering, OH, USA

June, 2001 ..... Bachelor of Science, Microbiology
Ohio University

2005 – 2009..... Graduate Research Associate
The Ohio State University

PUBLICATIONS

Research Publications

1. **Sullivan NJ**, Sasser AK, Axel A, Vesuna F, Raman V, Ramirez N, Oberyszyn TM, Hall BM. Interleukin-6 induces an epithelial-mesenchymal transition phenotype in human breast cancer cells. Oncogene 2009 (Epub ahead of print).

2. **Sullivan NJ**, Hall BM. Mesenchymal stem cells in tumor stroma. Stem Cells and Cancer 2009;2: 27-34. Humana Press; ISBN: 978-1-60327-933-8

3. Sasser AK, **Sullivan NJ**, Studebaker AW, Hendey LF, Axel AE, Hall BM. Interleukin-6 is a potent growth factor for ER-alpha-positive human breast cancer. FASEB J 2007;21(13):3763-70.

FIELD OF STUDY

Major Field: Integrated Biomedical Science
Specialization in Cancer Biology

TABLE OF CONTENTS

LIST OF FIGURES

LIST OF ABBREVIATIONS

2D	2-dimensional
3D	3-dimensional
α	alpha
ATCC	American Type Culture Collection
β	beta
BCC	basal cell carcinoma
BME	basement membrane extract
BSF-2	B-cell stimulating factor-2
C	cytosine
°C	degrees Celsius
cDNA	complementary DNA
CFDA-SE	carboxyfluorescein diacetate-succinimidyl ester
CNTF	ciliary neurotrophic factor
CPD	cyclobutane pyrimidine dimers
CRP	C-reactive protein
Δ	delta; mutant
DCIS	ductal carcinoma in situ
DTT	dithiothreitol

ECM	extracellular matrix
EGF	epidermal growth factor
EGFR2	epidermal growth factor receptor 2
EMT	epithelial-mesenchymal transition
ER	estrogen receptor
FBS	fetal bovine serum
γ	gamma
g	gram
G	guanine
G418	Geneticin®
G-CSF	granulocyte-colony stimulating factor
GM-CSF	granulocyte/monocyte-colony stimulating factor
gp130	glycoprotein 130
H&E	hematoxylin and eosin
HDGC	hereditary diffuse gastric cancer
HER2	human epidermal growth factor receptor 2
HGF	hepatocyte growth factor
hpf	high power fields
IDC	invasive ductal carcinoma
IFN	interferon
IL	interleukin
IL-6R	IL-6 receptor
IL-6sR	IL-6 soluble receptor

ILC	invasive lobular carcinoma
ILEI	Interleukin-like EMT inducer
iNOS	inducible nitric oxide synthase
J	Joules
JAK	Janus kinase
l	liter(s)
LCIS	lobular carcinoma in situ
LIF	leukemia inhibitory factor
LOH	loss of heterozygosity
μ	micro-
m	milli-; meter
M	molar
MCF	Michigan Cancer Foundation
M-CSF	monocyte-colony stimulating factor
MDA	MD Anderson
MDSC	myeloid-derived suppressor cell
MET	mesenchymal-epithelial transition
MFI	mean fluorescence intensity
MPO	myeloperoxidase
MSC	mesenchymal stem cells
MTA3	metastatic tumor antigen 3
n	nano-; number
NF-κB	nuclear factor-kappaB

NMSC	non-melanoma skin cancer
NO	nitric oxide
O_2^-	superoxide anion
$ONOO^-$	peroxynitrite
OSM	oncostatin M
p	phorsphorylated; phospho-; pico-
PBS	phosphate-buffered saline
PBS-T	PBS containing 0.1% Tween-20
PIAS	protein inhibitors of activated STATs
PR	progesterone receptor
RE	DsRed-Express
ROS	reactive oxygen species
RPMI	Roswell Park Memorial Institute
SCC	squamous cell carcinoma
SCF	stem cell factor
SDS	sodium dodecyl sulfate
SERM	selective estrogen receptor modulator
sgp130	soluble glycoprotein 130
SNP	single nucleotide polymorphism
SOCS	suppressors of cytokine signaling
STAT	signal transducer and activator of transcription
TDLU	terminal duct lobular unit
TGA	tumor growth assay

TGF-β	transforming growth factor-beta
UVB	ultraviolet light B
VEGF	vascular endothelial growth factor
Y	tyrosine

CHAPTER 1: INTRODUCTION

1.1 Anatomy of the Breast

Human female breasts provide essential neonate nourishment and immunity in the form of milk, thus sustaining life since the dawn of humanity. The majority of our knowledge of gross breast anatomy dates back to essential dissections and descriptions of lactating female cadavers reported by Sir Astly Cooper in 1840 (Cooper, 1840). Breasts are composed of a branching system of glandular lobules and milk ducts surrounded by stroma including fibroblasts, immune cells, adipose tissue, and extracellular matrix (ECM) and overlay the pectoralis major muscle. The innermost functioning units of the breast are the fifteen to twenty mammary gland lobes which are composed of lobules. Fifteen to twenty-five draining milk ducts and connected lobule alveoli (or acini) collectively form terminal duct lobular units (TDLU) (Weigelt and Bissell, 2008). These ducts align radially and end at the outermost breast protrusion, the nipple. A single layer of luminal epithelial cells forms an epithelium that surrounds the duct lumen, and myoepithelial cells, so-called due to a phenotype and morphology similar to those of smooth muscle cells, comprise the outer layer of the duct and reside around the epithelium. A basement membrane lines the outer myoepithelial layer such that each duct is separate from surrounding breast stroma.

A major arterial blood supply enters the breast through the internal mammary artery as well as the lateral thoracic artery. The internal thoracic, axillary, and cephalic veins drain circulating blood from each breast. The lymphatic system circulates throughout the breast, and drainage to the axillary lymph nodes is the most common route.

The non-lactating ratio of glandular to adipose tissue is difficult to precisely assess due to the heterogeneous composition of breast tissue, but it has been estimated at 1:1. Conversely, although highly variable among women, lactating breasts have an increased mean glandular to adipose tissue ratio of approximately 2:1 (Geddes, 2007). Upon egg fertilization, female hormones such as estrogen and progesterone remain elevated to maintain a full-term pregnancy. Luminal epithelial cells differentiate into lactocytes that facilitate milk production during the secretory differentiation phase of lactation throughout mid to late stage pregnancy. Estrogen and progesterone levels fall sharply following parturition while prolactin levels continue to increase, thus promoting the second stage of lactation, the secretory activation phase in which milk is actively produced and secreted (Pang and Hartmann, 2007).

1.2 Breast Cancer Epidemiology, Therapy, and Cost

Breast cancer is the second most common type of female cancer behind non-melanoma skin cancer, and it is the second leading cause of cancer-associated female mortality behind lung cancer. Over 192,000 new cases of breast cancer will be diagnosed in the United States in 2009, and over 1.2 million patients are diagnosed with breast cancer every year worldwide. In addition, more than 40,000 deaths will occur due to the

disease in the United States in 2009 (www.cancer.gov), and worldwide, breast cancer was responsible for approximately 548,000 deaths in 2007 (www.who.org). Male breast cancer is rare, representing approximately 1% of annual total breast cancer incidence (www.cancer.gov), and will not be discussed in further detail. As with most cancers, breast cancer incidence increases with age, and the majority of diagnoses occur in postmenopausal women. In the United States, the median age at breast cancer diagnosis was 61 from 2002 through 2006, and during the same period approximately 0.0% were diagnosed under age 20; 1.9% 20-34; 10.5% 35-44; 22.5% 45-54; 23.7% 55-64; 19.6% 65-74; 16.2% 75-84; and 5.5% >85. Again from 2002 to 2006, the breast cancer incidence rate was 123.8 per 100,000 women per year, and the 5-year relative survival rate from 1999 through 2005 was 89.1% (www.cancer.gov). Developing invasive breast cancer can be predicted according to age-dependent relative risk as follows: 0.48% <39 (1 in 210); 3.86% 40-59 (1 in 26); 3.51% 60-69 (1 in 28); 6.95% >70 (1 in 15); and 12.28% lifetime risk (1 in 8) (www.cancer.org).

Invasive breast cancer is most commonly thought to arise from premalignant tumors within TDLU (Weigelt and Bissell, 2008). Most of these are diagnosed as ductal carcinoma in situ (DCIS), which describes hyperplasia of the luminal epithelial cells within mammary ducts of TDLU. DCIS is a noninvasive lesion retained within the boundaries of a ductal basement membrane, and therefore, the term “carcinoma” is perhaps inappropriate. Although up to 15% of patients demonstrate eventual invasive local recurrence, the 10-year disease-specific survival rate for DCIS is over 97%. Some patients demonstrate poorly differentiated DCIS with HER2 overexpression, mutated p53, and elevated markers of angiogenesis and cellular proliferation. These more

aggressive DCIS tumors are generally estrogen receptor (ER)/progesterone receptor (PR)-negative and progress rapidly compared to better differentiated ER/PR-positive DCIS that may take up to twenty years for clinical detection. Due to the invasive potential of DCIS, definitive surgical therapy in the form of breast conservation therapy (e.g., partial mastectomy/lumpectomy/quadrantectomy with negative margins, breast irradiation) or total mastectomy is indicated. Surgical options are determined by size of the lesion relative to the size of the breast and location and extent of the lesion based on mammography and biopsy results.

Unlike DCIS, lobular carcinoma in situ (LCIS) is a histologic diagnosis associated with increased breast cancer risk rather than a lesion requiring surgical resection (Frykberg, 1999). Although first described as a mammary lobule-specific tumor, it has since been shown to arise from discohesive ductal or lobular epithelial cells of TDLU. The exact incidence of LCIS is difficult to quantify due to its asymptomatic nature and subsequent complicated diagnosis. LCIS does not present as a hard palpable mass and cannot be routinely detected by mammography (Ho and Tan, 2009). Past studies showed equal risk of LCIS recurrence in ipsilateral and contralateral breasts (Li *et al.*, 2006) and upon diagnosis, it is usually bilaterally detected throughout most breast tissue (Frykberg, 1999). Risk reduction measures for patients with LCIS include close interval follow up with 6 monthly examinations, bilateral prophylactic mastectomies, and chemoprevention with tamoxifen.

DCIS or LCIS tumor cells may eventually acquire the capability to invade through the basement membrane into the breast parenchyma, which then initiates direct tumor-stroma interaction and ensuing invasive breast cancer. DCIS has the potential to

give rise to invasive ductal carcinoma of the breast (IDC), the most common type of invasive breast cancer representing approximately 80% of cases. Although LCIS is most commonly associated with subsequent IDC as well, LCIS is also found in association with invasive lobular carcinoma of the breast (ILC), which represents 15% of invasive breast cancer cases. IDC exhibits a diffuse glandular pattern of invasion, while ILC tends to invade in a single line composed of adjacent cells (Turashvili *et al.*, 2005).

Estrogen receptor-alpha (ERα) is a latent cytoplasmic ligand-activated transcription factor utilized by clinicians to classify the heterogeneous disease of breast cancer. ERα-positive breast cancer incidence increases up to age 51, the mean age of menopause, and continues to increase until age 80. Conversely, ERα-negative breast cancer incidence plateaus and even decreases at age 51, while demonstrating an increase prior to age 50 comparable to that of ERα-positive disease. This discrepancy between the two incidence rates at menopause produces an inflection in the incidence rate of all breast cancer cases which has been termed Clemmesen's hook (Anderson and Matsuno, 2006). Whereas the prevalence of ERα-positive cells within TDLU of healthy premenopausal women has been reported at 7%, this number is estimated at 42% in postmenopausal women (Shoker *et al.*, 1999). In addition, approximately two-thirds of all breast cancers are diagnosed as ERα-positive, and 75% of postmenopausal breast cancers are ERα-positive (Macedo *et al.*, 2009). Progesterone receptor (PR) and epidermal growth factor receptor 2 (EGFR2; HER2; or ErbB2), a receptor tyrosine kinase involved in cellular proliferation, have also acquired clinical relevance following reports of dismal survival rates in "triple negative" (ERα negative/PR negative/HER2 not overexpressed) breast cancer. Triple negative breast cancer represents approximately 15 to 20% of all breast

cancer cases, typically presents with ductal histology, and can only be treated with standard chemotherapy as it lacks current adjuvant therapeutic targets. Such breast tumors are highly proliferative with a high mitotic index, increased necrosis, elevated apoptosis, and typically are of higher tumor grade. *TP53* gene and p53 protein mutations as well as loss of the Rb tumor suppressor protein are common. Familial breast cancer patients with congenital BRCA1 mutations often present with triple negative breast cancer, as do relatively younger breast cancer patients and African American women. Currently, triple negative breast cancers are associated with a poor prognosis largely due to poor survival rates and early relapse. The fact that these breast tumors respond well if not completely to initial chemotherapy may seem counterintuitive, but enhanced invasiveness dictates distant metastasis and residual local recurrence to promote poor clinical outcomes (Irvin and Carey, 2008).

Like many cancers, early detection has decreased breast cancer patient mortality over the last twenty years. Likewise, heightened public awareness and more prevalent mammography screening has improved patient outcome in this regard. Clinical assessment for probable breast cancer includes physical examination and radiological imaging including mammography. Upon diagnosis of invasive breast cancer, treatment options include surgery, radiation therapy, and/or systemic therapy depending on the stage of disease and patient and tumor characteristics. Surgical tumor resection is the primary standard of care, and selection of surgical treatment is based on the findings on clinical breast examination, imaging studies, pathology, and patient history. Whole-breast or in some instances partial-breast radiotherapy is recommended to follow breast lumpectomy to prevent cancer relapse due to residual local tumor cells.

Beyond surgical intervention and radiotherapy of primary breast cancer, both adjuvant chemotherapy and, if applicable, selectively targeted adjuvant therapy, are utilized to prevent the outgrowth of occult systemic micrometastases. Importantly, systemic adjuvant therapy increases disease-free and overall survival rates in early stage breast cancer patients. The most successful of these to date are the taxanes, including paclitaxel and docetaxel, which target cell microtubules to disrupt mitosis, and anthracycline antibiotics including doxorubicin (Benson *et al.*, 2009). Selective estrogen receptor modulators (SERM) are non-steroidal synthetic compounds that selectively target the estrogen receptor and demonstrate tissue-specific biological activity. For example, the first synthesized and most commonly utilized SERM, tamoxifen, is considered antiestrogenic in the breast but elicits the opposite effect in the endometrium where it increases the relative risk of endometrial cancer (Oseni *et al.*, 2008). Tamoxifen is currently used as selective adjuvant therapy in ERα-positive breast cancer. Aromatase inhibitors are also employed in the management of ER-positive breast cancer. Aromatase is an enzymatic complex which converts androgens (e.g., testosterone) to estrogens and is responsible for estrogen synthesis in postmenopausal women. Postmenopausal breast tissue exhibits aromatase activity, and therefore, aromatase inhibitors function to reduce breast tissue estrogen levels and therefore, are only utilized in postmenopausal patients. Third-generation aromatase inhibitors such as letrozole (Femara) are currently being used as initial selective adjuvant therapy to treat hormone responsive breast cancer in postmenopausal patients (Macedo *et al.*, 2009). Trastuzumab (Herceptin®), a monoclonal humanized anti-HER2 antibody, has proven effective for the management of early stage breast cancer with HER2 overexpression (Mariani *et al.*, 2009). Therefore, it

is not a treatment option for triple negative breast cancer due to a lack of HER2 overexpression in these tumors.

Patient survival rates continue to increase, but therapeutic management of breast cancer comes at a cost. Thus, continued studies and consequent utilization of breast cancer prevention strategies is paramount to alleviating breast cancer-associated heatlh care costs. The total amount paid by Medicare in 2002 for the first year following breast cancer diagnosis in patients aged 65 and older was $1,061,459,553. The mean Medicare payment for each of these patients was $20,964. Almost all (91%) newly diagnosed breast cancer patients undergo surgery as primary treatment following diagnosis, whether it is lumpectomy to remove only the tumor or mastectomy to completely remove the affected breast, and this surgical treatment averaged $5,674 in Medicare payments in 2002. Nearly one-quarter (24%) of first-year patients received chemotherapy, and Medicare paid an average of $12,802 for each patient. Over half (51%) of first-year patients received radiation therapy in 2002, and this cost Medicare approximately $4,500. Furthermore, Medicare paid approximately $16,000 in 2002 for first-year patient hospitalizations that were unrelated to cancer surgery (23%) (Warren *et al.*, 2008).

1.3 Breast Cancer Cell Lines

Since the inception of the first immortalized human cell line generated for research, HeLa cervical cancer cells, cell lines have been utilized to study many if not all diseases. Despite inherent disadvantages such as culture-induced genotypic divergence and risk of cellular contamination, cell lines have been used for over fifty years. In particular, established cell lines derived from primary or secondary tumor sites currently

serve as common models of human cancers (Burdall *et al.*, 2003). Cancer cell lines are invaluable resources and can be used *in vitro* to characterize specific oncogenic mechanisms or *in vivo* to model human cancer progression and metastasis. They are models of human malignancy and although essential to cancer research, cannot be considered definitive resources. Rather, they should be exploited to scrutinize hypotheses and generate well-characterized conclusions prior to ultimate preclinical and clinical trials. Likewise, they are also powerful tools which can be used to define clinical anomalies, as was the case in the current body of work.

Breast cancer is one of the most widely studied cancers, and therefore, over one hundred human and murine breast cancer cell lines are available for purchase through the American Type Culture Collection (ATCC). Although breast cancer cell lines are easily propagated *in vitro* on plastic dishes with simple growth medium and supplemental fetal bovine serum (FBS), these two-dimensional (2D) conditions are not representative of the dimensionality and stiffness of *in vivo* tumor microenvironments (Paszek *et al.*, 2005). While this more traditional 2D cell culture will continue to be used due to its convenience and demonstrated productivity, the necessity for three-dimensional (3D) cell culture models has recently become more evident. In fact, microarray gene expression analysis has demonstrated distinct gene expression profiles between breast cancer cell lines grown in 2D versus 3D culture (Kenny *et al.*, 2007). Furthermore, gene expression profiles from breast cancer cell lines grown in 3D models have been used for accurate prediction of clinical patient outcome among multiple datasets (Martin *et al.*, 2008).

Another advantage to breast cancer cell lines is their capacity to model multiple clinical subtypes of breast cancer. For example, breast cancer cell lines including MCF-

7, BT474, T47D, and ZR-75-1 cells are all classified as estrogen receptor-alpha (ERα)-positive and luminal breast cancer subtype, while MDA-MB-231 cells are ERα-negative and basal breast cancer subtype. ERα and clinical breast cancer subtypes will be discussed in more detail below. Additionally, these breast cancer cell lines can also be distinguished based on morphologies and phenotypes consistent with epithelial-mesenchymal transition (EMT), which again, will be discussed in further detail below. The four ERα-positive breast cancer cell lines utilized in our current studies all express E-cadherin, lack mesenchymal gene expression, and exhibit mass or spheroid morphology. Conversely, ERα-negative MDA-MB-231 cells lack E-cadherin, express Vimentin, and exhibit stellate morphology (Blick *et al.*, 2008; Kenny *et al.*, 2007). Concerning detailed accounts of IL-6, STAT3, and EMT below, the ERα-positive breast cancer cell lines studied here lack IL-6 production and constitutive STAT3 activation, whereas ERα-negative MDA-MB-231 cells produce IL-6 and exhibit constitutive STAT3 activation (Sasser *et al.*, 2007b).

1.4 Interleukin-6 and STAT3 in Breast Cancer Progression

Interleukin-6 (IL-6) is a 26 kDa protein product of the *IL6* gene on human chromosome 7 and represents a quintessential pleiotropic cytokine. First characterized as a T-cell-derived factor that induced proliferation, differentiation, and immunoglobulin production in B-cells, IL-6 was originally named B-cell stimulating factor-2 (BSF-2). It was later thought to be a novel interferon (IFN-β_2) due to studies demonstrating the ability of IL-6 to activate signal transducer and activator of transcription 3 (STAT3) (Kishimoto, 2006). Complementary DNA (cDNA) encoding the human IL-6 gene was

subsequently cloned, and human IL-6 transgenic mice were generated with a polyclonal IgG1 plasmacytosis phenotype (Suematsu *et al.*, 1989). Next, IL-6 knockout (IL-$6^{-/-}$) mice were generated and characterized. These mice demonstrated normal development, but adults exhibited reduced numbers of peripheral T-cells, and impaired antiviral cytotoxic T-cell activity (Kopf *et al.*, 1994). Cutaneous wound healing studies in IL-$6^{-/-}$ mice revealed the essential role of IL-6 to induce keratinocyte migration during the re-epithelialization phase of skin repair (Gallucci *et al.*, 2000). IL-6 is now known to be an inflammatory cytokine as the major inducer of C-reactive protein (CRP) throughout the acute phase inflammatory response. It is a critical factor to hematopoiesis and subsequent lymphocyte differentiation and activation, and fibroblasts, T and B-cells, macrophages, and endothelial cells all have the potential to produce constitutive or inducible IL-6 (Kishimoto, 2006). IL-6 gene expression is nuclear factor-kappaB (NF-κB)-dependent (Chauhan *et al.*, 1996), and if present, ERα directly binds to NF-κB, thus preventing transactivation of IL-6 expression (Galien and Garcia, 1997).

IL-6 primarily signals through the Janus kinase (JAK)/STAT3 pathway (Hodge *et al.*, 2005). To do so, a plasma membrane-associated IL-6 receptor (IL-6R/CD126) homodimer first ligates two soluble IL-6 molecules which leads to gp130 (CD126) homodimer ligation. Whereas IL-6Rα is only expressed on hepatocytes, neutrophils, monocytes, macrophages, and some lymphocytes under normal physiological conditions, gp130 is a ubiquitous and promiscuous receptor involved in multiple cytokine signaling pathways (e.g., IL-11, leukemia inhibitory factor (LIF), oncostatin M (OSM), and ciliary neurotrophic factor (CNTF)) (Rose-John *et al.*, 2006). To initiate IL-6-induced gp130 intracellular signal transduction, JAK are recruited to the intracellular domain of the

gp130 receptor where they bind and autophosphorylate. Subsequent gp130 phosphorylation via activated JAK offers docking sites for STAT3 and other receptor-associated proteins. Once bound to the intracellular domain of gp130, STAT3 is specifically phosphorylated (pSTAT3) by adjacent JAK on a C-terminal tyrosine residue (Y705), which grants its disengagement from the receptor. Dissociation of $pSTAT3^{Y705}$ from gp130 facilitates its homodimerization within the cytoplasm, and the $pSTAT3^{Y705}$ homodimer translocates to the nucleus. There, $pSTAT3^{Y705}$ binds to specific promoters whereby it initiates the transcription of multiple downstream target genes (Clevenger, 2004). An inhibitory feedback loop maintains rapid and transient STAT3 activation under normal physiological conditions, but this is not the case in many human cancers which exhibit constitutive STAT3 activity. Following activation in normal cells, STAT3 induces suppressors of cytokine signaling (SOCS) and protein inhibitors of activated STATs (PIAS) expression. While SOCS-1 specifically inhibits JAK function, SOCS-3 binds the IL-6R complex to inhibit IL-6 signal transduction. PIAS-3 directly interacts with STAT3 to inhibit all STAT3 target gene expression (Kishimoto, 2006).

Alternatively, IL-6 *trans*-signaling describes an IL-6 signaling pathway whereby an IL-6 soluble receptor (IL-6sR) binds IL-6 and subsequently ligates gp130 to provoke STAT3 activation in cells that only express gp130. IL-6sR is naturally produced by either proteolytic cleavage of the membrane-bound IL-6R or alternative splicing of IL-6R mRNA (Rose-John *et al.*, 2006). Whereas IL-6 serum levels continue to increase with age, levels of serum IL-6sR rise until approximately age 70 at which time they gradually decline (Giuliani *et al.*, 2001). Likewise, IL-6sR expression has been demonstrated in human breast cancer cell lines (Crichton *et al.*, 1996; Oh *et al.*, 1996; Singh *et al.*, 1995),

suggesting that IL-6 *trans*-signaling mediates the effects of IL-6 in breast cancer cells. A naturally occurring soluble form of gp130 (sgp130) specifically antagonizes IL-6 *trans*-signaling by exclusively binding to the IL-6-IL-6sR complex, thus having no effect on cells that express the membrane-bound IL-6R (Rose-John *et al.*, 2006).

Aberrantly elevated IL-6 is associated with a poor breast cancer prognosis (Bachelot *et al.*, 2003; Salgado *et al.*, 2003; Zhang and Adachi, 1999). Human breast tumors produce significantly more IL-6 when compared to matched healthy breast tissue (*P*-value < 0.0001), and IL-6 levels increase with tumor grade. ERα-negative human breast tumors produce significantly more IL-6 than tumors that express ERα. (*P*-value <0.001) (Chavey *et al.*, 2007), and IL-6 serum levels are significantly higher in ERα-negative breast cancer patients compared to ERα-positive patients (*P*-value < 0.05) (Jiang *et al.*, 2000). Furthermore, increased serum IL-6 has been demonstrated in breast cancer patients compared to normal donors and correlates with advanced breast tumor stage (Kozlowski *et al.*, 2003) and increased number of metastatic sites (Salgado *et al.*, 2003). Finally, a single nucleotide polyporphism (SNP) exists at position -174 in the IL-6 gene promoter region, noted as IL-6 (-174 G>C). The IL-6 (-174 G>C) SNP has the following allele frequency in a Caucasion population: 36% G/G, 44% G/C, and 18% C/C. Following an inflammatory stimulus such as *Salmonella typhii* vaccination, those individuals with the G/G allele exhibit higher serum IL-6 from 6 to 24-hours post-vaccination (Bennermo *et al.*, 2004). Although the IL-6 (-174 G>C) SNP is not associated with increased risk of developing breast cancer (Gonzalez-Zuloeta Ladd *et al.*, 2006; Litovkin *et al.*, 2007), it is significantly associated with disease-free (*P*-value = 0.02) and overall (*P*-value = 0.01) survival in breast cancer patients (DeMichele *et al.*,

2003). Moreover, ERα-negative breast cancer patients, whose tumors produce more IL-6 than those that express ERα (Chavey *et al.*, 2007), demonstrate no difference in survival between the G/G allele (higher inducible systemic IL-6) and any C allele (G/C or C/C; lower inducible systemic IL-6). In contrast, ERα-positive breast cancer patients demonstrate a significant difference in disease-free (*P*-value = 0.003) and overall (*P*-value = 0.001) survival between the G/G allele and any C allele (DeMichele *et al.*, 2003).

Although the mechanisms that underlie the association between IL-6 and unfavorable clinical outcomes in breast cancer remain poorly understood, the oncogenic capacity of STAT3 may shed some light. STATs are latent cytoplasmic proteins, but upon tyrosine phosphorylation, they are granted access to the nucleus where they induce a plethora of target genes. For example, oncogenes such as c-Myc, cyclin D1, BCL-X_L, and HGF and immunosuppressive genes including TGF-β, IL-10, and VEGF are direct downstream transcriptional targets of STAT3. Likewise, multiple growth factors are capable of activating STAT3 including hepatocyte growth factor (HGF), vascular endothelial growth factor (VEGF), and epidermal growth factor (EGF). Most relevant to this body of work, we and others have previously demonstrated that paracrine or autocrine IL-6 signaling in human breast cancer cells can induce $pSTAT3^{Y705}$, a surrogate for transcriptionally active STAT3 (Berishaj *et al.*, 2007; Sasser *et al.*, 2007b). STAT3 was demonstrated to be required for Src-dependent cellular transformation, which led to extensive characterization of its oncogenic potential (van 't Veer *et al.*, 2002). Active STAT3 has since been detected in various human hematopoietic malignancies such as multiple myeloma, acute and chronic mylogenous leukemias, non-Hodgkin's lymphoma

as well as solid tumors such as breast, ovarian, lung, pancreatic, and prostate carcinomas (Wang *et al.*, 2004).

Interestingly, STAT3 knockout mice ($STAT3^{-/-}$) are embryonic lethal while individual ablation of all other STATs generates viable phenotypes (Takeda *et al.*, 1997). To overcome STAT3-dependent embryogenesis, STAT3 inhibition and knockdown strategies have been utilized to evaluate the role of constitutive STAT3 activation in breast cancer cell lines. Consistent with this and offering further evidence of the effect of IL-6 in human breast cancer, MDA-MB-231 human breast cancer cells expressing a dominant negative isoform of gp130 lacked constitutively active STAT3 and exhibited impaired tumorigenicity in an orthotopic nude mouse xenograft model (Selander *et al.*, 2004). Likewise, MDA-MB-468 human breast cancer cells treated with AG490, a selective JAK inhibitor, demonstrated growth arrest and eventual apoptosis (Burke *et al.*, 2001). Highly tumorigenic 4T1 mouse mammary carcinoma cells expressing stable STAT3-specific shRNA with little to no STAT3 or $pSTAT3^{Y705}$ protein were unable to form orthotopic tumors in immunocompetent mice. STAT3 knockdown had no effect on 4T1 cell proliferation or apoptosis in standard 2-dimensional culture (Ling and Arlinghaus, 2005), suggesting that STAT3 activation may promote immunoevasion in this model as in others (Wang *et al.*, 2004).

1.5 Breast Cancer Metastasis and Epithelial-Mesenchymal Transition

Tumor metastasis is the culmination of a complex cascade in which disseminated primary tumor cells grow and colonize at a secondary tissue site. Primary tumors rarely have the capacity to cause patient death, but rather, tumor metastasis governs nearly all

cancer-associated mortalities. Successful growth at a secondary site is a somewhat daunting task that requires disseminated tumor cell survival at multiple sequential steps including: detachment from the primary neoplasm, local invasion through the confining basement membrane, and subsequent intravasation into vasculature or lymphatics; resistance to anoikis and shear stress once in circulation; embolism formation within a capillary or lymphatic vessel; extravasation through that vessel wall followed by invasion, proliferation, and ultimate colonization within a secondary tissue microenvironment, all while evading immunosurveillance. An introduction to metastasis would be remiss without the mention of Stephen Paget's "seed and soil" hypothesis, first proposed in 1889. At that time, tumor metastasis was thought to be a random event. However, as an English surgeon, Paget recognized a recurrent pattern of breast cancer metastasis, particularly to bone, that did not coincide with the current dogma of his time. He postulated that a metastatic primary tumor cell, or "seed," would only grow in a congenial "soil," now accepted as a favorable tissue microenvironment (Fidler, 2003; Paget, 1889). Incidentally, primary mammary tumor cell dissemination has been quantified at 3 to 4 x 10^6 primary tumor cells in circulation per 24 hours per gram of tumor in a rat mammary carcinoma model, which exemplifies the inefficient nature of metastasis (Butler and Gullino, 1975).

Although metastasis has been generally accepted as a relatively late event during carcinogenesis, recent work has revealed evidence of early primary tumor cell dissemination, thus refuting this paradigm (Klein, 2009). In particular, it has reently been demonstrated that untransformed triple transgenic (doxycycline-inducible K-ras, MYC, and polyoma middle T antigen) mammary epithelial cells are capable of lung

colonization when tail vein-injected into immunocompromised female mice on doxycycline. This work showed that untransformed "normal" mammary epithelial cells can colonize ectopic lung tissue, and upon oncogene activation, disseminated mammary epithelial cells within circulation or a foreign host microenvironment are capable of forming tumors at the ectopic site (Podsypanina *et al.*, 2008). Additionally, reports of bone marrow cytokeratin-positive epithelial cells in up to 48% of breast cancer patients without overt metastases also lend support to early primary tumor cell dissemination. Decreased survival in patients with such cells was demonstrated in all studies (Braun *et al.*, 2000; Diel *et al.*, 1996; Gebauer *et al.*, 2001; Pantel *et al.*, 2003; Vannucchi *et al.*, 1998). Furthermore, only 8% of these patients with bone marrow micrometastases exhibited cytokeratin-positive/Ki67-positive cells, suggesting that lack of overt bone metastasis may be due to disseminated tumor cell dormancy (Pantel *et al.*, 2003).

Breast cancer most commonly metastasizes to bone, followed by lung, liver, and brain. Owed to the heterogeneity of breast tumors, few prognostic molecular biomarkers have been demonstrated to accurately predict metastatic potential. One of the most important of these is ERα, which is clinically exploited as a predictor of bone metastasis (Kominsky and Davidson, 2006). Whereas ERα-positive breast cancers have a strong tendency to metastasize to bone if at all (James *et al.*, 2003), their ERα-negative counterparts favor visceral organs such as lung and liver (Hess *et al.*, 2003). Meanwhile, histopathological tumor characterization including primary tumor size, axillary lymph node involvement, and histological grade has proven clinically relevant. A primary breast tumor of less than 2 cm is associated with low metastatic risk, while a tumor greater than 5 cm is associated with a very high metastatic risk. Detection of 4 or more

axillary lymph node metastases is associated with a very high risk of distant metastasis, and metastatic risk increases with tumor grade such that poorly differentiated grade 3 tumors are highly prone to metastasize (Weigelt *et al.*, 2005).

More recently, genetic profiling studies have identified breast tumor subtypes based on distinct gene expression patterns, and each subtype can be used as a prognostic marker to effectively predict patient survival. Three predominant breast tumor subtypes were initially identified: luminal, basal-like, and ERBB2 (HER2)-positive breast tumors in which the luminal subtype was associated with ERα expression and the basal-like and ERBB2-positive subtypes both showed little to no ERα expression (Perou *et al.*, 2000). A subsequent study by Sorlie, *et al*. not only confirmed these findings but also elucidated three subclasses of luminal breast tumors, termed luminal subtypes A, B, and C. Although these three additional luminal subtypes all expressed ERα to some degree, luminal subtype A breast tumors expressed the highest ERα levels while luminal subtypes B and C shared features of basal-like and ERBB2-positive subtypes. Perhaps the most clinically relevant finding was that these breast tumor subtypes predicted patient survival. In particular, the poorest outcome was in basal-like and ERBB2-positive patients compared to patients with luminal breast tumors (Sorlie *et al.*, 2001). Consequent studies have since corroborated these findings by identification of a gene expression signature capable of predicting breast cancer patient survival (Buyse *et al.*, 2006; van 't Veer *et al.*, 2002; van de Vijver *et al.*, 2002).

Another prognostic molecular biomarker clinically utilized to project the metastatic propensity of breast cancer is E-cadherin. Whereas very few studies have failed to demonstrate E-cadherin as an independent prognostic marker in breast cancer

patients (Lipponen *et al.*, 1994; Parker *et al.*, 2001), the overwhelming majority of reports on this matter have revealed E-cadherin as one of the strongest predictors of patient survival. Specifically, impaired E-cadherin expression in human breast tumors correlates with enhanced invasiveness, metastatic potential (Oka *et al.*, 1993), and significantly decreased breast cancer patient survival (P-value < 0.0001) (Heimann and Hellman, 2000; Pedersen *et al.*, 2002). While appropriate E-cadherin function is essential to the maintenance of epithelial cell morphology, phenotype, and homeostasis, regulation of E-cadherin expression is of equal importance. *CDH1*, the gene that encodes E-cadherin, is located on human chromosome 16q22.1 (Rakha *et al.*, 2006) and is susceptible to inactivation by promoter hypermethylation, somatic mutation, or aberrant overexpression of repressive transcription factors including Twist, Snail, and Slug among others (Hirohashi, 1998). Likewise, E-cadherin loss of function can arise due to extracellular domain-specific proteolytic cleavage. Although uncommon, germline mutations of *CDH1* predispose individuals to hereditary diffuse gastric cancer (HDGC) syndrome, and a proportion of these patients present with other cancers, including breast cancer (Guilford, 1999).

Initially termed uvomorulin in mice and L-CAM in chicks, E-cadherin was concomitantly discovered as a 120 kDa calcium-dependent trypsin-labile cell surface glycoprotein required for intercellular adhesion in mouse blastomeres (Hyafil *et al.*, 1981) and chick embryos (Brackenbury *et al.*, 1981). It now represents the best studied member of the cadherin family of tissue-specific homophilic intercellular adhesion molecules. E-cadherin knockout studies have demonstrated early embryonic lethality due to impaired maintenance of epithelial polarity and failure to form an intact epithelium in

E-cadherin$^{-/-}$ embryos (Larue *et al.*, 1994). E-cadherin is localized on the cell surface of epithelial cells, and each E-cadherin protein consists of an amino-terminal extracellular domain, a single-pass transmembrane segment, and a carboxy-terminal intracellular domain. Five calcium-binding repeated subunits comprise an extracellular domain that promotes homophilic interaction to ultimately form anti-parallel trans-E-cadherin dimers between adjacent cells (Guilford, 1999). The intracellular domain is comprised of a juxtamembrane p120-catenin binding subdomain and a C-terminal beta (β)-catenin binding subdomain. β-catenin, a potent transcription factor, binds E-cadherin and alpha (α)-catenin subsequently binds β-catenin. Although contentious (Weis and Nelson, 2006), it is generally acknowledged that α-catenin interacts with F-actin and thereby, facilitates the linkage of E-cadherin to the cytoskeleton. This E-cadherin-catenin-actin complex localizes to epithelial intercellular junctions called adherens junctions and is critical to epithelial cell adhesion, polarity, and morphology (Hartsock and Nelson, 2008). Furthermore, E-cadherin sequesters β-catenin at the cell surface as one means to inhibit β-catenin nuclear translocation and consequent expression of β-catenin responsive genes (Perez-Moreno *et al.*, 2003).

CDH1, the gene that encodes E-cadherin, is regarded as a major tumor suppressor gene due to frequent loss of heterozygosity (LOH) at the 16q locus in breast cancer (Rakha *et al.*, 2006). In contrast to DCIS and IDC (i.e., ductal tumors), nearly all cases of LCIS and ILC (i.e, lobular tumors) (Acs *et al.*, 2001; Berx *et al.*, 1995) lack E-cadherin protein expression due to LOH at the *CDH1* locus. Consequently, E-cadherin expression can be utilized in the clinic to distinguish lobular from ductal carcinoma diagnoses (Acs *et al.*, 2001; Bertucci *et al.*, 2008; Yoder *et al.*, 2007). In addition, conditional knockout

of epithelial tissue-specific E-cadherin, combined with loss of p53, has been shown to promote mammary tumor initiation, subsequent invasive lobular mammary carcinoma, and ultimately metastasis in a mouse model of ILC (Derksen *et al.*, 2006).

Another prominent role of E-cadherin is that of an invasion/metastasis suppressor protein. Upon loss of E-cadherin and subsequent dissociation of adherens junctions, epithelial cells acquire enhanced invasive capability (Behrens *et al.*, 1989). This is corroborated by the conversion of benign adenoma to invasive carcinoma upon loss of E-cadherin in a murine model of pancreatic β-cell carcinogenesis (Perl *et al.*, 1998). More specific to human breast cancer, MDA-MB-231 cells lack E-cadherin whereas MCF-7 cells express high levels of E-cadherin (Kenny *et al.*, 2007), and Sommers *et al*. demonstrated enhanced invasive capability in MDA-MB-231 cells compared to MCF-7 cells (Sommers *et al.*, 1991). Naturally, E-cadherin expression and consequent invasive capacity regulate the propensity of breast cancer metastasis. Multiple signaling pathways are activated following loss of E-cadherin protein, which promote transformed human breast epithelial cell metastasis in a xenograft model. Interestingly, Twist, a transcriptional repressor of *CDH1*, is induced upon loss of E-cadherin and is necessary for metastasis in this model. Furthermore, the E-cadherin binding partner, β-catenin, was shown to be necessary but not sufficient for the EMT phenotype induced following loss of E-cadherin (Onder *et al.*, 2008). Ectopic expression of murine E-cadherin in highly metastatic human MDA-MB-231 cells significantly reduced osteolytic bone metastases in a murine intracardiac dissemination model (Mbalaviele *et al.*, 1996). Likewise, aberrant cytoplasmic or diminished to negative E-cadherin immunostaining patterns are commonly detected in invasive poorly differentiated breast carcinomas compared to

noninvasive well-differentiated breast carcinomas and are associated with increased probability of breast carcinoma metastasis (Oka *et al.*, 1993). The finding that distant metastases often express E-cadherin even in patients which exhibit primary breast carinomas which lack E-cadherin suggests that ultimate re-expression may be necessary for colonization of secondary tissues (Kowalski *et al.*, 2003; Saha *et al.*, 2007).

Loss of E-cadherin is a prerequisite for epithelial-mesenchymal transition (EMT), a highly conserved process which exemplifies the aberrant induction of an embryonic gene expression program during carcinoma progression. EMT is critical for multiple steps of developmental metazoan cellular morphogenesis as demonstrated in well-characterized *Drosophila* and *Xenopus* models. Throughout embryonic development, EMT whereby epithelial cells give rise to more motile mesenchymal cells is essential for mesoderm and neural crest formation. Importantly, this is a transient process and mesenchymal-epithelial transition (MET) allows for cellular reversion (Yang and Weinberg, 2008).

Whereas EMT has been extensively studied for its essential role in embryogenesis, the concept of EMT-like cellular changes in human cancers has gained acceptance as a major mechanism to promote primary tumor cell invasion and subsequent tumor metastasis. A carcinoma cell must first detach from the primary tumor and invade through the basement membrane into the underlying tissue parenchyma to initiate the metastasic cascade. Although cancer-associated EMT was considered a controversial notion even in recent years (Tarin *et al.*, 2005), it has been demonstrated in multiple human carcinomas, including breast cancer (Cheng *et al.*, 2008; Heimann and Hellman, 2000; Moody *et al.*, 2005; Sarrio *et al.*, 2008), and is now recongnized as a putative

mediator of tumor metastasis. An EMT phenotype including impaired E-cadherin expression with concominant induction of Vimentin, Alpha-smooth-muscle-actin, and/or N-cadherin is associated with the basal breast cancer subtype, suggesting that EMT may promote characteristic aggressiveness in these tumors and contribute to poor breast cancer patient survival (Sarrio *et al.*, 2008). Likewise, relatively noninvasive ERα-positive MCF-7 cells exhibit a characteristic epithelial phenotype and are classified as luminal subtype whereas highly invasive ERα-negative MDA-MB-231 cells show more of an EMT phenotype (i.e., lack E-cadherin and aberrant Vimentin expression) and are classified as basal subtype (Blick *et al.*, 2008). While EMT may enhance carcinoma cell invasion and subsequent dissemination which would increase metastatic potential, it is not synonymous with metastasis in all models. For example, Lou, *et al*. demonstrated that EMT alone was insufficient for spontaneous murine mammary carcinoma metastasis (Lou *et al.*, 2008). Yet, Weinberg and colleagues described the promotion of metastasis with loss of E-cadherin and a consequent EMT phenotype in transformed human breast epithelial cells (Onder *et al.*, 2008).

1.6 Non-Melanoma Skin Cancer

Human skin functions primarily as a direct physical barrier between us and our environment and is composed of three histologically distinguishable layers termed the epidermis, dermis, and hypodermis (or subcutis). The outermost layer, the epidermis, is composed of progressively differentiating keratinocytes which form a stratified squamous epithelium comprised of basal, spinous, and granular sublayers. These epidermal sublayers are delineated by basal to superficial keratinocyte differentiation. Basal cells

serve as epidermal stem cells and give rise to keratinocytes which will differentiate upward through the spinous and granular sublayers. Upon arrival at the surface of the skin, terminally differentiated keratinocytes are termed corneocytes and form the stratum corneum. These flat anucleated cells are full of nothing more than cytokeratin intermediate filaments and are destined for flaking off the skin, or desquamation. In this manner, the epidermis is constantly turning over through cellular loss at the surface and concomitant cellular proliferation arising from the basal level. Underlying the epidermis is the dermis, the layer that gives skin its structure. The dermis is comprised of connective tissue and fibroblasts. The lowest layer of the skin is the hypodermis, a layer comprised of adipose tissue and blood vessels. (Bouwstra, 2006).

Without the sun, life as we know it would not exist. The sun not only provides optimal temperatures for life on Earth, but it also provides a sunlight which is critical to the process of photosynthesis and subsequent oxygen production. The ultraviolet (UV) portion of sunlight exceeds the energy of the visible light spectrum and has a wavelength range of approximately 100 to 400 nanometers (nm). UV radiation can be subdivided into three different wavelengths which include UVA, UVB, and UVC. The highest energy UV radiation, UVC, ranges from 100 to 280 nm and is almost entirely absorbed by the Earth's atmosphere. Thus, solar UVC has no impact on Earth's surface. UVB represents the second highest energy UV radiation and ranges from 280 to 320 nm. As with UVC, most solar UVB does not make it past the Earth's atmosphere, but the longer wavelength UVB does reach the Earth's surface. The third wavelength of UV radiation is UVA and ranges from 320 to 400 nm.

Whereas both UVA and UVB contribute to initiate and promote skin carcinogenesis (Boukamp, 2005), UVB is the most dominant etiologic wavelength and accounts for 75% of non-melanoma skin cancer (NMSC) risk (van Steeg and Kraemer, 1999). UVB is classified as a complete carcinogen capable of provoking tumor initiation, promotion, and progression (Baliga and Katiyar, 2006). The initiation phase of UVB-induced NMSC is the irreversible culmination of direct DNA damage due to accumulation of cyclobutane pyrimidine dimers (CPD) and (6-4) photoproducts within critical tumor suppressor genes such as *TP53* or indirect DNA damage induced by infiltrating inflammatory cell-derived reactive oxygen species (ROS). Subsequent inflammatory responses and increased genetic mutations drive the promotion and ultimate progression stages of UVB-induced NMSC. UVB exposure causes acute cutaneous inflammation characterized by increased vascular permeability and blood flow and consequent erythema and edema (Clydesdale *et al.*, 2001; Terui *et al.*, 2001). Although higher NMSC incidence rates in men have historically been attributed to increased sun exposure compared to women, gender differences in acute UVB-induced inflammation have also been demonstrated. In particular, female Skh-1 mice have significantly higher skin fold thickness and myeloperoxidase (MPO) expression 48 hours post-UVB exposure (P-value <0.05). (Thomas-Ahner *et al.*, 2007).

Epidermal skin carcinomas are of two major clinical types, melanoma and non-melanoma skin cancer. Greater than one million cases of NMSC will be diagnosed this year in the United States, and the incidence rates continue to increase annually (www.cancer.gov). The two most common forms of NMSC are basal cell carcinoma (BCC) and squamous cell carcinoma (SCC), which account for 80% and 16% of skin

cancer cases, respectively. Conversely, melanoma accounts for 4% of all skin cancer cases (Bowden, 2004). The lifetime risk of developing SCC is estimated at 7% to 11% and 28% to 33% for BCC. Although melanoma is the rarest form of skin cancer, it causes 79% of all skin cancer-specific mortalities. Conversely, NMSC represent almost all skin cancer cases but account for approximately 1,300 to 2,300 deaths in the United States per year with most due to metastatic SCC (Abdulla *et al.*, 2005).

Outbred Skh-1 hairless mice are readily susceptible to UVB-induced SCC skin cancer, which reflects that of human SCC and are therefore the most commonly used mouse model for NMSC. Skh-1 mice develop normally and have hair at birth. However, at approximately day thirteen following birth, they exhibit rapid and complete hair loss. They are albino, euthymic, and fully immunocompetent. Individual skin tumors develop through pathologically distinct epithelial hyperplasia to papilloma to SCC progression but are rarely fatal, thus allowing evaluation of acute as well as chronic UVB effects (Benavides *et al.*, 2009). Furthermore, Skh-1 mice demonstrate a large number of tumors relatively quickly following UVB exposure three times per week for up to 25 weeks. More specifically, median time to first tumor for male mice is 10 weeks and by 25 weeks, male mice have a mean of approximately 30 tumors. In contrast, median time to first tumor for female mice is 12 weeks and by 25 weeks, female mice have a mean of approximately 22 tumors. All Skh-1 mice develop UVB-induced skin tumors by 16 weeks. As previously stated, this is an SCC skin cancer model and thus, a fraction of papillomas will progress to SCC but never to BCC or melanoma (Thomas-Ahner *et al.*, 2007).

1.7 Myeloid-Derived Suppressor Cells

Although immunosuppressive myeloid cells were first detected in tumor-bearing mice over twenty years ago, their contribution to tumor-induced immunosuppression has gained more recent appreciation. A plethora of murine transplantable and spontaneous tumor models including melanoma, neuroblastoma, and breast, lung, colon, and cervical cancers have demonstrated the aberrant systemic expansion of myeloid-derived suppressor cells (MDSC). MDSC are a heterogeneous population of immature cells of myeloid lineage which are mobilized from the bone marrow to peripheral lymphoid tissues upon various pathological stimuli such as infection, sepsis, trauma, and cancer. In mice, Gr-1 (Ly-6G and Ly-6C) and CD11b are exploited as specific MDSC immunophenotypic markers and whereas MDSC comprise 20% to 30% of normal mouse bone marrow cells, very few can be detected in peripheral lymphoid tissues. Conversely, in tumor-bearing mice, MDSC can represent as many as 20% to 40% of total splenocytes and are found within local tumor tissue. Furthermore, up to tenfold greater numbers of MDSC in peripheral blood samples can be detected in patients with various cancers.

MDSC expansion and activation is regulated by a growing number of tumor-derived factors which indirectly stimulate MDSC expansion by inducing myelopoiesis and inhibiting myeloid cell maturation. Additionally, activated T-cell and tumor stroma-derived factors are capable of directly activating MDSC. Vascular endothelial growth factor (VEGF), granulocyte-colony stimulating factor (G-CSF), monocyte-CSF (M-CSF), granulocyte/monocyte-CSF (GM-CSF), stem cell factor (SCF), transforming growth factor-beta (TGF-β), interferon-gamma (IFN-γ), interleukin-1-beta (IL-1β), and other inflammatory cytokines have all been shown to induce the expansion and activation of

MDSC in various tumor models. Intriguingly, IL-6 has been characterized as one such inflammatory cytokine capable of inducing MDSC in a 4T1 murine mammary carcinoma model. The majority of these factors ultimately lead to the constitutive induction of active STAT3 in MDSC. Chronic STAT3 activation concomitantly increases MDSC survival and proliferation while inhibiting their maturation and differentiation.

MDSC are potent suppressors of T-cell proliferation, activation, and effector function. L-arginine is an amino acid necessary for T-cell proliferation as well as a substrate for arginase 1 and inducible nitric oxide synthase (iNOS), both of which are overexpressed by MDSC. Furthermore, MDSC produce high levels of ROS, particularly superoxide anion (O_2^-), and nitric oxide (NO) which chemically combine to form peroxynitrite ($ONOO^-$). Peroxynitrite consequently induces antigen-specific T-cell anergy (Gabrilovich and Nagaraj, 2009). In addition, MDSC have been shown to produce elevated levels of IL-10 and TGF-β, which are individually immunosuppressive but also synergize to promote the induction of regulatory T-cells. IL-10 production can also generate a Th2 $CD4^+$ T-cell response rather than an appropriate Th1 anti-tumor response, the latter characterized by interferon responsiveness and subsequent STAT1 activation (Ostrand-Rosenberg and Sinha, 2009).

1.8 Hypotheses

1.8.1 Breast Cancer Studies

Although our hypotheses have always been influenced by clinical literature, the current body of breast cancer work directly emerged from our previously reported studies regarding the interactions between tissue-specific fibroblasts and breast cancer cells.

Briefly, in coculturing primary human mesenchymal stem cells (MSC; bone marrow fibroblasts), and subsequently primary breast fibroblasts, with human breast cancer cell lines in a 3-dimensional (3D) tumor growth assay (TGA), we noted enhanced growth rates in ERα-positive breast cancer cells (Sasser *et al.*, 2007a; Studebaker *et al.*, 2008). We would later postulate and show that IL-6 was necessary for fibroblast-dependent breast cancer cell growth and sufficient for cell growth *in vitro* as well as in an orthotopic xenograft model (Sasser *et al.*, 2007b). Throughout these studies, we detected aberrant mesenchymal or fibroblastoid morphologies in ERα-positive breast cancer cells following exposure to fibroblast conditioned medium. We therefore hypothesized that these cells had acquired an EMT phenotype and that IL-6 may be required for this induction. We consequently demonstrated IL-6-inducible E-cadherin repression and induction of an EMT phenotype (Chapter 2), which provoked us to further assess the role of E-cadherin in breast cancer cell growth. The notion that IL-6-dependent E-cadherin repression played a role in ERα-positive cell growth was supported by our preliminary findings as well as those of other groups. In particular, Perrais, *et al*. showed that homophilic E-cadherin binding inhibits primary human breast epithelial cell and breast cancer cell growth (Perrais *et al.*, 2007). Thus, we hypothesized that impaired E-cadherin expression would promote breast cancer cell growth (Chapter 3). The stated hypotheses were proposed with the intention of elucidating molecular mechanisms by which IL-6 impacts breast cancer progression.

1.8.2 Non-Melanoma Skin Cancer Studies

Likewise, the current body of skin cancer studies was pursued based largely on our previous reports as well as those of others. We and others have previously published studies involving UVB-induced skin tumors in Skh-1 mice (Benavides *et al.*, 2009). However, unlike many other mouse tumor models (Gabrilovich and Nagaraj, 2009), the impact of MDSC in UVB-induced skin tumorigenesis has yet to be evaluated. UVB irradiation induces cutaneous inflammation, and potentially IL-6, in Skh-1 mice and has been shown to induce IL-6 expression in primary human keratinocytes (De Haes *et al.*, 2003). Moreover, we have previously demonstrated gender disparities in UVB-induced skin tumorigenesis in which male Skh-1 mice acquire a higher tumor burden with less inflammation compared to females (Thomas-Ahner *et al.*, 2007). Systemic MDSC activation and expansion has been characterized in a number of mouse tumor models, and IL-6 is capable of promoting MDSC induction in a 4T1 mammary carcinoma model (Bunt *et al.*, 2007). We therefore hypothesized that tumor-bearing Skh-1 mice would exhibit higher percentages of peripheral MDSC than control mice not exposed to UVB radiation. Furthermore, we hypothesized that MDSC induction would be elevated in male tumor-bearing mice due to an expected higher tumor burden and decreased inflammatory response relative to females. The stated hypotheses were proposed with the intention of further characterizing gender discrepancies in skin tumor burden and inflammation in a mouse model of UVB-induced cutaneous SCC.

CHAPTER 2: Interleukin-6 Induces an Epithelial-Mesenchymal Transition Phenotype in Human Breast Cancer Cells

2.1 Introduction

Despite recent well-documented molecular and pathological evidence of epithelial-mesenchymal transition (EMT) phenotypes in human breast tumors (Cheng *et al.*, 2008; Heimann and Hellman, 2000; Moody *et al.*, 2005; Sarrio *et al.*, 2008), few tumor microenvironment-derived extracellular cues capable of provoking this transition have been identified. While EMT comprises a dynamic process critical to metazoan development (Yang and Weinberg, 2008), such phenotypes also promote carcinoma cell invasiveness (Thiery, 2002). In particular, impaired E-cadherin expression in human breast tumors correlates with enhanced invasiveness, metastatic potential (Oka *et al.*, 1993), and decreased breast cancer patient survival (Heimann and Hellman, 2000; Pedersen *et al.*, 2002). Moreover, human breast tumors exhibit increased interleukin-6 (IL-6) expression compared to matched healthy breast tissue, and these IL-6 levels increase with tumor grade (Chavey *et al.*, 2007). Elevated serum IL-6 has been demonstrated in breast cancer patients compared to normal donors (Jiang *et al.*, 2000; Kozlowski *et al.*, 2003) and correlates with advanced breast tumor stage (Kozlowski *et al.*, 2003), increased number of metastatic sites (Salgado *et al.*, 2003), and an overall poor prognosis (Bachelot *et al.*, 2003; Salgado *et al.*, 2003; Zhang and Adachi, 1999).

Normal polarized epithelial cells exhibit "cobblestone" homophilic morphology and express specific proteins including E-cadherin, cytokeratins, occludins, and claudins. However, carcinoma cells may develop a fibroblastoid morphology and a mesenchymal phenotype characterized by distinct proteins including Vimentin, N-cadherin, Fibronectin, and Alpha-smooth-muscle-actin (Thiery and Sleeman, 2006). Carcinomas, including breast carcinoma, often present with reduced expression of E-cadherin, a calcium-dependent intercellular adhesion molecule and dominant constituent of epithelial cell adherens junctions. Among other mechanisms, this can be a result of germline mutations, promoter hypermethylation, or aberrantly expressed repressive transcription factors such as Twist, Snail (SNAI1), Slug (SNAI2) (Yang and Weinberg, 2008).

The role of cytokines in cancer has been well-studied (Massague, 2008; Naugler and Karin, 2008), particularly in breast cancer (Chavey *et al.*, 2007; Nicolini *et al.*, 2006). Some cytokines have been shown to induce phenotypes consistent with EMT in transformed epithelial as well as carcinoma cell lines. For example, TGF-β1 and Interleukin-like EMT inducer (ILEI) have independently been shown to promote an EMT phenotype in mouse mammary epithelial cells (Thuault *et al.*, 2006; Waerner *et al.*, 2006). Interleukin-6 (IL-6) is a pleiotropic cytokine which participates in acute inflammation as the major inducer of C reactive protein, plays a central role in hematopoiesis (Kishimoto, 2006), and enhances proliferation of breast cancer cells (Sasser *et al.*, 2007b). IL-6 signaling utilizes a specific IL-6 receptor (IL-6R/CD126) as well as a promiscuous transmembrane signal transducer, gp130 (CD130), to initiate the Jak/STAT3 pathway.

To our knowledge, this is the first study to demonstrate the induction of an EMT phenotype in carcinoma cells exposed to IL-6. We utilized a three-dimensional (3D) culture assay and an orthotopic xenograft model to reveal that IL-6 effectively promoted an EMT phenotype in estrogen receptor-alpha (ERα) positive human breast cancer cells. Specifically, IL-6 exposure induced Vimentin, N-cadherin, Snail, and Twist and repressed E-cadherin. This phenotype was further characterized by enhanced invasiveness *in vitro* and increased tumor cell proliferative index, advanced histologic grade, and poor differentiation *in vivo*.

2.2 Results

2.2.1 IL-6 exposure represses E-cadherin protein expression. We and others have previously shown that ERα positive human breast cancer cells, including MCF-7, BT474, T47D, and ZR-75-1, do not express IL-6 (Sansone *et al.*, 2007; Sasser *et al.*, 2007b). E-cadherin protein levels were assessed following exposure to IL-6 within a 3D culture assay (Sasser *et al.*, 2007a; Sasser *et al.*, 2007b), which allowed us to physiologically model the dimensionality and stiffness of *in vivo* mammary tumor microenvironments (Paszek *et al.*, 2005). IL-6 exposure resulted in decreased E-cadherin in MCF-7 cells at 2, 4, 8, and 24-hour time points by western blot analysis (Figure 2.1A). Likewise, BT474, T47D, and ZR-75-1 cells showed almost complete abrogation of E-cadherin protein levels at 24 hours of IL-6 exposure (Figure 2.1B).

2.2.2 Autocrine IL-6 expression promotes an EMT phenotype. To characterize the extent to which IL-6 is capable of inducing an EMT phenotype, we evaluated MCF-7 cells that constitutively express ectopic IL-6 (MCF-$7^{IL\text{-}6}$). Quantitative real-time PCR

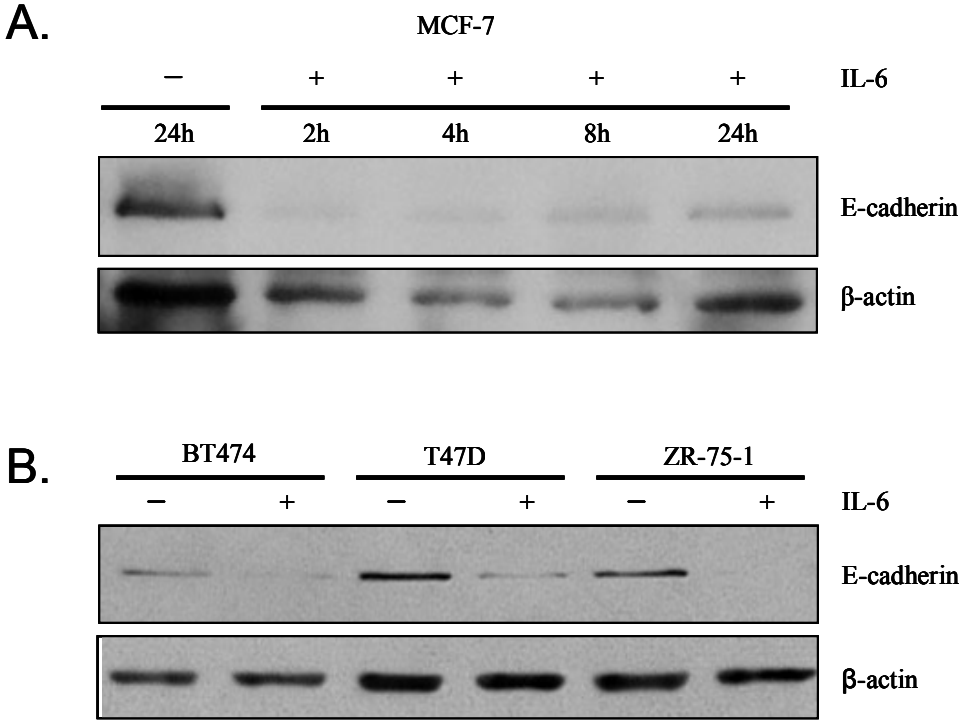

Figure 2.1 IL-6 induces E-cadherin protein repression. *A*, Western blot analysis of MCF-7 cells exposed to 50 ng/ml IL-6 in a 3D culture assay revealed a decrease in E-cadherin levels at 2, 4, 8, and 24-hours compared to untreated cells in the 3D assay. *B*, BT474, T47D, and ZR-75-1 cells were exposed to 50 ng/ml IL-6 for 24 hours in a 3D culture assay, and western blot analysis revealed almost complete abrogation of E-cadherin compared to untreated cells.

analysis demonstrated a gene expression pattern consistent with EMT including *E-cadherin* repression and concomitant induction of *Vimentin*, *N-cadherin*, *Snail*, and *Twist* in MCF-7^{IL-6} cells compared to control cells (Figure 2.2A). Western blot analysis of MCF-7^{IL-6} cells showed nearly complete abrogation of E-cadherin that coincided with induction of N-cadherin and Vimentin (Figure 2.2B). Immunofluorescence microscopy was utilized to compare immunostaining of E-cadherin and Vimentin in MCF-7 control versus MCF-7^{IL-6} cells. MCF-7 control cells showed typical epithelial homophilic adhesion, E-cadherin localization at cell-cell junctions, and lacked Vimentin expression. Meanwhile, MCF-7^{IL-6} cells lacked E-cadherin and expressed prominent cytoplasmic Vimentin intermediate filaments (Figure 2.2C).

2.2.3 IL-6 enhances invasiveness. EMT phenotypes are associated with enhanced tumor cell invasiveness. To determine whether IL-6 exposure functionally enhanced the invasive capacity of MCF-7 cells, an *in vitro* basement membrane extract (BME) invasion assay was utilized. MCF-7 control cells demonstrated minimal invasion through BME in the presence or absence of fetal bovine serum (FBS), which served as a chemoattractant. In contrast, MCF-7^{IL-6} cells were significantly (P-value < 0.05) more invasive in the presence or absence of FBS and attained over a 20-fold increase in directional invasiveness toward FBS compared to MCF-7 control cells (Figure 2.3).

2.2.4 Ectopic Twist expression stimulates IL-6 production and STAT3 activation. Constitutive expression of Twist in MCF-7 cells (MCF-7^{Twist}) has been shown to induce a morphology and phenotype consistent with EMT (Mironchik *et al.*, 2005) analogous to those currently noted for MCF-7^{IL-6} cells. Accordingly, we examined cellular supernatants from MCF-7 vector control cells (MCF-7^{vector}) and MCF-7^{Twist} cells for

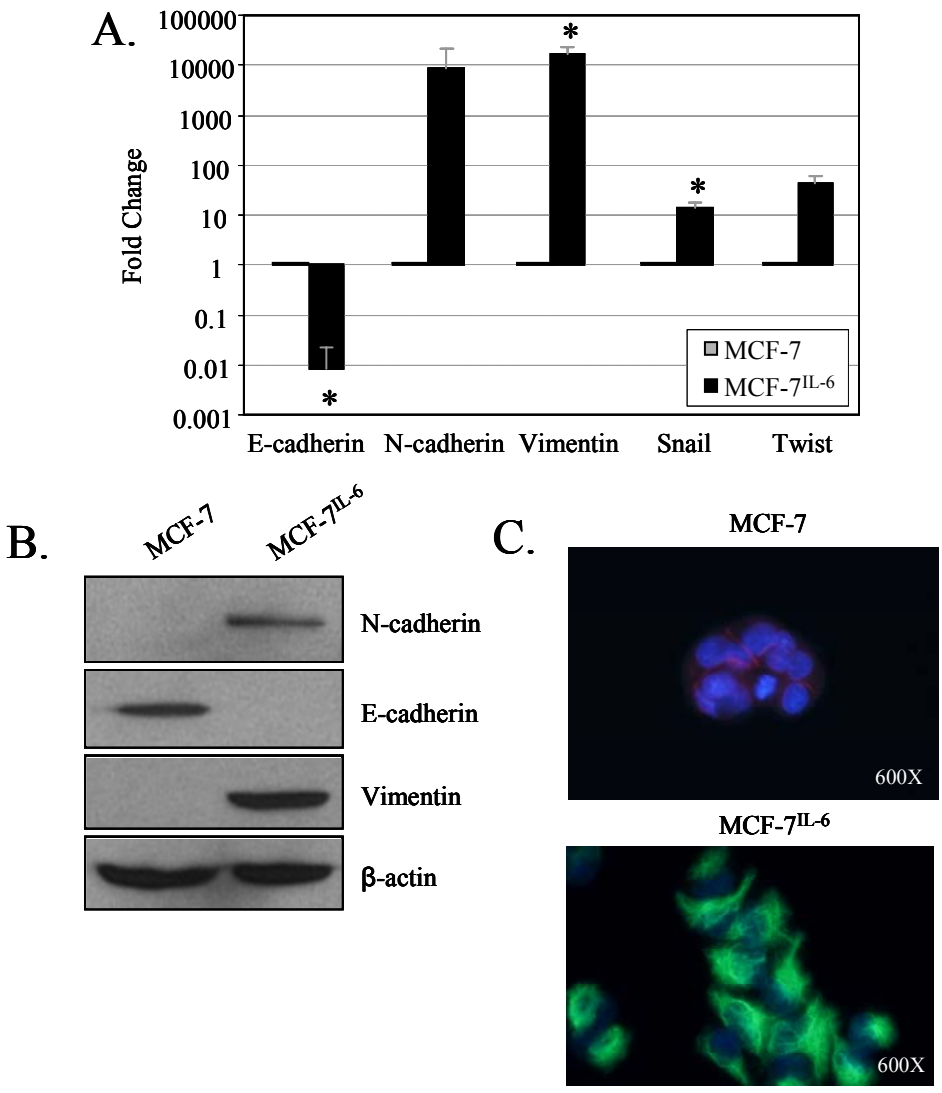

Figure 2.2 Constitutive IL-6 expression promotes a gene expression pattern and phenotype consistent with EMT. *A*, Real-time quantitative PCR analysis of MCF-$7^{IL\text{-}6}$ cells demonstrated a robust decrease in *E-cadherin* (**P*-value = 0.00003) gene expression and concomitant increase in *N-cadherin*, *Vimentin* (**P*-value < 0.05), *Snail* (**P*-value < 0.05), and *Twist*. Real-time PCR data are shown normalized to *GAPDH* expression and on a logarithmic scale. *B*, Western blot analysis of MCF-$7^{IL\text{-}6}$ cells revealed the induction of N-cadherin and Vimentin and abrogation of E-cadherin. *C*, Immunofluorescent staining of MCF-7 control cells demonstrated normal immunopositive E-cadherin (red; Alexa Fluor 594) localization and no detectable Vimentin (green; Alexa Fluor 488). Conversely, MCF-$7^{IL\text{-}6}$ cells exhibited no detectable E-cadherin and strong immunopositive staining for Vimentin. DAPI nuclear stain is shown in blue.

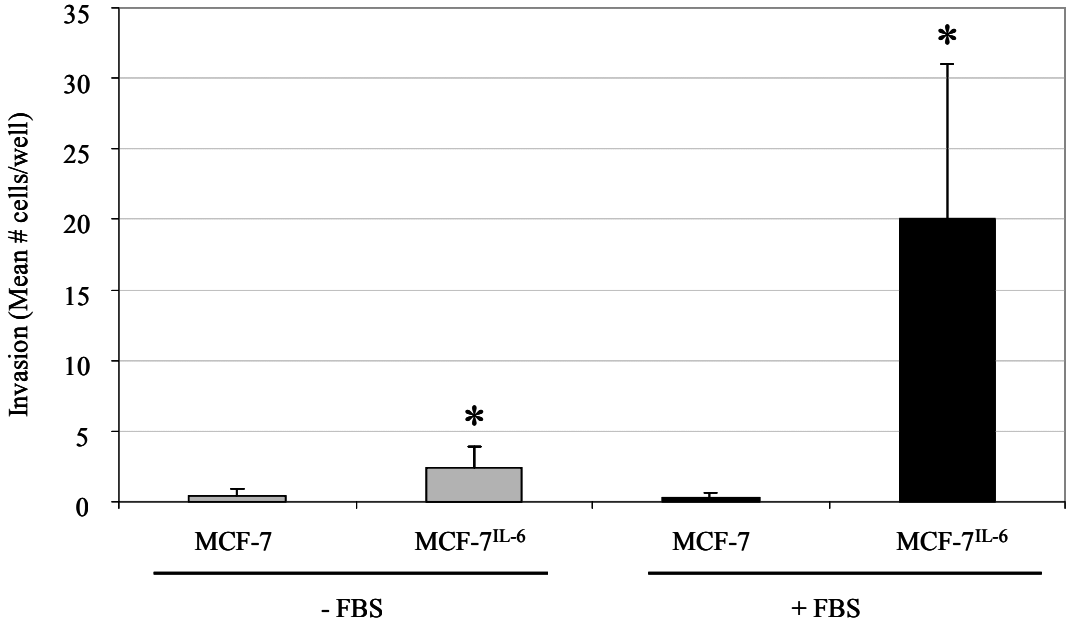

Figure 2.3 IL-6 expression enhances invasiveness *in vitro*. MCF-7 control cells showed minimal invasion through BME both with (black bars) and without (gray bars) the addition of FBS as a chemoattractant. In contrast, MCF-7^{IL-6} cells demonstrated significantly (**P*-value < 0.05) increased invasiveness, particularly with FBS supplementation.

production of soluble IL-6 by enzyme-linked immunosorbent assay. While MCF-7^{vector} cells produced an undetectable concentration of IL-6 as expected (Sansone *et al.*, 2007; Sasser *et al.*, 2007b), MCF-7^{Twist} cells produced more than 350 pg/ml of IL-6 (Figure 2.4A). We therefore examined the baseline level of phospho-STAT3^{Y705} in MCF-7^{vector} and MCF-7^{Twist} cells, and only the MCF-7^{Twist} cells displayed aberrantly activated STAT3 (Figure 2.4B). To determine if STAT3 was required for the EMT phenotypes in human breast cancer cells, we inhibited STAT3 activation in MCF7^{IL-6} and MCF-7^{Twist} cells with JSI-124, a highly selective small molecular inhibitor of the Jak/STAT3 signaling pathway (Blaskovich *et al.*, 2003). STAT3 inhibition induced rapid cell death in our cell lines (data not shown), which was corroborated by similar reports in other carcinoma cells (Barton *et al.*, 2004; Gritsko *et al.*, 2006; Lin *et al.*, 2005).

2.2.5 Constitutive IL-6 expression maintains an EMT phenotype and promotes cell proliferation in an orthotopic xenograft model of breast cancer. Tumor sections from all orthotopic xenograft tumors (n=12 xenografts per cell line) were blindly evaluated and graded by a trained pathologist. Microscopic evaluation of a representative section of MCF-7 control tumor revealed rare tubule formation (<10% of the tumor, 3 points), high nuclear grade (3 points) and mitotic activity averaging 2 mitotic figures per hpf, including abnormal forms (1 point). The histologic grade of this tumor was 2 (moderately differentiated) based on an overall score of 7. Individual tumor cell necrosis comprising less than 10% of the tumor was also noted. The tumor cells were strongly immunopositive for membranous E-cadherin and immunonegative for Vimentin. Patchy intracytoplasmic mucin positivity comprised less than 10% of the tumor and was mostly

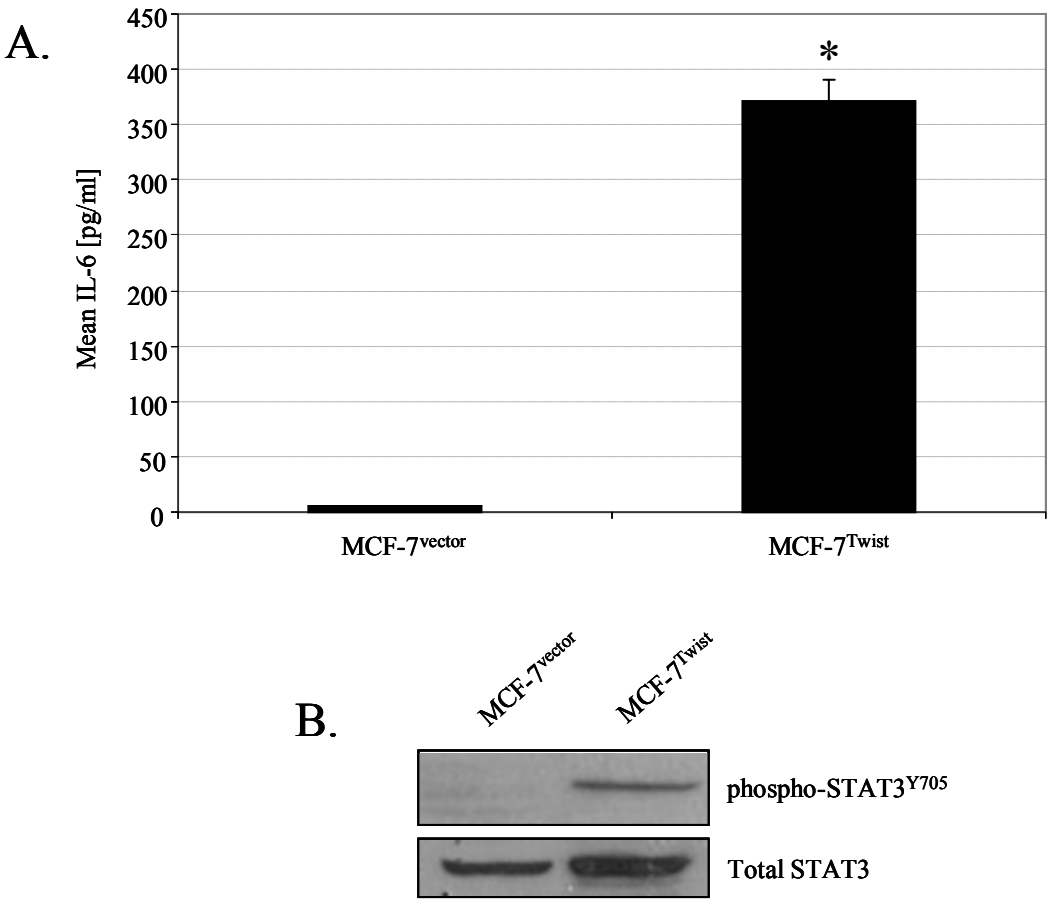

Figure 2.4 Ectopic Twist expression stimulates secretion of IL-6 and constitutive STAT3 activation. *A*, 48-hour cellular supernatants were assessed by enzyme-linked immunosorbent assay and demonstrated no detectable soluble IL-6 production in MCF-7^{vector} cells compared to greater than 350 pg/ml IL-6 in MCF-7^{Twist} cells (**P*-value = 0.01). *B*, MCF-7^{Twist} cells expressed elevated phosphorylated STAT3Y705 (phospho-STAT3Y705) as shown by western blot analysis.

associated with tubule formation. These results can also be seen in association with moderately differentiated tumors.

Microscopic evaluation of a representative section of MCF-7^{IL-6} tumor revealed no tubule formation (3 points), high nuclear grade (3 points) and mitotic activity averaging 8 mitotic figures per hpf, including abnormal forms (2 points). The histologic grade of this tumor is 3 (poorly differentiated), based on an overall score of 8. The presence of 10-20% geographic areas of tumor necrosis was noted. E-cadherin was immunonegative and cytoplasmic immunopositivity for Vimentin was diffuse and strong in the tumor cells. Also noted was the absence of intracytoplasmic mucin. These results can also be seen in association with poorly differentiated tumors.

In agreement with our *in vitro* data, MCF-7 control tumors expressed membranous E-cadherin whereas MCF-7^{IL-6} tumors did not. Vimentin expression was immunonegative in MCF-7 control tumors, but MCF-7^{IL-6} tumors demonstrated robust Vimentin protein expression. Importantly, the human IL-6 receptor does not recognize murine IL-6 (van Dam *et al.*, 1993), and consequently, E-cadherin repression and Vimentin induction are only evident in MCF-7^{IL-6} tumors, as these tumors expressed human IL-6. Consistent with our previously published report of enhanced MCF-7^{IL-6} tumor engraftment and size compared to MCF-7 control tumors (Sasser *et al.*, 2007b), MCF-7^{IL-6} tumors showed more mitotic figures than MCF-7 control tumors by H&E, suggestive of a higher proliferation rate (Figure 2.5)

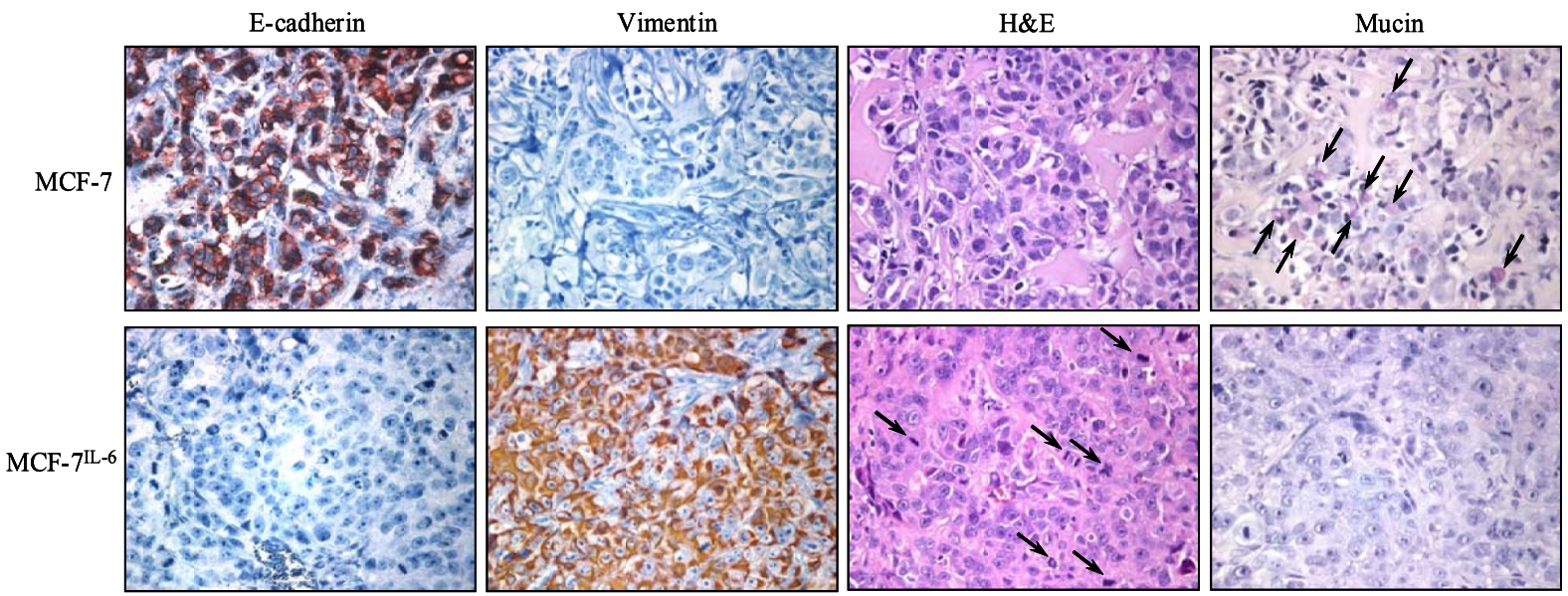

Figure 2.5 Autocrine IL-6 production maintains an EMT phenotype in orthotopic xenograft tumors. $2x10^6$ BME-embedded cancer cells were orthotopically injected into the fifth and tenth mammary fat pad of 6 mice per group (n=12 xenografts per cell line), and tumors were resected at 6 weeks. Tumors shown are representative of all stained tumor sections in that group. E-cadherin expression was immunopositive and localized at intercellular junctions in MCF-7 control tumors and immunonegative in MCF-7^{IL-6} tumors. Vimentin expression was immunonegative in MCF-7 control tumors and highly immunopositive in MCF-7^{IL-6} tumors. H&E staining showed increased mitotic figures (arrows) in MCF-7^{IL-6} tumors compared to MCF-7 control tumors. Mucicarmine staining revealed focal expression of mucin in MCF-7 control tumors (arrows), suggestive of better differentiated MCF-7 cells within these xenografts. MCF-7^{IL-6} tumors lacked mucin, suggestive of poorly differentiated MCF-7 cells within these xenografts.

2.3 Discussion

Collectively, these data demonstrate that IL-6 promotes an EMT phenotype in human breast cancer cells. In particular, we showed IL-6-dependent E-cadherin repression in four ERα positive human breast cancer cell lines (Figure 2.1). Likewise, constitutive IL-6 expression induced a gene expression pattern (Figure 2.2A) and EMT phenotype (Figures 2.2B and 2.2C) in MCF-$7^{IL\text{-}6}$ cells. As a functional consequence of IL-6 signaling, MCF-$7^{IL\text{-}6}$ cells displayed significantly increased invasiveness when compared to MCF-7 control cells (P-value < 0.05) (Figure 2.3). We also showed that ectopic Twist expression in MCF-7 cells induced aberrant IL-6 production (Figure 2.4A) and constitutive STAT3 activation (Figure 2.4B). Finally, MCF-$7^{IL\text{-}6}$ xenograft tumors exhibited a phenotype consistent with EMT and associated with poor clinical prognosis in breast cancer which included loss of E-cadherin, Vimentin induction, high mitotic activity, advanced histologic grade, and poor differentiation (Figure 2.5).

Although IL-6 is elevated in human breast tumors as well as breast cancer patient sera and associated with a poor prognosis in breast cancer, the source of this IL-6 remains poorly defined. Primary human breast tumor cells (Sansone *et al.*, 2007) and human breast cancer cell lines (Sasser *et al.*, 2007b) are capable of producing autocrine IL-6, suggesting carcinoma cells as one source of aberrantly increased tumor and serum IL-6. We now demonstrate that upon aberrant IL-6 overexpression, human breast carcinoma cells acquire a more aggressive phenotype. We have also recently shown that primary breast fibroblasts and fibroblasts isolated from common sites of breast cancer metastasis produce IL-6 (Studebaker *et al.*, 2008), which demonstrates one potential mechanism of paracrine IL-6 signaling in human breast cancer. Whether IL-6 signaling in the tumor

microenvironment is autocrine-mediated from carcinoma cells or paracrine-mediated from stromal cells such as fibroblasts, activated immune cells, or endothelial cells, we have previously shown that sustained IL-6 signaling constitutively activates STAT3 in human breast cancer cells (Sasser *et al.*, 2007b). A recent study found that STAT3 has the capacity to transactivate *Twist* gene expression (Cheng *et al.*, 2008) and therefore, our current findings suggest that STAT3 may serve as a molecular mediator between IL-6, Twist, and ultimate activation of an EMT phenotype in human breast cancer. Furthermore, MCF-7^{Twist} cells aberrantly expressed IL-6 and active STAT3, suggesting evidence of a vicious cycle whereby IL-6 signals through STAT3 to transactivate Twist and subsequently promote autocrine-mediated IL-6 signaling events.

Stromal fibroblasts represent a major cell type within the tumor microenvironment, and soluble factors from mammary carcinoma-associated fibroblasts were shown to induce an EMT phenotype in PMC42-LA human breast carcinoma cells. The authors could not reproduce the phenotype with recombinant proteins known to be present in fibroblast conditioned medium including IGF-I, IGF-II, TNF-α, VEGF, and TGF-β (Lebret *et al.*, 2007). However, IL-6, a factor produced by human breast fibroblasts (Singh *et al.*, 1999), was not tested. In another relevant study, Karnoub *et al*. found that bone marrow-derived human mesenchymal stem cells, a predominant population of bone marrow stromal fibroblasts that produces IL-6 (Sasser *et al.*, 2007b), enhanced breast cancer metastasis (Karnoub *et al.*, 2007). Our findings suggest that IL-6 may be involved in fibroblast-mediated EMT phenotypes and enhanced metastasis in breast cancer.

The IL-6 signaling network has been targeted with several therapeutic antagonists in various human cancer preclinical and clinical trials, but this strategy has yet to be employed for breast cancer. We have demonstrated an IL-6-mediated EMT phenotype in breast cancer cells which is clinically associated with unfavorable outcome in numerous types of human carcinomas. These data support a potential link between poor breast cancer patient survival associated with high serum IL-6 (Bachelot *et al.*, 2003; Jiang *et al.*, 2000; Kozlowski *et al.*, 2003; Salgado *et al.*, 2003; Zhang and Adachi, 1999) and impaired tumor E-cadherin expression (Heimann and Hellman, 2000; Oka *et al.*, 1993; Pedersen *et al.*, 2002). Although further studies are needed to fully define the role of IL-6 in breast cancer progression and eventual metastasis, our findings strengthen the rationale for evaluation of anti-IL-6 therapies in breast cancer.

2.4 Materials and Methods

2.4.1 Breast cancer cell lines. ERα positive human breast cancer cell lines MCF-7, BT474, T47D, and ZR-75-1 were purchased from the American Type Culture Collection (ATCC, Manassas, VA)**.** MCF-7$^{IL\text{-}6}$ cells were kindly provided by Dr. Mercedes Rincón (University of Vermont, Burlington, VT) (Conze *et al.*, 2001), and MCF-7^{vector} and MCF-7^{Twist} cells were previously published by Dr. Venu Raman (Mironchik *et al.*, 2005). All cell lines were maintained in humidified incubators at 37^{o}C and 5% CO_2 and cultured in RPMI-1640 medium (Invitrogen, Carlsbad, CA) containing 5% characterized FBS (HyClone, Logan, UT), 2mM L-glutamine, 10 units/ml penicillin, and 10 μg/ml streptomycin, hereafter termed complete medium.

2.4.2 Real-time quantitative PCR. Total cellular RNA was isolated using a PureLink™ Micro-to-Midi Total RNA Purification System (Invitrogen), and cDNA was synthesized using a RT^2 First Strand Kit (SABiosciences, Frederick, MD). Real-time PCR was performed using RT^2 Real-Time™ SYBR Green/ROX PCR Master Mix (SABiosciences) on an ABI Prism® 7000 Sequence Detection System (Applied Biosystems, Foster City, CA). Data are shown normalized to *GAPDH* expression and averaged between three repeated experiments. Primer sequences were as follows. *E-cadherin*, forward: 5′-CCCACCACGTACAAGGGTC-3′, reverse: 5′-CTGGGGTATTGGGGGCATC-3′; *N-cadherin*, forward: 5′-CAACTTGCCAGAAAACTCCAGG-3′, reverse: 5′-ATGAAACCGGGCTATCTGCTC 3′; *Vimentin*, forward: 5′ CGCCAGATGCGTGAAATGG 3′, reverse: 5′ ACCAGAGGGAGTGAATCCAGA 3′; *Snail*, forward: 5′ AATCGGAAGCCTAACTACAGCG 3′, reverse: 5′ GTCCCAGATGAGCATTGGCA 3′; *Twist*, forward: 5′ GTCCGCAGTCTTACGAGGAG 3′, reverse: 5′ GCTTGAGGGTCTGAATCTTGCT 3′; *GAPDH*, forward: 5′ GATGCTGGCGCTGAGTACG 3′, reverse: 5′ GCTAAGCAGTTGGTGGTGC 3′.

2.4.3 Western blot analysis. Whole cell lysates were harvested and western blot analysis was performed as previously described (Sasser *et al.*, 2007b). Primary antibodies included rabbit anti-N-cadherin 1:1000 (Santa Cruz Biotechnology, Santa Cruz, CA), rabbit anti-E-cadherin 1:1000 (Cell Signaling, Danvers, MA), mouse anti-Vimentin 1:500 (Clone V9, Dako, Denmark), rabbit anti-phospho-$STAT3^{Y705}$ 1:1000 (Cell Signaling), rabbit anti-STAT3 1:1000 (Cell Signaling) and mouse anti-β-actin 1:10,000 (Clone AC-15, Sigma, St. Louis, MO). Secondary antibodies included goat

anti-rabbit IgG-HRP 1:1000 (Santa Cruz Biotechnology) and sheep anti-mouse IgG-HRP 1:1000 (GE Healthcare, Chalfont St. Giles, United Kingdom). All antibodies were diluted with 5% milk in PBS containing 0.1% Tween-20 (PBS-T) and incubated for either 1 hour at room temperature or overnight at 4°C. All western blots were visualized with ECL western blotting substrate (Pierce, Rockford, IL).

2.4.4 Immunofluorescence. 1.5 x 10^5 cells per chamber were plated into Lab-Tek™ two-chamber slides (Nunc; Thermo Fisher Scientific, Rochester, NY) overnight. The next day, cells were 50-70% confluent, washed one time with PBS, and fixed and permeabilized in cold 100% methanol at -20°C for 20 minutes. Chambers were given three five-minute washes in 0.1% Tween-20/PBS (PBS-T) and were then incubated in 3% BSA/0.1% Tween-20/PBS blocking buffer for one hour at room temperature. Following one PBST wash, chambers were incubated with primary antibodies: rabbit anti-E-cadherin 1:200 (Santa Cruz Biotechnology) and mouse anti-Vimentin 1:200 (Dako) in blocking buffer for two hours at room temperature. Chambers were given three five-minute PBST washes and were then incubated with secondary antibodies: donkey anti-rabbit-Alexa Fluor 594 1:1,000 (Molecular Probes; Invitrogen) and goat anti-mouse-Alexa Fluor 488 1:1,000 (Molecular Probes; Invitrogen) in blocking buffer for one hour at room temperature in the dark. Secondary antibody alone was used as a negative immunofluorescent control. Following three five-minute PBST washes, chambers were incubated with 0.25 μg/ml DAPI (Molecular Probes; Invitrogen) for one minute at room temperature in the dark. Chambers were given three five-minute PBST washes, plastic chamber inserts were removed, and slides were coverslipped with ProLong® Gold antifade reagent (Molecular Probes; Invitrogen). Slides were evaluated

with a Nikon Eclipse E400 microscope, and images were taken with a Nikon DXM1200 digital camera using Nikon Act-1 version 2.63 imaging software. Merged images were created with SPOT Advanced version 4.0.9 imaging software (Diagnostic Instruments, Sterling Heights, MI).

2.4.5 Invasion assay. BD Falcon™ FluoroBlok™ Cell Culture Inserts for 24-well plates (BD Biosciences, San Jose, CA) were pre-coated with 3 mg/ml Matrigel™ basement membrane extract (BME) (BD Biosciences) diluted in phenol red-free RPMI-1640 medium (Invitrogen) containing 2 mM GlutaMax™ (Invitrogen), hereafter termed serum-free medium. Breast cancer cells were labeled with 1 μM carboxyfluorescein diacetate succinimidyl ester (CFDA-SE) (Invitrogen) and then plated in complete medium overnight. The following day, adherent cells were trypsinized, and 100,000 cells per well were added to a BME-coated 24-well invasion assay plate. Fluorescent cells that had invaded through the BME layer to the underside of the insert were counted at 20 hours. Assay was repeated to confirm.

2.4.6 3D culture assay. Cultrex® basement membrane extract (BME) (Trevigen, Gaithersburg, MD) was diluted in serum-free medium and plated at a concentration of 6 mg/ml per well into a 24-well plate and allowed to solidify for a minimum of 1 hour at 37˚C. All cells were harvested with CellStripper™ non-enzymatic cell dissociation solution (Mediatech, Manassas, VA) according to the manufacturer's protocol to prevent trypsin-mediated E-cadherin cleavage between standard 2D culture and 3D assays. For 24-hour 3D studies, 250,000 cells embedded in 3 mg/ml BME with or without 50 ng/ml recombinant human IL-6 (Peprotech) were plated per well. Cells were harvested at each time point by dilution with serum-free medium, centrifugation out of BME suspension,

and lysed with SDS lysis buffer (62.5 mM Tris-HCl, 2% w/v SDS, 10% glycerol, 50nM DTT, 0.01% w/v bromophenol blue). For 2-week MCF-7 3D studies, 150,000 cells were plated per well and harvested as described for 24-hour 3D studies with one exception. At day 7, a sample of IL-6-treated cells was harvested from BME and expanded in the absence of IL-6 for another 7 days of 3D culture. Western blot analysis was performed as described above.

2.4.7 Quantification of soluble IL-6 protein. 750,000 cells were plated into a 6-well plate and allowed to adhere overnight. The next day, cells were washed once with PBS and 1 ml complete medium was gently added. Cells were allowed to grow for 48 hours, at which time cellular supernatants were harvested and 0.2 μm filtered. Supernatants were assayed for soluble IL-6 protein using the Human IL-6 DuoSet® ELISA Development Kit (R&D Systems, Minneapolis, MN) according to the manufacturer's protocol. Data are shown averaged between two repeated experiments.

2.4.8 Xenografts, histopathology, and immunohistochemistry. Immunocompromised athymic nude (nu/nu) female mice were purchased at 3-4 weeks of age (The Jackson Laboratory, Bar Harbor, ME). $2x10^6$ MCF-7 control or MCF-7^{IL-6} cells suspended in 6 mg/ml Cutlrex® BME (Trevigen) were orthotopically injected into the fifth and tenth mammary fat pad of 6 mice per group (n = 12 xenografts per cell line). Tumors were resected at 6 weeks, formalin-fixed, and paraffin-embedded using standard methods.

Xenograft tissue sections of MCF-7 control and MCF-7^{IL-6} tumors were blindly evaluated microscopically for proliferative indices and degree of differentiation using H&E and mucicarmine stained sections, respectively. E-cadherin and Vimentin protein expression was also evaluated by IHC. The H&E stained tumors were graded using the

Nottingham combined histologic grading system (Elston-Ellis modification of the Scarff-Bloom-Richardson grading system) for invasive breast cancers which includes evaluation of morphologic features, such as tubule formation, nuclear pleomorphism and mitotic count (Elston and Ellis, 1991). Mitotic counts were averaged upon evaluation of 5 separate high power fields (hpf).

Thin 5 μm tissue sections from the surface of tissue blocks were mounted onto glass slides, stained with H&E, and coverslipped in the usual manner. A second set of thin tissue sections were mounted onto glass slides, stained with mucicarmine using the standard method, and coverslipped in the usual manner. Immunoperoxidase staining was performed on a third set of thin tissue sections, placed onto charged slides, and deparaffinized. Slides were then immersed in Antigen Retrieval Citra Solution (BioGenex, San Ramon, CA) in a pressure cooker at 120˚C, blocked in Power Block™ Universal Blocking Reagent (BioGenex) for 10 minutes at room temperature, and washed one time with PBS. Primary antibodies were diluted in Power Block™ reagent. Slides were incubated with rabbit anti-E-cadherin 1:50 (Cell Signaling) or mouse anti-Vimentin 1:200 (Clone V9, Dako) primary antibody overnight at 4˚C and subsequently washed three times with Super Sensitive™ Wash Buffer (BioGenex). Slides were then incubated with 1X Universal Link biotinylated goat anti-mouse and rabbit IgG secondary antibody (Biocare Medical, Concord, CA) for 10 minutes at room temperature, washed three times with wash buffer, and incubated with streptavadin-HRP (Biocare Medical) in the dark for 30 minutes at room temperature. Following three wash buffer washes, AEC substrate chromogen (Dako) was added, and the IHC sections were coverslipped in the usual manner. All experiments involving animals were conducted in accordance with The

Research Institute at Nationwide Children's Hospital Institutional Animal Care and Usage Committee (IACUC).

2.4.9 Statistical Analysis. Student's t-test was performed to determine statistically significant differences between groups, and a *P*-value < 0.05 was considered significant.

CHAPTER 3: E-cadherin Suppresses Breast Cancer Cell Growth and IL-6 Production

3.1 Introduction

E-cadherin is critical to epithelial cell adhesion and subsequent polarity and phenotype, whereas its dysfunction promotes breast carcinoma aggressiveness. Impaired E-cadherin expression correlates with decreased breast cancer patient survival (Heimann and Hellman, 2000; Pedersen *et al.*, 2002), and it serves as one of the strongest independent prognostic biomarkers for breast cancer. Although rare, germline mutations in the E-cadherin gene (*CDH1*) are major risk factors for hereditary diffuse gastric cancer (HDGC) and predispose HDGC patients to invasive lobular breast carcinoma (Ripperger *et al.*, 2009). Normal epithelial cells express E-cadherin, a well-characterized member of the cadherin family of tissue-specific calcium-dependent homophilic intercellular adhesion molecules. β-catenin, a potent transcription factor, binds to E-cadherin at an intracellular binding domain and subsequently binds alpha (α)-catenin. Ligated α-catenin then binds F-actin, thereby linking E-cadherin to the cytoskeleton. This E-cadherin-catenin-actin complex localizes to adherens junctions, which form between adjacent cells to preserve epithelial cell homeostasis (Hartsock and Nelson, 2008).

Estrogen receptor-alpha (ERα), another prognostic biomarker utilized to classify breast cancer patients, is expressed in luminal subtype breast tumors (Perou *et al.*, 2000) and therefore associated with improved patient survival (Buyse *et al.*, 2006; Sorlie *et al.*,

2001) (Sorlie *et al.*, 2001) (Buyse *et al.*, 2006). Estrogen-dependent signaling through ERα maintains E-cadherin expression through indirect transactivation of metastatic tumor antigen 3 (MTA3), which subsequently inhibits Snail, a potent E-cadherin repressor (Fujita *et al.*, 2003). Furthermore, we just showed that interleukin-6 (IL-6) induces E-cadherin repression in ERα-positive breast cancer cells (Chapter 2). IL-6 expression is NF-κB-dependent (Chauhan *et al.*, 1996) and negatively regulated by ERα, whereby direct ERα-NF-κB interactions prohibit NF-κB transactivation of IL-6 (Galien and Garcia, 1997).

Intercellular contact inhibition of proliferation remains a poorly understood phenomenon, but E-cadherin has been implicated as a putative mediator of epithelial cell growth. Utilizing microbeads with chimeric fusion proteins of the E-cadherin extracellular domain and an IgG Fc domain, E-cadherin homophilic ligation was demonstrated to significantly reduce E-cadherin-positive carcinoma cell proliferation (*P*-value < 0.05) (Perrais *et al.*, 2007). Alternatively, E-cadherin sequesters β-catenin at the cell surface as one means to inhibit its nuclear translocation and consequent transactivation of β-catenin responsive genes (Perez-Moreno *et al.*, 2003). Direct β-catenin target genes include major proliferative oncogenes such as c-Myc and cyclin D1 (Dihlmann and von Knebel Doeberitz, 2005). Work by Gottardi, *et al*. further demonstrated cell growth inhibition upon ectopic expression of full-length E-cadherin in a colorectal tumor cell line. However, ectopic expression of E-cadherin which lacks an intracellular β-catenin binding activity did not inhibit colorectal tumor cell growth, suggesting that the β-catenin binding domain is necessary for E-cadherin-mediated growth suppression by retaining β-catenin at the plasma membrane (Gottardi *et al.*,

2001). Likewise, extracellular cleavage of E-cadherin has been shown to maintain growth suppressive properties of E-cadherin (Sasaki *et al.*, 2000).

In the present study we evaluated the effects of E-cadherin expression levels on breast cancer cell growth rates in a 3-dimensional (3D) tumor growth assay (TGA). In particular, we showed that IL-6 enhanced human ERα-positive breast cancer cell growth and concomitantly induced E-cadherin protein repression in a dose-dependent manner. Furthermore, primary human mesenchymal stem cells (MSC) enhanced breast cancer cell growth and reduced E-cadherin protein expression. Although we unexpectedly demonstrated that estrogen had no effect on breast cancer cell growth, estrogen did slightly up-regulate E-cadherin protein levels as expected. MCF-7 cells which express Twist (MCF-7^{Twist}) and therefore lack E-cadherin exhibited no growth enhancement upon IL-6 or MSC exposure. Finally, we stably expressed ectopic full-length E-cadherin or E-cadherin which lacked β-catenin binding activity in MDA-MB-231 cells and showed inhibition of soluble IL-6 expression and decreased cell growth.

3.2 Results

3.2.1 IL-6 enhances the growth of ERα-positive breast cancer cells in a dose-dependent manner. ERα positive human breast cancer cells, including MCF-7 and BT474, do not express IL-6 (Sansone *et al.*, 2007; Sasser *et al.*, 2007b). Therefore, we assessed the effects of IL-6 on MCF-7 and BT474 cells in a 3-dimensional (3D) tumor growth assay (TGA) (Sasser *et al.*, 2007a) to model the dimensionality and stiffness of the mammary gland microenvironment (Paszek *et al.*, 2005). As expected from our previous findings (Sasser *et al.*, 2007b), IL-6 increased the growth rates of both

BT474^{VSVgR2} (Figure 3.1A) MCF-7^{VSVgR2} cells (Figure 3.1B), but we further demonstrated a dose-dependent growth enhancement.

3.2.2 IL-6 down-regulates E-cadherin protein expression in a dose-dependent manner. We have previously revealed that IL-6 represses E-cadherin in breast cancer cells (Chapter 2) and thus, hypothesized that IL-6-induced E-cadherin repression may promote breast cancer cell growth. To test this, we assessed E-cadherin protein levels on day eight of a 3D TGA by western blot analysis. In accordance with a dose-dependent increase in cell growth upon IL-6 treatment (Figure 3.1), increasing IL-6 concentration induced concomitant decreased E-cadherin expression in BT474^{VSVgR2} (Figure 3.2A) and MCF-7^{VSVgR2} (Figure 3.2B) cells.

3.2.3 E-cadherin protein levels are associated with cell growth rates. To further characterize the association between E-cadherin status and cell growth, we compared E-cadherin expression in MCF-7^{VSVgR2} cells on TGA day one and day eight. As expected based on our IL-6 dose response experiments, IL-6 exposure decreased E-cadherin expression in a dose-dependent manner and was associated with increased growth rates in MCF-7^{VSVgR2} cells. As expected (Fujita *et al.*, 2003), estrogen treatment slightly up-regulated E-cadherin expression, but the combination of estrogen and increasing doses of IL-6 showed a marked decrease in E-cadherin (Figure 3.3A). Furthermore, cells cultured with MSC exhibited the most robust reduction in E-cadherin as well as the largest cell growth enhancement (Figure 3.3B).

3.2.4 Cells which lack E-cadherin do not demonstrate IL-6 or MSC-induced growth. To investigate the growth effects of IL-6 and MSC on E-cadherin-negative breast cancer

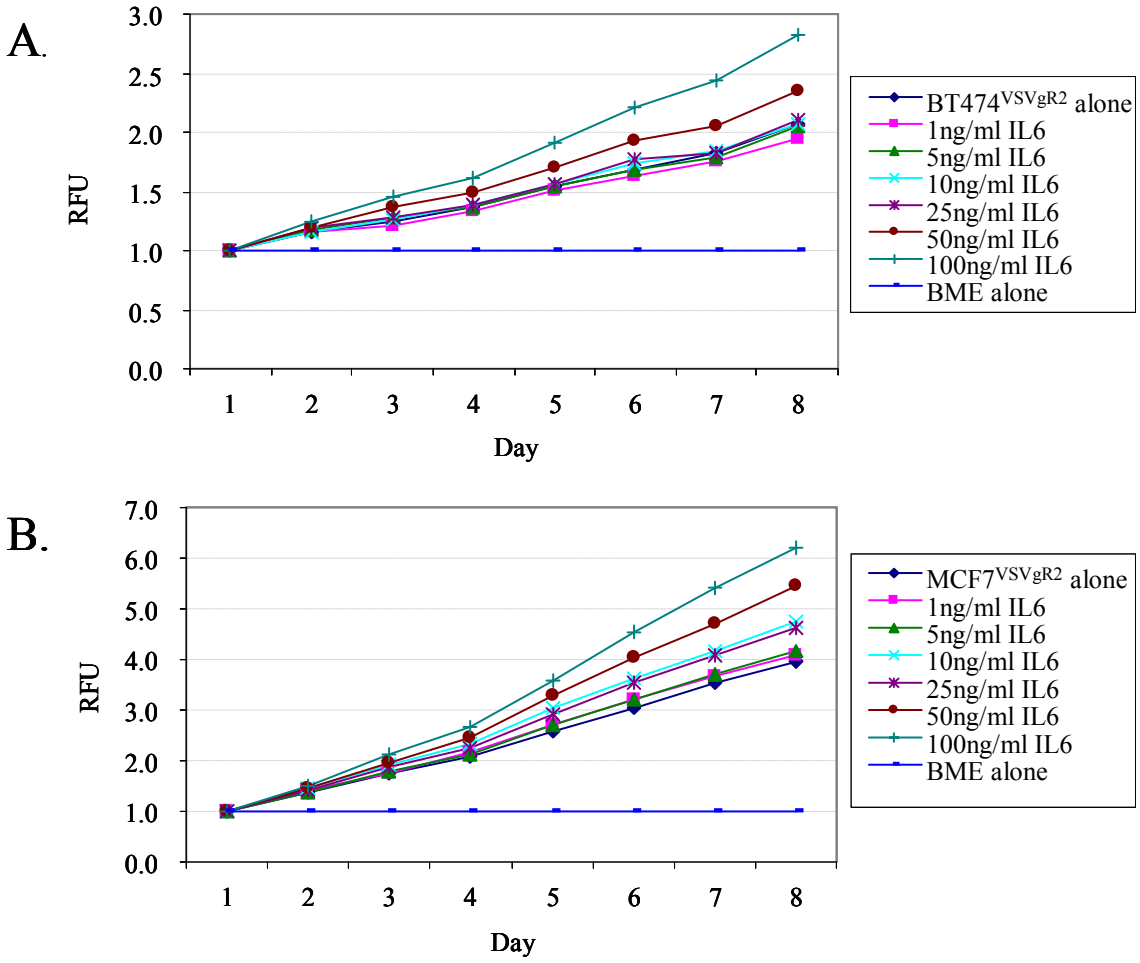

Figure 3.1 IL-6 dose-dependent growth rate enhancement in ERα-positive breast cancer cells. *A*, BT474^{VSVgR2} cells grown in a 3D TGA demonstrated increased growth with increasing doses of recombinant human IL-6. *B*, Similar yet more robust cell growth was demonstrated in MCF-7^{VSVgR2} cells exposed to increasing doses of IL-6 in a 3D TGA. Data are shown relative to day 1 and daily BME alone background fluorescence. RFU, relative flurorescence units.

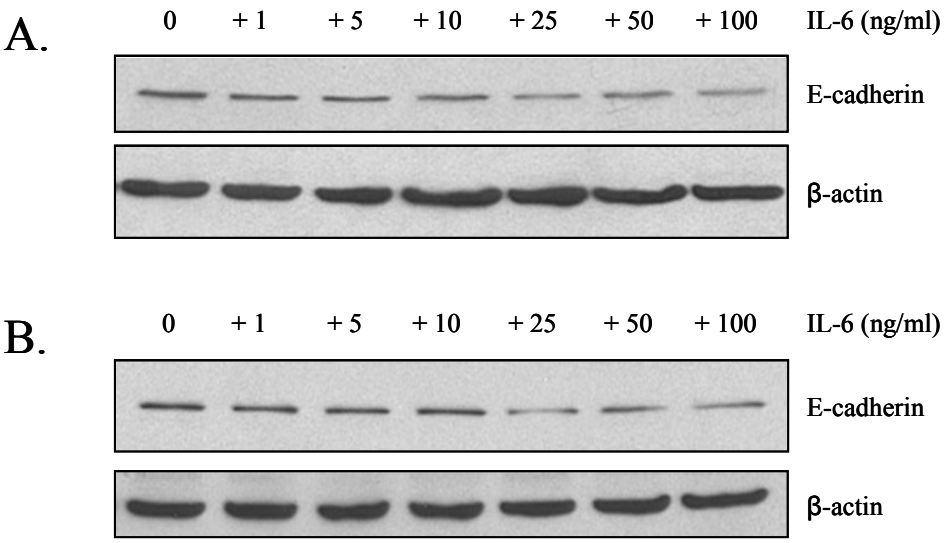

Figure 3.2 Increasing IL-6 dose correlates with increased E-cadherin protein repression. *A*, Western blot analysis of E-cadherin expression in BT474^{VSVgR2} cells grown in a 3D TGA. At day 8, E-cadherin protein is increasingly diminished following exposure to increasing doses of IL-6. *B*, Western blot analysis of E-cadherin expression in MCF-7^{VSVgR2} cells grown in a 3D TGA. At day 8, a similar pattern of IL-6-inducible E-cadherin repression was evident.

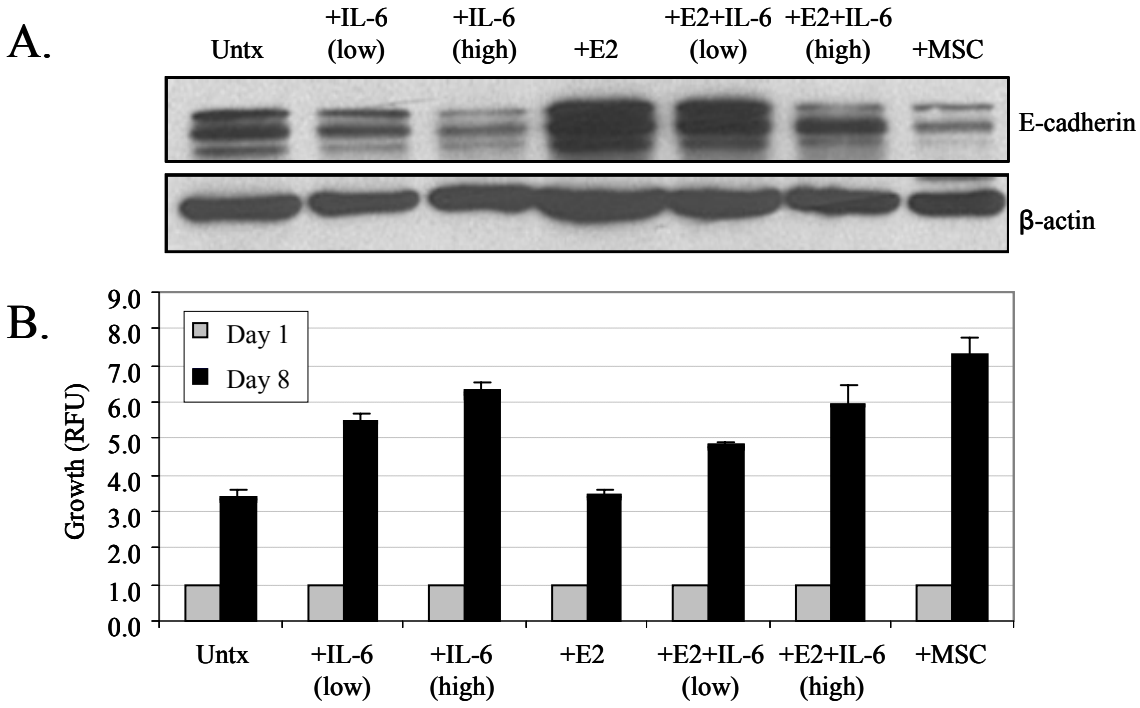

Figure 3.3 E-cadherin expression level is associated with cell growth. *A*, Western blot analysis of E-cadherin expression in MCF-7^{VSVgR2} cells at day 8 of a 3D TGA. Cells alone (Untx) expressed E-cadherin as expected, and E-cadherin levels decreased with low (10 ng/ml) and high (100 ng/ml) IL-6 treatment. 10 nM estrogen (E2) alone up-regulated E-cadherin as expected, but when combined with low and high IL-6, E2-induced E-cadherin expression was abrogated. When grown with mesenchymal stem cells (MSC) at a MCF-7:MSC ratio of 10:1, MSC exposure induced the largest decrease in E-cadherin expression. *B*, 3D TGA growth data normalized to cell growth at day 1. Cell growth rate was inversely associated with E-cadherin expression levels in each treatment group. IL-6 and MSC enhanced cell growth, whereas E2 alone had a minimal effect on cell growth.

cells, we utilized MCF-7 cells which ectopically express Twist (MCF-7^{Twist}) and therefore lack E-cadherin (Mironchik *et al.*, 2005). Monomeric DsRed-positive cells were generated (MCF-7$^{Twist/VSVgR}$), and cell growth was assessed in a 3D TGA for eight days. Cells treated with 50 ng/ml IL-6 or MSC at a tumor cell:MSC ratio of 10:1 showed no increase in growth compared to untreated cells (Figure 3.4).

3.2.5 E-cadherin expression inhibits IL-6 production and cell growth. To investigate the effects of E-cadherin expression on IL-6 production and cell growth, we utilized E-cadherin-negative DsRed-Express-positive MDA-MB-231 breast cancer cells (MDA-MB-231RE) (Sasser *et al.*, 2007a) to express full-length E-cadherin (MDA-MB-231$^{RE/E\text{-}cadherin\text{-}FL}$) or E-cadherin lacking β-catenin binding activity (MDA-MB-231$^{RE/E\text{-}cadherin\text{-}\Delta\beta\text{-}catenin}$). It should be noted that each E-cadherin cDNA has an intact extracellular domain, thereby capable of extracellular homophilic adhesion. Stable expression of both E-cadherin proteins was demonstrated by western blot analysis while vector control cells exhibited no E-cadherin expression. Ectopic E-cadherin expression had no effect on constitutive levels of phoshporylated STAT3 (pSTAT3^{Y705}) (Figure 3.5A).

Due to reports of ERα-positive E-cadherin-positive breast cancer cells which lack IL-6 expression and ERα-negative breast cancer cells which lack E-cadherin but express high levels of IL-6 (Chavey *et al.*, 2007; Sasser *et al.*, 2007b), we hypothesized that E-cadherin may regulate IL-6 production. Therefore, we assessed 24-hour cellular supernatants from MDA-MB-231$^{RE/E\text{-}cadherin}$ cells for IL-6 production. Whereas vector control cells exhibited IL-6 production as expected from our previous studies, cells expressing either E-cadherin protein expressed significantly less IL-6 than vector control cells (*P*-value = 0.03). Our findings also indicated that MDA-MB-231$^{RE/E\text{-}cadherin\text{-}\Delta\beta\text{-}catenin}$

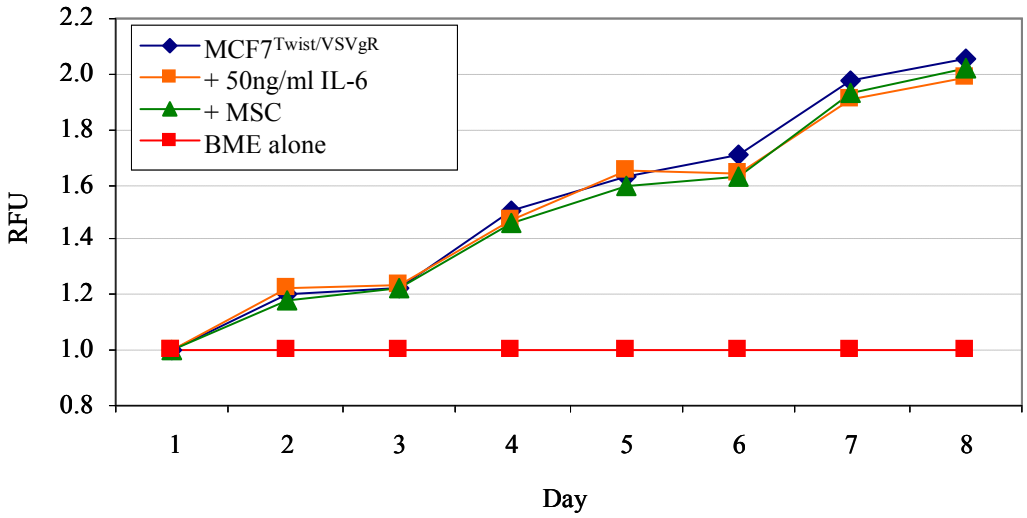

Figure 3.4 Cells which lack E-cadherin show no change in growth rate by IL-6 or MSC. 3D TGA growth rates in MCF-$7^{Twist/VSVgR}$ cells. 50 ng/ml IL-6 or mesenchymal stem cells (MSC) did not enhance growth compared to cells alone. Data are shown relative to day 1 and daily BME alone background fluorescence. RFU, relative fluorescence units.

cells produced significantly more IL-6 than MDA-MB-231$^{RE/E\text{-}cadherin\text{-}FL}$ cells (*P*-value = 0.001), which produced virtually no IL-6 (Figure 3.5B). Cell growth was subsequently evaluated in a 3D TGA. When compared to MDA-MB-231RE cells, MDA-MB-231 cells expressing either E-cadherin construct demonstrated impaired cell growth rates. Moreover, MDA-MB-231$^{RE/E\text{-}cadherin\text{-}\Delta\beta\text{-}catenin}$ cells retained a higher growth rate compared to MDA-MB-231$^{RE/E\text{-}cadherin\text{-}FL}$ cells, implicating the capability of β-catenin to induce cell growth in breast cancer cells (Figure 3.5C).

3.3 Discussion

The current study characterized the extent to which E-cadherin expression affects breast cancer cell growth in a 3D TGA. We demonstrated a dose-dependent increased growth rate in breast cancer cells exposed to IL-6 (Figure 3.1) and concomitant dose-dependent IL-6-induced E-cadherin repression (Figure 3.2). Similar findings were revealed in breast cancer cells cultured with MSC. Although estrogen had no effect on ERα-positive breast cancer cell growth in this system, it did stimulate slight E-cadherin induction compared to untreated cells (Figure 3.3). MCF-7 cells which expressed Twist and therefore no E-cadherin did not exhibit an increase in cell growth when exposed to IL-6 or MSC (Figure 3.4). Finally, stable E-cadherin expression in E-cadherin-negative MDA-MB-231 cells inhibited soluble IL-6 expression and decreased growth (Figure 3.5).

Although breast cancer-specific increases in serum and tumor microenvironment IL-6 levels are associated with poor patient survival (Bachelot *et al.*, 2003; Salgado *et al.*, 2003; Zhang and Adachi, 1999), this has been generally disregarded as the consequence

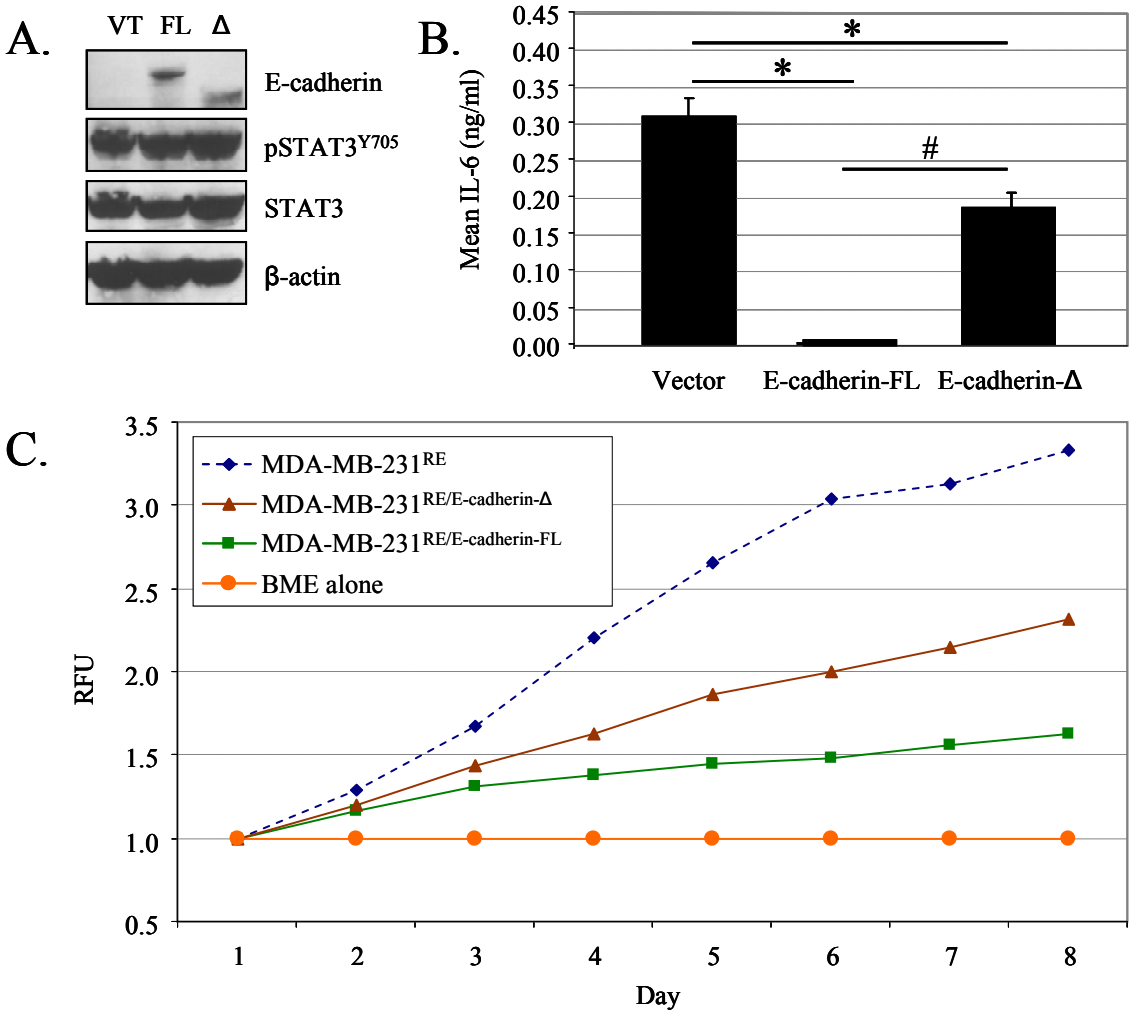

Figure 3.5 Ectopic E-cadherin expression suppresses IL-6 production and cell growth. *A*, MDA-MB-231RE cells were stably transfected with vector only (VT), full-length E-cadherin (FL), or E-cadherin which lacks a β-catenin binding domain (Δ). Western blot analysis shows that VT cells lack E-cadherin, whereas transfected cells expressed appropriate ectopic E-cadherin proteins. E-cadherin did not affect constitutive STAT3 phosphorylation (pSTAT3^{Y705}). *B*, Vector only cells exhibited IL-6 production as expected, whereas E-cadherin-FL cells showed complete abrogation of IL-6 and E-cadherin-Δ showed suppressed IL-6 production. *C*, 3D TGA data demonstrated that ectopic E-cadherin suppressed cell growth. Compared to control cells, E-cadherin-FL cells showed the most robust decrease in growth, whereas E-cadherin-Δ cells showed an intermediate growth rate. Data are shown relative to day 1 and daily BME alone control. RFU, relative fluorescence units. *P-value = 0.03; # P-value = 0.001

of an elevated anti-tumor inflammatory response. Conversely, we have previously demonstrated that IL-6 is a potent growth factor for ERα-positive breast cancer cells (Sasser *et al.*, 2007b) which is now corroborated by dose-dependent IL-6-induced cell growth and decreased E-cadherin expression. Thus, our results suggest that IL-6 is capable of mediating breast cancer progression rather than merely serving as an inflammatory marker.

We have previously demonstrated that MSC have no proliferative effect on MDA-MB-231 cells (Sasser *et al.*, 2007b), human ERα-negative breast cancer cells which express IL-6 and lack E-cadherin. To investigate if this would be the case in other cells which lack E-cadherin, we utilized human ERα-positive MCF-7 cells which ectopically express Twist (MCF-7^{Twist}) and therefore lack E-cadherin. MCF-7$^{Twist/VSVgR}$ cell growth was unaffected by IL-6 or MSC to further suggest that E-cadherin repression promotes breast cancer cell growth. Interestingly, we recently showed that ectopic Twist expression induces soluble IL-6 production (Chapter 2), which may account for the lack of growth enhancement in the presence of exogenous IL-6 or MSC.

MDA-MB-231 breast cancer cells represent a well-characterized cell line commonly used to model highly aggressive breast cancer. The fact that MDA-MB-231 cells are E-cadherin-negative allowed us to study the biological impact of two E-cadherin constructs, one full-length (E-cadherin-FL) and one without β-catenin binding activity (E-cadherin-Δβ-catenin), in these cells. Full-length E-cadherin expression was sufficient to significantly abrogate IL-6 production in MDA-MB-231 cells (*P*-value = 0.03), demonstrating the potential of E-cadherin to regulate IL-6 expression. Although E-cadherin-Δβ-catenin expression significantly reduced IL-6 production compared to vector

control cells (*P*-value = 0.03), it sustained significantly more IL-6 production than full-length E-cadherin expression (*P*-value = 0.001). These results suggest that E-cadherin suppresses evident β-catenin-mediated transactivation of IL-6 in breast cancer cells. In addition to abrogating IL-6 production, full-length E-cadherin expression in MDA-MB-231 cells induced a robust decrease in cell growth rate. Interestingly, an elevated growth rate was demonstrated upon E-cadherin-Δβ-catenin expression compared to the full-length E-cadherin but remained much lower than control cell growth. These data implicate β-catenin as a promoter of MDA-MB-231 cell growth in our 3D TGA model while also providing evidence that E-cadherin-mediated extracellular adhesion may also inhibit breast cancer cell growth.

E-cadherin is more commonly regarded as a major invasion/metastasis suppressor, but the current study highlights its competence as a bona fide tumor suppressor protein. Furthermore, we have revealed that E-cadherin inhibits aberrant IL-6 production and breast cancer cell growth, which support the fact that impaired E-cadherin expression is a strong indicator of poor prognosis in breast cancer patients. In conclusion, our findings demonstrate the capacity of E-cadherin to control multiple facets of breast cancer progression beyond simply curbing invasion and metastasis, particularly through IL-6 repression and growth inhibition.

3.4 Materials and Methods

3.4.1 Breast cancer cell lines. MCF-7, BT474, and MDA-MB-231 cells were purchased from the American Type Culture Collection (ATCC, Manassas, VA). MCF-7^{Twist} cells were kindly provided and previously published by Dr. Venu Raman at Johns Hopkins

University (Mironchik *et al.*, 2005). All cell lines were maintained in humidified incubators at 37°C and 5% CO2 and cultured in RPMI-1640 medium (Invitrogen, Carlsbad, CA) containing 5% characterized FBS (HyClone, Logan, UT), 2 mM L-glutamine, 10 U/ml penicillin, and 10 μg/ml streptomycin, hereafter termed complete medium.

3.4.2 Primary bone marrow-derived human mesenchymal stem cells (MSC). Primary human bone marrow-derived MSC (also known as bone marrow stromal cells or bone marrow fibroblasts) were obtained from Dr. Darwin Prockop at Tulane University (http://www.som.tulane.edu/gene_therapy/distribute.shtml). MSC were maintained in MEM-alpha medium (Invitrogen) containing 10% defined FBS (HyClone), 2 mM L-glutamine, 10 U/ml penicillin, 10 μg/ml streptomycin.

3.4.3 Stable red fluorescent breast cancer cell lines. Stable red fluorescent protein expressing cell lines were generated as previously described (Sasser *et al.*, 2007a). Briefly, we generated stable monomeric DsRed-positive MCF-7 and BT474 cell lines using VSV-G pseudotyped MLV retrovirus containing the pRetroQ-DsRed Monomer-C1 packaging construct (Clontech, Mountain View, CA). Retrovirus was produced by co-transfecting pVSV-G and pRetroQ-DsRed into the PG2-293 MLV packaging cell line and collecting virus from cellular supernatants, which was subsequently used to transfect MCF-7 and BT474 cells with TransFast™ lipid-based transfection reagent (Promega, Madison, WI). Following two weeks of selection with 5 μg/ml puromycin (Invivogen, San Diego, CA), cells underwent two sequential rounds of sterile cell sorting (MCF-7^{VSVgR2} and $BT474^{VSVgR2}$). Likewise, monomeric DsRed-containing retrovirus was also used to generate stable MCF-$7^{Twist/VSVgR}$ cells. In addition to stable monomeric DsRed-

positive cells, MDA-MB-231 cells were transfected with pDsRed-Express-C1 DNA plasmid (Clontech, Mountain View, CA) using TransFast™ lipid-based transfection reagent (Promega, Madison, WI). After 48 hours, DsRed-Express-positive cells were selected with 200 μg/ml G418 (Invivogen) for two weeks. Stable red fluorescent cells were sequentially sterile cell sorted using a Becton Dickinson FACSVantage/DiVa (Becton Dickinson; Mountain View, CA) (MDA-MB-231RE).

Full-length E-cadherin cDNA (E-cadherin-FL) and truncated E-cadherin cDNA (E-cadherin-Δβ-catenin) which lacks intracellular β-catenin binding activity were kindly provided and previously published by Dr. Barry Gumbiner at University of Virginia (Gottardi *et al.*, 2001) (Perrais *et al.*, 2007). E-cadherin cDNA was subcloned into a pcDNA3.1/Hygro DNA vector (Invitrogen) which contained a hygromycin resistance gene. MDA-MB-231 were transfected with E-cadherin cDNA using TransFast™ lipid-based transfection reagent (Promega) and selected with 400 μg/ml hygromycin (Invivogen) to generate stable cell lines (MDA-MB-231$^{RE/E\text{-}cadherin\text{-}FL}$ and MDA-MB-231$^{RE/E\text{-}cadherin\text{-}\Delta\beta\text{-}catenin}$).

3.4.4 3D Tumor Growth Assay (TGA). The 3D TGA is a fluorescence-based *in vitro* proliferation assay that we previously designed to monitor cell growth over time (Sasser *et al.*, 2007a; Sasser *et al.*, 2007b; Studebaker *et al.*, 2008). Briefly, red fluorescent cells (MCF-7^{VSVgR2}, BT474^{VSVgR2}, and MDA-MB-231RE) were embedded in 3 mg/ml Cultrex® basement membrane extract (BME) (Trevigen, Gaithersburg, MD) in the presence or absence of recombinant human IL-6 (PeproTech, Rocky Hill, NJ) or with MSC. BME is diluted in serum-free phenol red-free RPMI-1640, and cells were plated into black-walled clear bottom 96-well plates at 12,500 cells/well in triplicate.

Fluorescence, which correlates with cell number (Sasser *et al.*, 2007a), was measured daily up to eight days on a SpectraMax M2^{e} Microplate Reader (Molecular Devices, Sunnyvale, CA).

3.4.5 Western blot analysis. Cells were harvested from the 3D TGA by dilution with serum-free medium, centrifugation out of BME suspension at 4°C, and lysed with SDS lysis buffer (62.5 mM Tris-HCl, 2% w/v SDS, 10% glycerol, 50nM DTT, 0.01% w/v bromophenol blue). Western blot analysis was performed as previously described (Sasser *et al.*, 2007b). Primary antibodies included rabbit anti-E-cadherin 1:1000 (Cell Signaling, Danvers, MA), rabbit anti-E-cadherin 1:1000 (Santa Cruz Biotechnology, Santa Cruz, CA) (Figure 3 only), mouse anti-β-actin 1:10,000 (Clone AC-15, Sigma, St. Louis, MO), rabbit anti-phospho-STAT3^{Y705} 1:1000 (Cell Signaling), and rabbit anti-STAT3 1:1000 (Cell Signaling). Secondary antibodies included goat anti-rabbit IgG-HRP 1:1000 (Santa Cruz Biotechnology) and sheep anti-mouse IgG-HRP 1:1000 (GE Healthcare, Chalfont St. Giles, United Kingdom). All antibodies except rabbit anti-phospho-STAT3^{Y705} were diluted with 5% milk in PBS containing 0.1% Tween-20 (PBS-T) and incubated for either 1 hour at room temperature or overnight at 4°C. Rabbit anti-phospho-STAT3^{Y705} was diluted with 5% BSA in PBS-T and incubated overnight at 4°C All western blots were visualized with ECL western blotting substrate (Pierce, Rockford, IL).

3.4.6 Quantification of soluble IL-6 protein. 750,000 cells were plated per well into a 6-well plate and allowed to adhere overnight. The next day, cells were approximately 75% confluent, washed once with PBS, and 1 ml complete medium was gently added. Cells were allowed to grow for 24 hours, at which time cellular supernatants were

harvested and 0.2 μm filtered. Supernatants were assayed for soluble IL-6 protein using the Human IL-6 DuoSet® ELISA Development Kit (R&D Systems, Minneapolis, MN) according to the manufacturer's protocol.

3.4.7 Statistical analysis. Student's t-test was performed to determine statistically significant differences between groups, and a P-value < 0.05 was considered significant.

CHAPTER 4: Tumor-Induced Gender Disparities in Myeloid-Derived Suppressor Cell Expansion and Immune Competence in a Murine Model of Cutaneous Squamous Cell Carcinoma

4.1 Introduction

Non-melanoma skin cancer (NMSC), which includes basal cell and squamous cell carcinomas, represents the most common type of human malignancy and incidence rates continue to rise annually. More than one million cases will be diagnosed this year in the United States (www.cancer.gov). Furthermore, male incidence rates are approximately double those for females (Foote *et al.*, 2001). Ultraviolet light B (UVB) is the most dominant etiologic wavelength of UV radiation in NMSC (van Steeg and Kraemer, 1999) and is categorized as a complete carcinogen due to its capacity to induce tumor initiation, promotion, and progression (Baliga and Katiyar, 2006). Thus, the gender anomaly was initially attributed to more male sun exposure, but recent reports from our laboratory have revealed gender differences in cutaneous inflammation and consequent skin carcinogenesis upon equivalent cumulative UVB exposure. In particular, male mice get more tumors faster and demonstrate less inflammation while exhibiting more oxidative DNA damage compared to females (Thomas-Ahner *et al.*, 2007).

Immunosuppression promotes tumorigenesis in mice and humans. In fact, immunodeficient mice are more susceptible to spontaneous or chemically-induced tumors, particularly in skin (Koebel *et al.*, 2007; Shankaran *et al.*, 2001). Likewise,

human transplant recipients on chronic immunosuppressive therapy or acquired immunodeficiency syndrome (AIDS) patients exhibit an increased risk of cancer (Bernstein *et al.*, 2006; Veness *et al.*, 1999). Therefore, a predominant hypothesis of cancer immunosurveillance has reemerged which proposes that under normal circumstances, the immune system is capable of recognizing and eliminating abnormal tumor cells, thereby effectively preventing malignancy. In addition, an immunoediting hypothesis has more recently emerged, which takes into account the fact that tumor infiltrating immune cells may promote immune evasion and subsequent tumor progression through selection of poorly immunogenic tumor cells (Dunn *et al.*, 2004).

Myeloid-derived suppressor cells (MDSC), a heterogeneous population of immature myeloid cells capable of robust immunosuppression, have gained recent appreciation despite being initially described in tumor-bearing mice over twenty years ago. Bone marrow-derived MDSC are mobilized to peripheral lymphoid tissue in response to infection, sepsis, and trauma. Moreover, multiple murine tumor models such as melanoma, neuroblastoma, breast, lung, colon, and cervical cancers as well as peripheral blood specimens from patients with various types of cancer have confirmed aberrant peripheral induction of MDSC. In mice, MDSC exhibit a Gr-1/CD11b double-positive immunophenotype and are normally scant in peripheral tissue. In tumor-bearing mice however, MDSC can make up to 40% of total splenocytes and can be detected within tumor microenvironments.

Tumor-derived as well as inflammatory cytokines including VEGF, G-CSF, M-CSF, GM-CSF, SCF, TGF-β, IFN-γ, IL-1β, and IL-6 are capable of regulating MDSC expansion and activation either directly or by inducing myelopoiesis and inhibiting

myeloid cell maturation. MDSC suppress T-cell proliferation through metabolism of L-arginine, a required amino acid for T-cell proliferation and substrate for arginase-1 and inducible nitric oxide synthase (iNOS), both of which are overexpressed by MDSC. Furthermore, MDSC produce high levels of reactive oxygen species (ROS), which consequently induce antigen-specific T-cell anergy (Gabrilovich and Nagaraj, 2009). Additionally, MDSC have been shown to produce elevated levels of IL-10 and TGF-β, immunosuppressive cytokines capable of *de novo* regulatory T-cell induction. IL-10 production can also generate a Th2 T-cell response rather than an appropriate Th1 anti-tumor response, the latter characterized by interferon responsiveness and subsequent STAT1 activation (Ostrand-Rosenberg and Sinha, 2009).

Although aberrant peripheral MDSC induction is well-established in diverse murine tumor models and human cancers, it has yet to be described in UVB-induced non-melanoma skin cancer. In the current pilot study, we utilized the Skh-1 mouse model of UVB-induced cutaneous squamous cell carcinoma to investigate the role of MDSC in skin tumorigenesis. Specifically, our results confirmed higher male tumor burden compared to females as expected (Thomas-Ahner *et al.*, 2007), as well as offered evidence of gender differences in consequent MDSC expansion in male compared to female tumor-bearing mice. We demonstrated impaired immune competence as evaluated by interferon-induced STAT1 phosphorylation in male splenocytes, suggesting systemic immunosuppression that may be associated with MDSC induction.

4.2 Results

4.2.1 Male mice exhibit higher UVB-induced skin tumor burden. Fifteen female and fifteen male 4-week old outbred Skh-1 mice underwent UVB irradiation three times per week for 25 weeks. At week 25, individual tumor burdens were calculated, taking into account total tumor number per mouse and individual tumor area per mouse. In accordance with our previous findings in this model of UVB-induced cutaneous SCC (Thomas-Ahner *et al.*, 2007), male mice had significantly higher skin tumor burdens compared to female mice receiving equivalent cumulative doses of UVB (P-value < 0.05) (Figure 4.1).

4.2.2 UVB-induced skin tumorigenesis promotes peripheral MDSC expansion. Ten outbred Skh-1 mice of each gender received no UVB exposure and served as tumor-free controls. Total female and male splenocytes from mice lacking tumors (no UVB controls) and those from mice with relatively low (n = 2 per gender) and high (n = 2 per gender) tumor burdens following 25 weeks of UVB exposure were stained for Gr-1 and CD11b for flow cytometric analysis. Gr-1/CD11b double-positive cells were considered MDSC, and representative dot plots are shown from each group of mice. MDSC were present at low levels in no UVB control mice, and a basal gender discrepancy was not evident. However, mice with relatively low UVB-induced skin tumor burden demonstrated elevated MDSC levels, particularly in male tumor-bearing mice. Furthermore, mice with relatively high UVB-induced skin tumor burden showed more robust MDSC induction, which was particularly apparent in male tumor-bearing mice (Figure 4.2).

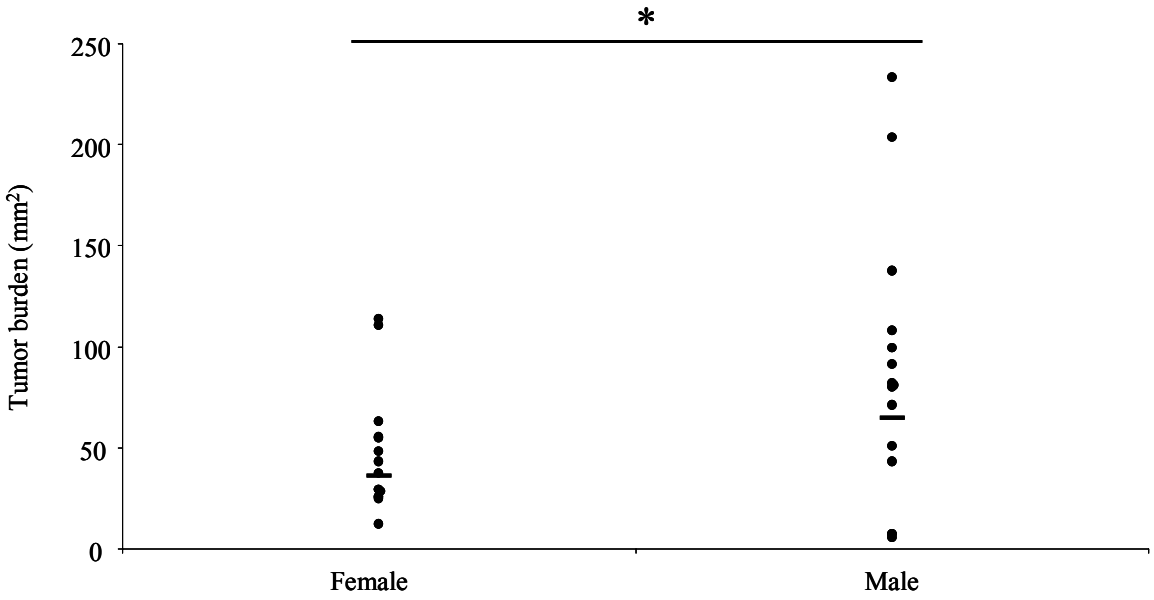

Figure 4.1 Higher UVB-induced skin tumor burden in male Skh-1 mice. Female and male outbred Skh-1 mice were exposed to UVB irradiation 3 times per week for 25 weeks. Individual tumor burdens were calculated, taking into account tumor number and individual tumor area. Horizontal bars represent mean tumor burden. *P-value < 0.05

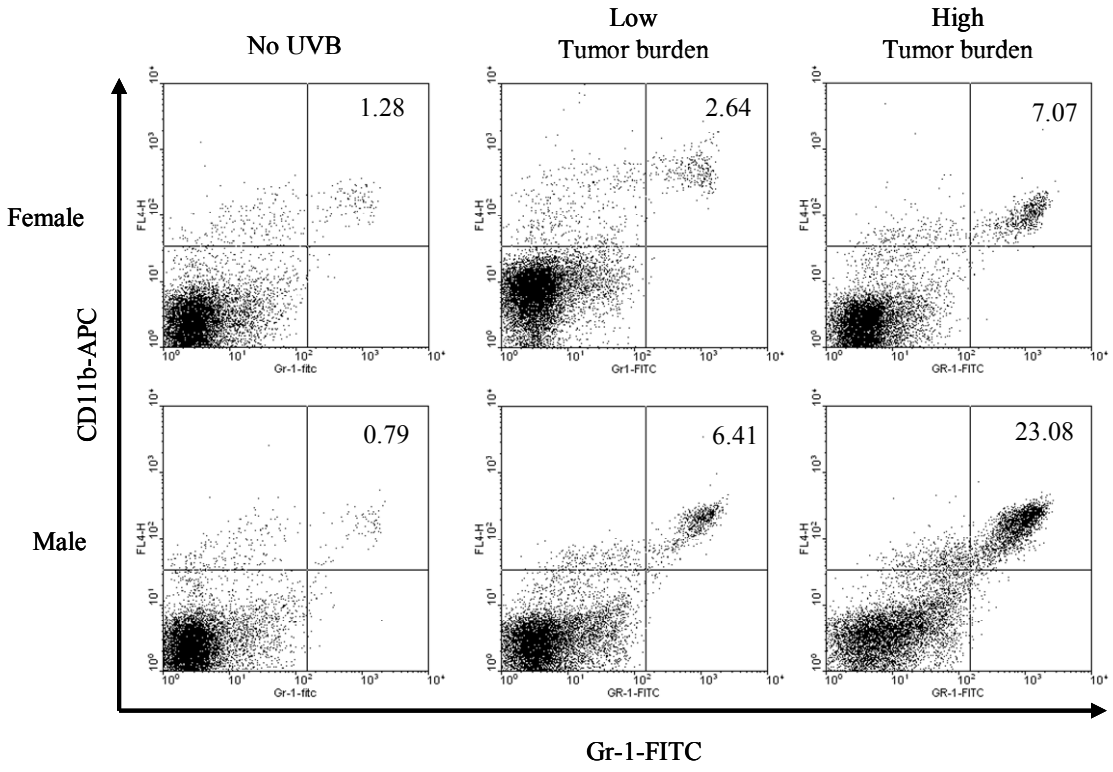

Figure 4.2 Peripheral MDSC expansion in skin tumor-bearing mice. Following chronic UVB exposure, mice were sacrificed, and splenocytes from the two highest and two lowest tumor burden mice per gender were stained for Gr-1-FITC (x-axis) and CD11b-APC (y-axis). Gr-1+/CD11b+ events were considered MDSC, and representative dot plots are shown. No UVB tumor-free control mice showed low levels of baseline MDSC. Compared to No UVB controls, tumor-bearing mice exhibited elevated peripheral MDSC expansion, and high tumor burden mice demonstrated more MDSC than low tumor burden mice. MDSC levels were higher in male compared to female tumor-bearing mice.

4.2.3 Male mice with relatively high skin tumor burden demonstrate elevated peripheral MDSC levels. Whereas female skin tumor-bearing mice showed no significant difference in skin tumor-induced MDSC levels, the data are suggestive that MDSC numbers increase with tumor burden. In contrast, male skin tumor-bearing mice showed significantly more MDSC in high compared to low tumor burden groups (*P*-value = 0.002). Additionally, the data are suggestive of a gender disparity in skin tumor-induced MDSC expansion, whereby male mice are more susceptible to increased MDSC levels following UVB-induced skin tumorigenesis compared to females (Figure 4.3).

4.2.4 Abrogation of splenocyte interferon responsiveness in male UVB-induced skin tumor-bearing mice. To investigate the potential systemic immunosuppressive consequences of skin tumor-induced aberrant MDSC induction, female and male splenocytes were stimulated with interferon-alpha (IFN-α) and gamma (IFN-γ) and subsequently stained for intracellular phosphorylated STAT1 (pSTAT1) as a marker of interferon responsiveness. Basal levels of pSTAT1 in PBS-treated splenocytes were similar to those of isotype control stained splenocytes (data not shown), and therefore, data are shown compared to isotype control. Splenocytes from female and male tumor-free control mice exhibited normal pSTAT1 induction following IFN-α and IFN-γ stimulation. Although female mice with relatively low tumor burden showed IFN responsiveness consistent with female tumor-free mice, male tumor-bearing mice demonstrated impaired IFN responsiveness even with relatively low tumor burden. While female splenocytes from mice with relatively high tumor burden were still capable of responding to IFN-γ, IFN-α responsiveness was diminished. However, male

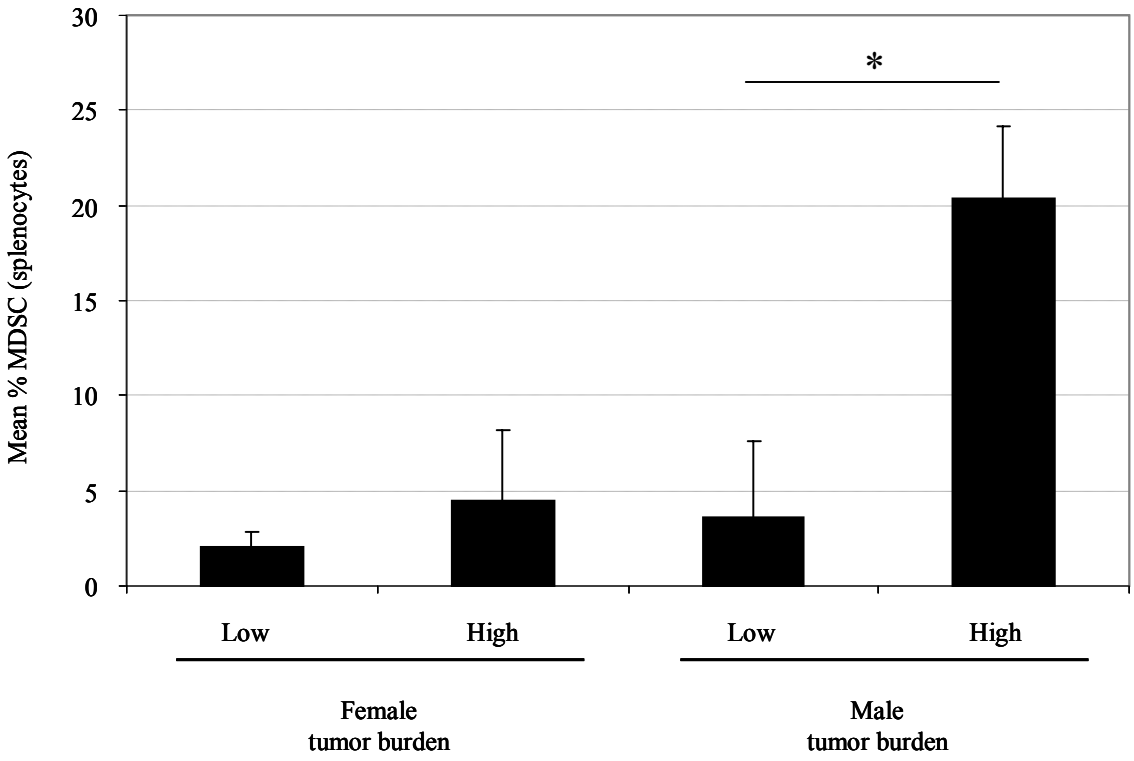

Figure 4.3 Male mice demonstrate more skin tumor-induced peripheral MDSC compared to female mice. Flow cytometric analysis of Gr-1+/CD11b+ MDSC suggests a gender discrepancy in susceptibility to MDSC induction. Male low and high tumor burden mice (n = 2 per group) exhibit higher mean MDSC levels compared to respective female tumor-bearing mice (n = 2 per group). Male high compared to low tumor burden mice showed significantly more peripheral MDSC (**P*-value = 0.002)

splenocyte responsiveness to either IFN-α or IFN-γ was severely abrogated in relatively high tumor burden mice (Figure 4.4).

We evaluated pSTAT1 mean fluorescence intensity, a measure of target protein expression level. No gender discrepancy in basal IFN responsiveness was evident in tumor-free control mice (Figure 4.5A). In relatively high tumor burden mice, the data are suggestive of a difference between female and male splenocyte IFN responsiveness (*P*-value = 0.1) (Figure 4.5B). When we compared IFN responsiveness between tumor-free and relatively high tumor burden male mice, high tumor burden males showed significantly less pSTAT1 induction upon IFN-α stimulation compared to tumor-free males (*P*-value = 0.01). Likewise, high tumor burden males showed significantly less pSTAT1 induction upon IFN-γ stimulation compared to tumor-free males (*P*-value = 0.001) (Figure 4.5C).

4.3 Discussion

To our knowledge, this is the first report of peripheral MDSC expansion in a mouse model of UVB-induced NMSC and furthermore, of a gender disparity in susceptibility to MDSC induction. Our findings were in accordance with our previous reports, which demonstrated that male Skh-1 mice acquire higher UVB-induced tumor burdens compared to female Skh-1 mice (Figure 4.1). We showed low basal levels of MDSC in tumor-free female and male Skh-1 mice and a subsequent robust induction of peripheral MDSC following chronic exposure to UVB irradiation (Figure 4.2). Male mice with high tumor burden maintained significantly more MDSC than those with low tumor burden (*P*-value = 0.002) (Figure 4.3). Furthermore, these data suggest that male

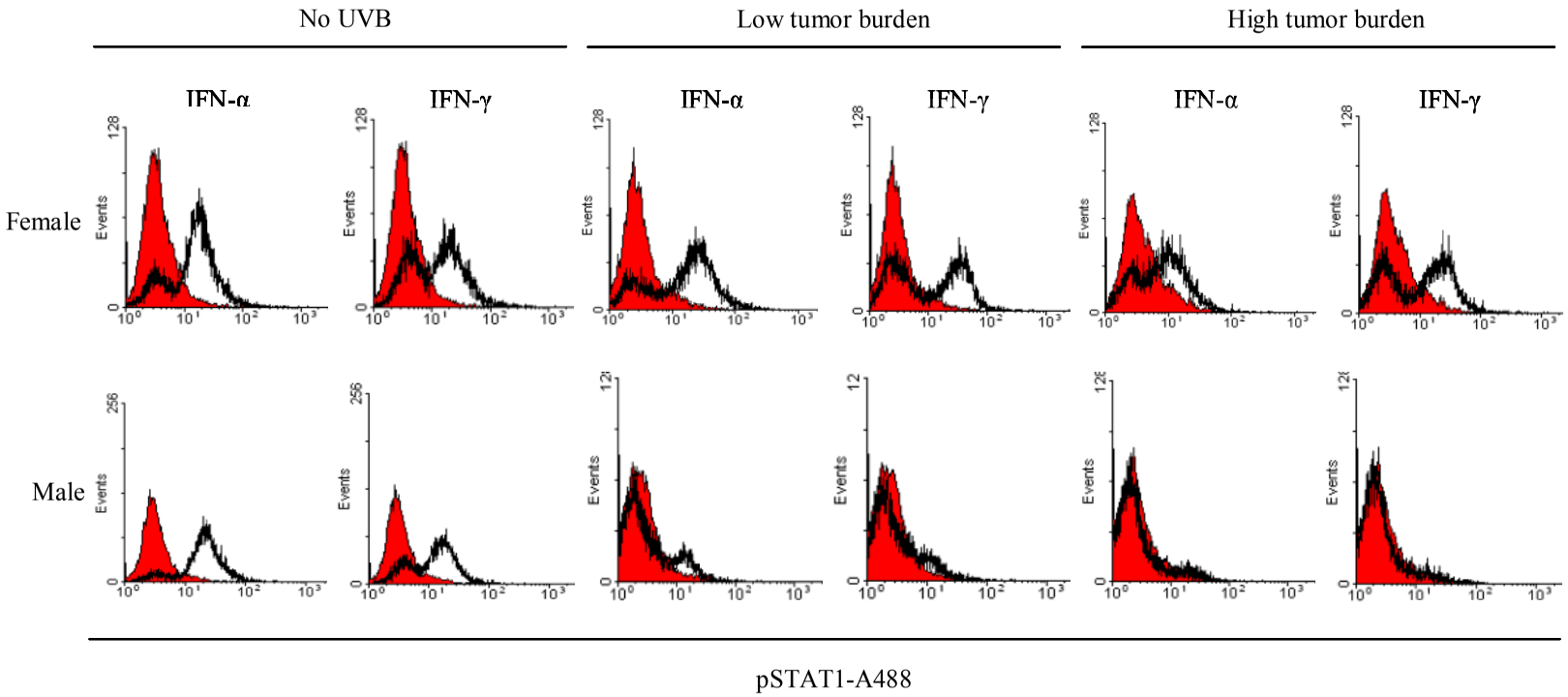

Figure 4.4 Abrogated systemic interferon responsiveness in tumor-bearing mice. Splenocytes from the two highest and two lowest tumor burden mice per gender were stimulated with 10^4 units/ml IFN-α or 10 ng/ml IFN-γ for 15 minutes. Intracellular flow cytometric analysis with anti-pSTAT1-AlexaFluor488 (pSTAT1-A488) was used as a marker of interferon responsiveness, and representative histograms are shown. No gender discrepancy was detected in tumor-free (no UVB) control splenocytes. Whereas female low tumor burden mice exhibited similar pSTAT1 induction compared to female tumor-free mice, those with high tumor burden showed slight suppression of pSTAT1 induction. Male compared to female tumor-bearing mice demonstrated almost complete abrogation of interferon responsiveness. Data are shown relative to isotype control staining (red histograms).

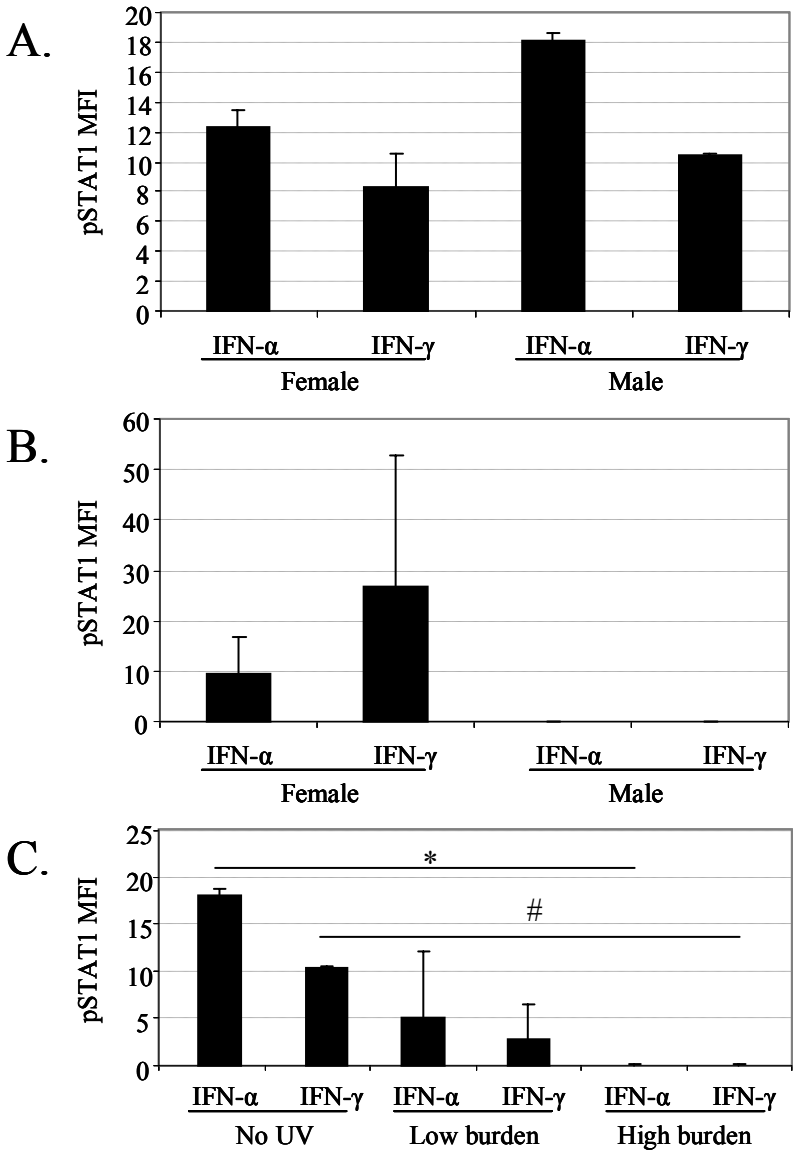

Figure 4.5 Inhibited STAT1 phosphorylation in male tumor-bearing mice. pSTAT1 mean fluorescence intensity (MFI) is shown for IFN-stimulated slenocytes. *A*, Tumor-free mice showed no gender difference in IFN-induced pSTAT1. *B*, High tumor burden mice revealed an apparent gender disparity in IFN-induced pSTAT1. *C*, Male high tumor burden mice exhibited significantly abrogated IFN-induced pSTAT1. (**P*-value = 0.01; #*P*-value = 0.001)

skin tumor-bearing mice are more susceptible to MDSC induction compared to female skin tumor-bearing mice. Finally, male skin tumor-bearing mice exhibited severely abrogated pSTAT1 induction following IFN stimulation (Figures 4.4 and 4.5).

Work from our laboratory has previously demonstrated gender differences in UVB-induced inflammation and subsequent skin tumorigenesis in the currently used and well-established Skh-1 mouse model. In particular, the UVB-induced inflammatory response was significantly higher in female mice (P-value < 0.05), while total tumor burden was significantly higher in male mice (P-value = 0.0177) (Thomas-Ahner *et al.*, 2007). The current study confirmed a significantly higher UVB-induced skin tumor burden in male mice (P-value < 0.05), but our findings also suggest a novel gender disparity in peripheral MDSC expansion following chronic UVB exposure and consequent skin tumorigenesis. Our results suggest that male mice are inherently more prone to skin tumor-induced MDSC induction than females. Moreover, peripheral MDSC were significantly higher in male mice with relatively high compared to relatively low tumor burden, and these results correlate with systemic abrogation of IFN responsiveness in high tumor burden male mice. These data provide evidence of a functional consequence of aberrant peripheral MDSC expansion, whereby male skin tumor-bearing mice had more MDSC and demonstrated impaired systemic immune competence compared to females. These data also correlate with the decreased inflammatory response we have shown in male compared to female mice following UVB exposure (Thomas-Ahner *et al.*, 2007).

As stated, this was a pilot study to characterize MDSC induction in our Skh-1 mouse model of UVB-inuduced NMSC. Thus, we only harvested spleens from the two

highest tumor burden mice and spleens from the two lowest tumor burden mice for each gender. Although this was not enough to show significant discrepancies in the MDSC population or immune competence of total splenocytes between female and male tumor-bearing mice, we were able to demonstrate some significant differences within male mice.

Future studies will expand on these findings of the effects of UVB-induced skin tumorigenesis on MDSC induction and potentially consequent systemic immune competence. *In vivo* studies will be performed to determine the time course of MDSC induction and evolution of systemic immunodeficiency following acute and chronic UVB exposure. UVB irradiation induces cutaneous inflammation, and of particular interest, IL-6 expression in primary human keratinocytes (De Haes *et al.*, 2003). IL-6 is a predominant factor capable of promoting MDSC expansion and activation in mouse tumor models, and we hypothesize that it may play a role in skin tumor-induced MDSC induction. Therefore, we will evaluate serum IL-6 levels during acute and chronic UVB exposure studies. Understanding gender disparities in MDSC expansion may reveal novel immunotherapeutics for NMSC patients and may potentially translate to other cancers as well.

4.4 Materials and Methods

4.4.1 Murine UVB-induced NMSC model. Outbred Skh-1 mice (Charles River Laboratories, Wilmington, MA) were housed at The Ohio State University's vivarium according to the requirements established by the American Association for Accreditation of Laboratory Animal Care. Procedures were approved by the appropriate Institutional

Animal Care Utilization Committee before the initiation of any studies. 15 female and 15 male four-week old Skh-1 mice were exposed to dorsal UVB irradiation as previously described (Thomas-Ahner *et al.*, 2007). Briefly, Phillips FS40UVB lamps (American Ultraviolet Company, Lebanon, IN) fitted with Kodacel filters (Eastman Kodak, Rochester, NY) were used to ensure only UVB (290–320 nm) emission. Animals were exposed to 2,240 J/m^2 (previously determined as 1 minimal erythemic dose) three times per week for 25 weeks. Skin tumors greater than 1 mm were counted and subsequently measured weekly with digital calipers. Animals were sacrificed 24 hours following the last UVB treatment, and spleens from the two highest and two lowest tumor burden mice of each gender were harvested. Spleen tissue was disaggregated into cellular splenocyte suspension and frozen in liquid nitrogen at -120ºC.

4.4.2 Interferon stimulation of total splenocytes. Splenocytes were thawed and washed in RPMI-1640 medium (Invitrogen, Carlsbad, CA) containing 10% FBS (HyClone, Logan, UT), hereafter referred to as splenocyte medium. 5 x 10^5 splenocytes were treated with 10^4 units/ml recombinant universal type I IFN (IFN-α) (PBL Biomedical Laboratories, Piscataway, NJ) or 10 ng/ml recombinant murine IFN-γ (R&D Sytems, Minneapolis, MN) at 37ºC for 15 minutes. Splenocytes treated with PBS were used as unstimulated baseline controls. Cells were washed with splenocyte medium, and immediately used for flow cytometric analysis of STAT1 phosphorylation (see below).

4.4.3 Flow cytometric analysis of myeloid-derived suppressor cells. Splenocytes were thawed and washed in splenocyte medium. 5 x 10^5 cells were double stained with rat anti-mouse Gr-1-FITC and rat anti-mouse CD11b-APC antibodies (BD Biosciences, San Jose, CA) in 100 µl splenocyte medium on ice in the dark for one hour. Appropriate

isotype control antibodies were used as negative controls. Stained cells were washed with PBS (Invitrogen) containing 5% FBS (HyClone), and resuspended in PBS containing 1% formalin. Flow cytometric analysis was performed using a BD FACSCalibur flow cytometer (BD Biosciences), and 10,000 events were collected for each sample. All flow cytometric data shown were analyzed and generated using WinMDI version 2.8 software (The Scripps Research Institute, San Diego, CA).

4.4.4 Flow cytometric analysis of STAT1 phosphorylation. Intracellular pSTAT1 flow cytometric staining was performed using the Fix & Perm® Cell Permeabilization Kit (Molecular Probes, Invitrogen). IFN-stimulated cells were fixed and permeabilized according to the manufacturer's methanol modification protocol and subsequently stained with mouse anti-STAT1 (pY701)-Alexa Fluor® 488 antibody (BD Biosciences). Appropriate isotype control antibody was used as a negative control and data are shown relative to isotype control staining.

4.4.5 Statistical Analysis. Student's t-test was performed to determine statistically significant differences between groups, and a P-value < 0.05 was considered significant.

CHAPTER 5: CONCLUSION

Far too many women have to endure unimaginable physical and emotional adversity during their battle with breast cancer, and the tragic reality is that the disease will take many of their lives while devastating the lives of family and friends. Therefore, researchers have devoted their efforts, in many cases a life's work, to unlocking the biological mechanisms that foster breast carcinogenesis and breast cancer progression. Curing and perhaps preventing breast cancer is going to be a difficult challenge for years to come, but great strides have been made to ameliorate the dismal implication of each breast cancer diagnosis. In fact, the current body of basic breast cancer research offers evidence of yet another potential mediator of breast cancer progression in the form of IL-6. Our findings suggest that breast cancer patient serum and tumor IL-6 levels are clinically relevant, and therefore, should be routinely evaluated upon diagnosis. Furthermore, this work supports the validation of currently available IL-6 signaling antagonists in breast cancer preclinical studies. Recombinant soluble gp130 (sgp130-Fc) has been shown to suppress murine colon carcinogenesis (Becker *et al.*, 2004), and our results suggest that this may be effective in breast cancer as well. sgp130-Fc would inhibit only IL-6 *trans*-signaling, thus preserving IL-6 signaling through membranous IL-6R in cells such as immune cells. If proven efficacious, IL-6 signaling antagonists could seize further clinical utility as breast cancer neoadjuvant or adjuvant therapy.

We demonstrated the potential of IL-6 to provoke an EMT phenotype in breast cancer cells in Chapter 2. EMT phenotypes are associated with poor patient survival in multiple types of carcinoma, and breast cancer is no exception. We can conclude from these studies that paracrine IL-6 signaling is capable of potent E-cadherin protein repression in ERα-positive breast cancer cells. Autocrine IL-6 signaling in MCF-7 breast cancer cells (MCF-$7^{IL\text{-}6}$) not only represses E-cadherin, but also induces aberrant N-cadherin, Vimentin, Twist, and Snail expression. IL-6 renders relatively noninvasive breast cancer cells highly invasive *in vitro*. Autocrine IL-6 signaling maintains a breast cancer-associated EMT phenotype *in vivo* while enhancing tumor growth and promoting poor tumor cell differentiation. Breast cancer cells which possess an EMT phenotype also demonstrate IL-6 overexpression and constitutive STAT3 activation.

Chapter 3 investigated the role of E-cadherin in breast cancer cell proliferation and IL-6 production. We have previously reported that IL-6 is a potent growth factor for ERα-positive breast cancer cells, but at the time, were unable to reveal a mechanism to explain this finding. As we showed in Chapter 2, E-cadherin expression is impaired following IL-6 exposure in breast cancer cells grown in 3D culture, and this prompted us to assess the impact of E-cadherin repression on IL-6-induced growth enhancement. It can be concluded from Chapter 3 that IL-6 enhances the growth rates of ERα-positive breast cancer cells in a dose-dependent manner. IL-6 dose also correlates with degree of E-cadherin protein repression, which suggests that loss of E-cadherin may be a dominant factor in IL-6-induced breast cancer cell growth. We have previously demonstrated that E-cadherin-negative MDA-MB-231 breast cancer cell growth is unaffected by IL-6, and we now show that MCF-7^{Twist} cells, another cell line which lacks E-cadherin, do not

respond to IL-6 exposure. Final experiments in Chapter 3 utilized MDA-MB-231 cells which ectopically expressed full-length E-cadherin or that which lacked β-catenin binding activity (mutant E-cadherin). Full-length E-cadherin expression completely abrogated IL-6 expression in MDA-MB-231 cells whereas mutant E-cadherin reduced IL-6 expression but to a lesser extent. Therefore, it appears that β-catenin may regulate IL-6 expression in breast cancer cells. Interestingly, E-cadherin expression impaired MDA-MB-231 cell growth, and although cells expressing mutant E-cadherin exhibited a slightly increased growth rate compared to those expressing full-length E-cadherin, cell growth was impaired in both cells compared to control cells. This not only shows that the extracellular domain of E-cadherin promotes growth suppression but also reveals a role for β-catenin as a mediator of breast cancer cell growth. Additionally, cells which expressed full-length E-cadherin demonstrated the most growth suppression and expressed little to no IL-6, suggesting that autocrine IL-6 expression may also promote MDA-MB-231 cell growth.

Non-melanoma skin cancer is the most common type of human cancer and incidence rates are rising annually. Solar-derived UVB radiation is one of the most dominant etiologic factors for skin carcinogenesis, whereby it is a complete carcinogen. Despite these facts, tanning beds which utilize UV irradiation to give Caucasian skin a more bronze appearance are still popular today. Unfortunately, the carcinogenic effect of outdoor or indoor tanning will take years to manifest, which probably plays a role in its continued popularity among younger generations. The current body of skin cancer basic research commenced with the intention to further characterize our Skh-1 mouse model of UVB-induced non-melanoma skin cancer. Although this work was only an initial pilot

study, it revealed skin tumor-induced peripheral MDSC expansion in mice following chronic UVB exposure. Furthermore, we detected an apparent gender discrepancy in peripheral MDSC levels and immune competence. Our findings support previous reports regarding skin cancer development in immunodeficient populations, and in particular, our previous report of decreased UVB-induced inflammation in male compared to female mice. Interestingly, UVB induces IL-6 in human epidermal keratinocytes and presumably throughout UVB-induced inflammation, and IL-6 has been shown to induce MDSC in murine tumor models. Therefore, we hypothesize that elevated levels of UVB-induced IL-6 may induce MDSC expansion in our model, thereby mediating skin carcinogenesis.

The work presented in Chapter 4 confirmed our previous results showing that male Skh-1 mice demonstrate higher skin tumor burden following chronic UVB exposure. Whereas both female and male tumor-bearing mice exhibited increased levels of peripheral MDSC compared to tumor-free control mice, our findings suggest that male mice are more susceptible to skin tumor-induced MDSC expansion. Furthermore, male mice with relatively high tumor burden showed significantly more peripheral MDSC compared to male mice with relatively low tumor burden (P-value = 0.002). To characterize the consequences of elevated peripheral MDSC, we assessed IFN-induced STAT1 phosphorylation (pSTAT1) as a surrogate of systemic immune function. In particular, male tumor-bearing mice demonstrated severely abrogated total splenocyte pSTAT1 induction following IFN-α and IFN-γ stimulation compared to either male tumor-free mice or female tumor-bearing mice. Although further studies will be necessary to confirm these findings, the data suggest that male compared to female

tumor-bearing mice exhibit elevated peripheral MDSC expansion, and this may consequently impair systemic immune competence, thus promoting skin carcinogenesis. Further characterization of serum cytokines will be necessary to determine the role of IL-6 during MDSC expansion and activation in our model.

Our work suggests that IL-6 may contribute to breast cancer progression, and to a more immature extent, skin carcinogenesis. However, the current body of knowledge has opened the door for more questions. For example, we demonstrated the ability of autocrine IL-6 signaling to maintain an EMT phenotype in a xenograft breast cancer model. Yet, it will be necessary to generate inducible IL-6 expressing murine mammary tumor cells for congenic tumor challenge studies to ask if IL-6 is capable of provoking an EMT phenotype consistent with E-cadherin repression *in vivo*. Furthermore, will IL-6-inducible E-cadherin repression be sufficient for enhanced tumor cell growth *in vivo*? We could also use the same inducible IL-6 murine mammary tumor cells for tumor challenge studies in IL-6 knockout mice to rule out the possibility of paracrine IL-6 signaling in this model. Additional MCF-7 xenograft studies in human IL-6-overexpressing mice could show the capability of paracrine IL-6 signaling to promote breast cancer progression. Finally, would IL-6 signaling antagonists such as sgp130-Fc, monoclonal anti-IL-6, monoclonal anti-IL-6R, or JAK/STAT3 inhibitors prove effective in these mouse models?

Likewise, our pilot study investigating peripheral MDSC expansion demonstrated promising preliminary data worthy of further characterization. In particular, future studies should determine the time course of MDSC induction in tumor-bearing mice. Or perhaps UVB is capable of inducing MDSC prior to skin tumorigenesis. Acute and

chronic UVB studies will be needed to assess MDSC induction pre- and post-tumor development. Intriguingly, IL-6 has been implicated as a tumor-derived factor capable of promoting peripheral MDSC expansion. What is the contribution of UVB-induced IL-6 in peripheral MDSC expansion? What role do peripheral MDSC play in suppression of systemic interferon responsiveness in our model? What role do they play in UVB-induced skin tumorigenesis? We have elucidated novel mechanisms by which IL-6 may potentially mediate human breast cancer progression and UVB-induced skin carcinogenesis, and we hope to see these findings one day translated into novel therapeutics for respective cancer patients.

References

Abdulla FR, Feldman SR, Williford PM, Krowchuk D, Kaur M (2005). Tanning and skin cancer. *Pediatr Dermatol* **22:** 501-12.

Acs G, Lawton TJ, Rebbeck TR, LiVolsi VA, Zhang PJ (2001). Differential expression of E-cadherin in lobular and ductal neoplasms of the breast and its biologic and diagnostic implications. *Am J Clin Pathol* **115:** 85-98.

Anderson WF, Matsuno R (2006). Breast cancer heterogeneity: a mixture of at least two main types? *J Natl Cancer Inst* **98:** 948-51.

Bachelot T, Ray-Coquard I, Menetrier-Caux C, Rastkha M, Duc A, Blay JY (2003). Prognostic value of serum levels of interleukin 6 and of serum and plasma levels of vascular endothelial growth factor in hormone-refractory metastatic breast cancer patients. *Br J Cancer* **88:** 1721-6.

Baliga MS, Katiyar SK (2006). Chemoprevention of photocarcinogenesis by selected dietary botanicals. *Photochem Photobiol Sci* **5:** 243-53.

Barton BE, Karras JG, Murphy TF, Barton A, Huang HF (2004). Signal transducer and activator of transcription 3 (STAT3) activation in prostate cancer: Direct STAT3 inhibition induces apoptosis in prostate cancer lines. *Mol Cancer Ther* **3:** 11-20.

Becker C, Fantini MC, Schramm C, Lehr HA, Wirtz S, Nikolaev A *et al* (2004). TGF-beta suppresses tumor progression in colon cancer by inhibition of IL-6 trans-signaling. *Immunity* **21:** 491-501.

Behrens J, Mareel MM, Van Roy FM, Birchmeier W (1989). Dissecting tumor cell invasion: epithelial cells acquire invasive properties after the loss of uvomorulin-mediated cell-cell adhesion. *J Cell Biol* **108:** 2435-47.

Benavides F, Oberyszyn TM, VanBuskirk AM, Reeve VE, Kusewitt DF (2009). The hairless mouse in skin research. *J Dermatol Sci* **53:** 10-8.

Bennermo M, Held C, Stemme S, Ericsson CG, Silveira A, Green F *et al* (2004). Genetic predisposition of the interleukin-6 response to inflammation: implications for a variety of major diseases? *Clin Chem* **50:** 2136-40.

Benson JR, Jatoi I, Keisch M, Esteva FJ, Makris A, Jordan VC (2009). Early breast cancer. *Lancet* **373:** 1463-79.

Berishaj M, Gao SP, Ahmed S, Leslie K, Al-Ahmadie H, Gerald WL *et al* (2007). Stat3 is tyrosine-phosphorylated through the interleukin-6/glycoprotein 130/Janus kinase pathway in breast cancer. *Breast Cancer Res* **9:** R32.

Bernstein WB, Little RF, Wilson WH, Yarchoan R (2006). Acquired immunodeficiency syndrome-related malignancies in the era of highly active antiretroviral therapy. *Int J Hematol* **84:** 3-11.

Bertucci F, Orsetti B, Negre V, Finetti P, Rouge C, Ahomadegbe JC *et al* (2008). Lobular and ductal carcinomas of the breast have distinct genomic and expression profiles. *Oncogene* **27:** 5359-72.

Berx G, Cleton-Jansen AM, Nollet F, de Leeuw WJ, van de Vijver M, Cornelisse C *et al* (1995). E-cadherin is a tumour/invasion suppressor gene mutated in human lobular breast cancers. *EMBO J* **14:** 6107-15.

Blaskovich MA, Sun J, Cantor A, Turkson J, Jove R, Sebti SM (2003). Discovery of JSI-124 (cucurbitacin I), a selective Janus kinase/signal transducer and activator of transcription 3 signaling pathway inhibitor with potent antitumor activity against human and murine cancer cells in mice. *Cancer Res* **63:** 1270-9.

Blick T, Widodo E, Hugo H, Waltham M, Lenburg ME, Neve RM *et al* (2008). Epithelial mesenchymal transition traits in human breast cancer cell lines. *Clin Exp Metastasis* **25:** 629-42.

Boukamp P (2005). Non-melanoma skin cancer: what drives tumor development and progression? *Carcinogenesis* **26:** 1657-67.

Bouwstra J, et al. (2006). Structure of the Skin Barrier. In: Elias P, Feingold, KR (ed). *Skin Barrier*. CRC Press. p 65.

Bowden GT (2004). Prevention of non-melanoma skin cancer by targeting ultraviolet-B-light signalling. *Nat Rev Cancer* **4:** 23-35.

Brackenbury R, Rutishauser U, Edelman GM (1981). Distinct calcium-independent and calcium-dependent adhesion systems of chicken embryo cells. *Proc Natl Acad Sci U S A* **78:** 387-91.

Braun S, Pantel K, Muller P, Janni W, Hepp F, Kentenich CR *et al* (2000). Cytokeratin-positive cells in the bone marrow and survival of patients with stage I, II, or III breast cancer. *N Engl J Med* **342:** 525-33.

Bunt SK, Yang L, Sinha P, Clements VK, Leips J, Ostrand-Rosenberg S (2007). Reduced inflammation in the tumor microenvironment delays the accumulation of myeloid-derived suppressor cells and limits tumor progression. *Cancer Res* **67:** 10019-26.

Burdall SE, Hanby AM, Lansdown MR, Speirs V (2003). Breast cancer cell lines: friend or foe? *Breast Cancer Res* **5:** 89-95.

Burke WM, Jin X, Lin HJ, Huang M, Liu R, Reynolds RK *et al* (2001). Inhibition of constitutively active Stat3 suppresses growth of human ovarian and breast cancer cells. *Oncogene* **20:** 7925-34.

Butler TP, Gullino PM (1975). Quantitation of cell shedding into efferent blood of mammary adenocarcinoma. *Cancer Res* **35:** 512-6.

Buyse M, Loi S, van't Veer L, Viale G, Delorenzi M, Glas AM *et al* (2006). Validation and clinical utility of a 70-gene prognostic signature for women with node-negative breast cancer. *J Natl Cancer Inst* **98:** 1183-92.

Chauhan D, Uchiyama H, Akbarali Y, Urashima M, Yamamoto K, Libermann TA *et al* (1996). Multiple myeloma cell adhesion-induced interleukin-6 expression in bone marrow stromal cells involves activation of NF-kappa B. *Blood* **87:** 1104-12.

Chavey C, Bibeau F, Gourgou-Bourgade S, Burlinchon S, Boissiere F, Laune D *et al* (2007). Oestrogen receptor negative breast cancers exhibit high cytokine content. *Breast Cancer Res* **9:** R15.

Cheng GZ, Zhang WZ, Sun M, Wang Q, Coppola D, Mansour M *et al* (2008). Twist is transcriptionally induced by activation of STAT3 and mediates STAT3 oncogenic function. *J Biol Chem* **283:** 14665-73.

Clevenger CV (2004). Roles and regulation of stat family transcription factors in human breast cancer. *Am J Pathol* **165:** 1449-60.

Clydesdale GJ, Dandie GW, Muller HK (2001). Ultraviolet light induced injury: immunological and inflammatory effects. *Immunol Cell Biol* **79:** 547-68.

Conze D, Weiss L, Regen PS, Bhushan A, Weaver D, Johnson P *et al* (2001). Autocrine production of interleukin 6 causes multidrug resistance in breast cancer cells. *Cancer Res* **61:** 8851-8.

Cooper A (1840). Anatomy of the Breast. *London: Longman, Orme, Green, Browne and Longmans*.

Crichton MB, Nichols JE, Zhao Y, Bulun SE, Simpson ER (1996). Expression of transcripts of interleukin-6 and related cytokines by human breast tumors, breast cancer cells, and adipose stromal cells. *Mol Cell Endocrinol* **118:** 215-20.

De Haes P, Garmyn M, Degreef H, Vantieghem K, Bouillon R, Segaert S (2003). 1,25-Dihydroxyvitamin D3 inhibits ultraviolet B-induced apoptosis, Jun kinase activation, and interleukin-6 production in primary human keratinocytes. *J Cell Biochem* **89:** 663-73.

DeMichele A, Martin AM, Mick R, Gor P, Wray L, Klein-Cabral M *et al* (2003). Interleukin-6 -174G-->C polymorphism is associated with improved outcome in high-risk breast cancer. *Cancer Res* **63:** 8051-6.

Derksen PW, Liu X, Saridin F, van der Gulden H, Zevenhoven J, Evers B *et al* (2006). Somatic inactivation of E-cadherin and p53 in mice leads to metastatic lobular mammary carcinoma through induction of anoikis resistance and angiogenesis. *Cancer Cell* **10:** 437-49.

Diel IJ, Kaufmann M, Costa SD, Holle R, von Minckwitz G, Solomayer EF *et al* (1996). Micrometastatic breast cancer cells in bone marrow at primary surgery: prognostic value in comparison with nodal status. *J Natl Cancer Inst* **88:** 1652-8.

Dihlmann S, von Knebel Doeberitz M (2005). Wnt/beta-catenin-pathway as a molecular target for future anti-cancer therapeutics. *Int J Cancer* **113:** 515-24.

Dunn GP, Old LJ, Schreiber RD (2004). The immunobiology of cancer immunosurveillance and immunoediting. *Immunity* **21:** 137-48.

Elston CW, Ellis IO (1991). Pathological prognostic factors in breast cancer. I. The value of histological grade in breast cancer: experience from a large study with long-term follow-up. *Histopathology* **19:** 403-10.

Fidler IJ (2003). The pathogenesis of cancer metastasis: the 'seed and soil' hypothesis revisited. *Nat Rev Cancer* **3:** 453-8.

Foote JA, Harris RB, Giuliano AR, Roe DJ, Moon TE, Cartmel B *et al* (2001). Predictors for cutaneous basal- and squamous-cell carcinoma among actinically damaged adults. *Int J Cancer* **95:** 7-11.

Frykberg ER (1999). Lobular Carcinoma In Situ of the Breast. *Breast J* **5:** 296-303.

Fujita N, Jaye DL, Kajita M, Geigerman C, Moreno CS, Wade PA (2003). MTA3, a Mi-2/NuRD complex subunit, regulates an invasive growth pathway in breast cancer. *Cell* **113:** 207-19.

Gabrilovich DI, Nagaraj S (2009). Myeloid-derived suppressor cells as regulators of the immune system. *Nat Rev Immunol* **9:** 162-74.

Galien R, Garcia T (1997). Estrogen receptor impairs interleukin-6 expression by preventing protein binding on the NF-kappaB site. *Nucleic Acids Res* **25:** 2424-9.

Gallucci RM, Simeonova PP, Matheson JM, Kommineni C, Guriel JL, Sugawara T *et al* (2000). Impaired cutaneous wound healing in interleukin-6-deficient and immunosuppressed mice. *Faseb J* **14:** 2525-31.

Gebauer G, Fehm T, Merkle E, Beck EP, Lang N, Jager W (2001). Epithelial cells in bone marrow of breast cancer patients at time of primary surgery: clinical outcome during long-term follow-up. *J Clin Oncol* **19:** 3669-74.

Geddes DT (2007). Inside the lactating breast: the latest anatomy research. *J Midwifery Womens Health* **52:** 556-63.

Giuliani N, Sansoni P, Girasole G, Vescovini R, Passeri G, Passeri M *et al* (2001). Serum interleukin-6, soluble interleukin-6 receptor and soluble gp130 exhibit different patterns of age- and menopause-related changes. *Exp Gerontol* **36:** 547-57.

Gonzalez-Zuloeta Ladd AM, Arias Vasquez A, Witteman J, Uitterlinden AG, Coebergh JW, Hofman A *et al* (2006). Interleukin 6 G-174 C polymorphism and breast cancer risk. *Eur J Epidemiol* **21:** 373-6.

Gottardi CJ, Wong E, Gumbiner BM (2001). E-cadherin suppresses cellular transformation by inhibiting beta-catenin signaling in an adhesion-independent manner. *J Cell Biol* **153:** 1049-60.

Gritsko T, Williams A, Turkson J, Kaneko S, Bowman T, Huang M *et al* (2006). Persistent activation of stat3 signaling induces survivin gene expression and confers resistance to apoptosis in human breast cancer cells. *Clin Cancer Res* **12:** 11-9.

Guilford P (1999). E-cadherin downregulation in cancer: fuel on the fire? *Mol Med Today* **5:** 172-7.

Hartsock A, Nelson WJ (2008). Adherens and tight junctions: structure, function and connections to the actin cytoskeleton. *Biochim Biophys Acta* **1778:** 660-9.

Heimann R, Hellman S (2000). Individual characterisation of the metastatic capacity of human breast carcinoma. *Eur J Cancer* **36:** 1631-9.

Hess KR, Pusztai L, Buzdar AU, Hortobagyi GN (2003). Estrogen receptors and distinct patterns of breast cancer relapse. *Breast Cancer Res Treat* **78:** 105-18.

Hirohashi S (1998). Inactivation of the E-cadherin-mediated cell adhesion system in human cancers. *Am J Pathol* **153:** 333-9.

Ho BC, Tan PH (2009). Lobular neoplasia of the breast: 68 years on. *Pathology* **41:** 28-35.

Hodge DR, Hurt EM, Farrar WL (2005). The role of IL-6 and STAT3 in inflammation and cancer. *Eur J Cancer* **41:** 2502-12.

Hyafil F, Babinet C, Jacob F (1981). Cell-cell interactions in early embryogenesis: a molecular approach to the role of calcium. *Cell* **26:** 447-54.

Irvin WJ, Jr., Carey LA (2008). What is triple-negative breast cancer? *Eur J Cancer* **44:** 2799-805.

James JJ, Evans AJ, Pinder SE, Gutteridge E, Cheung KL, Chan S *et al* (2003). Bone metastases from breast carcinoma: histopathological - radiological correlations and prognostic features. *Br J Cancer* **89:** 660-5.

Jiang XP, Yang DC, Elliott RL, Head JF (2000). Reduction in serum IL-6 after vacination of breast cancer patients with tumour-associated antigens is related to estrogen receptor status. *Cytokine* **12:** 458-65.

Karnoub AE, Dash AB, Vo AP, Sullivan A, Brooks MW, Bell GW *et al* (2007). Mesenchymal stem cells within tumour stroma promote breast cancer metastasis. *Nature* **449:** 557-63.

Kenny PA, Lee GY, Myers CA, Neve RM, Semeiks JR, Spellman PT *et al* (2007). The morphologies of breast cancer cell lines in three-dimensional assays correlate with their profiles of gene expression. *Mol Oncol* **1:** 84-96.

Kishimoto T (2006). Interleukin-6: discovery of a pleiotropic cytokine. *Arthritis Res Ther* **8 Suppl 2:** S2.

Klein CA (2009). Parallel progression of primary tumours and metastases. *Nat Rev Cancer* **9:** 302-12.

Koebel CM, Vermi W, Swann JB, Zerafa N, Rodig SJ, Old LJ *et al* (2007). Adaptive immunity maintains occult cancer in an equilibrium state. *Nature* **450:** 903-7.

Kominsky SL, Davidson NE (2006). A "bone" fide predictor of metastasis? Predicting breast cancer metastasis to bone. *J Clin Oncol* **24:** 2227-9.

Kopf M, Baumann H, Freer G, Freudenberg M, Lamers M, Kishimoto T *et al* (1994). Impaired immune and acute-phase responses in interleukin-6-deficient mice. *Nature* **368:** 339-42.

Kowalski PJ, Rubin MA, Kleer CG (2003). E-cadherin expression in primary carcinomas of the breast and its distant metastases. *Breast Cancer Res* **5:** R217-22.

Kozlowski L, Zakrzewska I, Tokajuk P, Wojtukiewicz MZ (2003). Concentration of interleukin-6 (IL-6), interleukin-8 (IL-8) and interleukin-10 (IL-10) in blood serum of breast cancer patients. *Rocz Akad Med Bialymst* **48:** 82-4.

Larue L, Ohsugi M, Hirchenhain J, Kemler R (1994). E-cadherin null mutant embryos fail to form a trophectoderm epithelium. *Proc Natl Acad Sci U S A* **91:** 8263-7.

Lebret SC, Newgreen DF, Thompson EW, Ackland ML (2007). Induction of epithelial to mesenchymal transition in PMC42-LA human breast carcinoma cells by carcinoma-associated fibroblast secreted factors. *Breast Cancer Res* **9:** R19.

Li CI, Malone KE, Saltzman BS, Daling JR (2006). Risk of invasive breast carcinoma among women diagnosed with ductal carcinoma in situ and lobular carcinoma in situ, 1988-2001. *Cancer* **106:** 2104-12.

Lin Q, Lai R, Chirieac LR, Li C, Thomazy VA, Grammatikakis I *et al* (2005). Constitutive activation of JAK3/STAT3 in colon carcinoma tumors and cell lines: inhibition of JAK3/STAT3 signaling induces apoptosis and cell cycle arrest of colon carcinoma cells. *Am J Pathol* **167:** 969-80.

Ling X, Arlinghaus RB (2005). Knockdown of STAT3 expression by RNA interference inhibits the induction of breast tumors in immunocompetent mice. *Cancer Res* **65:** 2532-6.

Lipponen P, Saarelainen E, Ji H, Aaltomaa S, Syrjanen K (1994). Expression of E-cadherin (E-CD) as related to other prognostic factors and survival in breast cancer. *J Pathol* **174:** 101-9.

Litovkin KV, Domenyuk VP, Bubnov VV, Zaporozhan VN (2007). Interleukin-6 -174G/C polymorphism in breast cancer and uterine leiomyoma patients: a population-based case control study. *Exp Oncol* **29:** 295-8.

Lou Y, Preobrazhenska O, auf dem Keller U, Sutcliffe M, Barclay L, McDonald PC *et al* (2008). Epithelial-mesenchymal transition (EMT) is not sufficient for spontaneous murine breast cancer metastasis. *Dev Dyn* **237:** 2755-68.

Macedo LF, Sabnis G, Brodie A (2009). Aromatase inhibitors and breast cancer. *Ann N Y Acad Sci* **1155:** 162-73.

Mariani G, Fasolo A, De Benedictis E, Gianni L (2009). Trastuzumab as adjuvant systemic therapy for HER2-positive breast cancer. *Nat Clin Pract Oncol* **6:** 93-104.

Martin KJ, Patrick DR, Bissell MJ, Fournier MV (2008). Prognostic breast cancer signature identified from 3D culture model accurately predicts clinical outcome across independent datasets. *PLoS One* **3:** e2994.

Massague J (2008). TGFbeta in Cancer. *Cell* **134:** 215-30.

Mbalaviele G, Dunstan CR, Sasaki A, Williams PJ, Mundy GR, Yoneda T (1996). E-cadherin expression in human breast cancer cells suppresses the development of osteolytic bone metastases in an experimental metastasis model. *Cancer Res* **56:** 4063-70.

Mironchik Y, Winnard PT, Jr., Vesuna F, Kato Y, Wildes F, Pathak AP *et al* (2005). Twist overexpression induces in vivo angiogenesis and correlates with chromosomal instability in breast cancer. *Cancer Res* **65:** 10801-9.

Moody SE, Perez D, Pan TC, Sarkisian CJ, Portocarrero CP, Sterner CJ *et al* (2005). The transcriptional repressor Snail promotes mammary tumor recurrence. *Cancer Cell* **8:** 197-209.

Naugler WE, Karin M (2008). The wolf in sheep's clothing: the role of interleukin-6 in immunity, inflammation and cancer. *Trends Mol Med* **14:** 109-19.

Nicolini A, Carpi A, Rossi G (2006). Cytokines in breast cancer. *Cytokine Growth Factor Rev* **17:** 325-37.

Oh JW, Revel M, Chebath J (1996). A soluble interleukin 6 receptor isolated from conditioned medium of human breast cancer cells is encoded by a differentially spliced mRNA. *Cytokine* **8:** 401-9.

Oka H, Shiozaki H, Kobayashi K, Inoue M, Tahara H, Kobayashi T *et al* (1993). Expression of E-cadherin cell adhesion molecules in human breast cancer tissues and its relationship to metastasis. *Cancer Res* **53:** 1696-701.

Onder TT, Gupta PB, Mani SA, Yang J, Lander ES, Weinberg RA (2008). Loss of E-cadherin promotes metastasis via multiple downstream transcriptional pathways. *Cancer Res* **68:** 3645-54.

Oseni T, Patel R, Pyle J, Jordan VC (2008). Selective estrogen receptor modulators and phytoestrogens. *Planta Med* **74:** 1656-65.

Ostrand-Rosenberg S, Sinha P (2009). Myeloid-derived suppressor cells: linking inflammation and cancer. *J Immunol* **182:** 4499-506.

Paget S (1889). The Distribution of Secondary Growths in Cancer of the Breast. *Lancet* **1:** 571-573.

Pang WW, Hartmann PE (2007). Initiation of human lactation: secretory differentiation and secretory activation. *J Mammary Gland Biol Neoplasia* **12:** 211-21.

Pantel K, Muller V, Auer M, Nusser N, Harbeck N, Braun S (2003). Detection and clinical implications of early systemic tumor cell dissemination in breast cancer. *Clin Cancer Res* **9:** 6326-34.

Parker C, Rampaul RS, Pinder SE, Bell JA, Wencyk PM, Blamey RW *et al* (2001). E-cadherin as a prognostic indicator in primary breast cancer. *Br J Cancer* **85:** 1958-63.

Paszek MJ, Zahir N, Johnson KR, Lakins JN, Rozenberg GI, Gefen A *et al* (2005). Tensional homeostasis and the malignant phenotype. *Cancer Cell* **8:** 241-54.

Pedersen KB, Nesland JM, Fodstad O, Maelandsmo GM (2002). Expression of S100A4, E-cadherin, alpha- and beta-catenin in breast cancer biopsies. *Br J Cancer* **87:** 1281-6.

Perez-Moreno M, Jamora C, Fuchs E (2003). Sticky business: orchestrating cellular signals at adherens junctions. *Cell* **112:** 535-48.

Perl AK, Wilgenbus P, Dahl U, Semb H, Christofori G (1998). A causal role for E-cadherin in the transition from adenoma to carcinoma. *Nature* **392:** 190-3.

Perou CM, Sorlie T, Eisen MB, van de Rijn M, Jeffrey SS, Rees CA *et al* (2000). Molecular portraits of human breast tumours. *Nature* **406:** 747-52.

Perrais M, Chen X, Perez-Moreno M, Gumbiner BM (2007). E-cadherin homophilic ligation inhibits cell growth and epidermal growth factor receptor signaling independently of other cell interactions. *Mol Biol Cell* **18:** 2013-25.

Podsypanina K, Du YC, Jechlinger M, Beverly LJ, Hambardzumyan D, Varmus H (2008). Seeding and propagation of untransformed mouse mammary cells in the lung. *Science* **321:** 1841-4.

Rakha EA, Green AR, Powe DG, Roylance R, Ellis IO (2006). Chromosome 16 tumor-suppressor genes in breast cancer. *Genes Chromosomes Cancer* **45:** 527-35.

Ripperger T, Gadzicki D, Meindl A, Schlegelberger B (2009). Breast cancer susceptibility: current knowledge and implications for genetic counselling. *Eur J Hum Genet* **17:** 722-31.

Rose-John S, Scheller J, Elson G, Jones SA (2006). Interleukin-6 biology is coordinated by membrane-bound and soluble receptors: role in inflammation and cancer. *J Leukoc Biol* **80:** 227-36.

Saha B, Chaiwun B, Imam SS, Tsao-Wei DD, Groshen S, Naritoku WY *et al* (2007). Overexpression of E-cadherin protein in metastatic breast cancer cells in bone. *Anticancer Res* **27:** 3903-8.

Salgado R, Junius S, Benoy I, Van Dam P, Vermeulen P, Van Marck E *et al* (2003). Circulating interleukin-6 predicts survival in patients with metastatic breast cancer. *Int J Cancer* **103:** 642-6.

Sansone P, Storci G, Tavolari S, Guarnieri T, Giovannini C, Taffurelli M *et al* (2007). IL-6 triggers malignant features in mammospheres from human ductal breast carcinoma and normal mammary gland. *J Clin Invest* **117:** 3988-4002.

Sarrio D, Rodriguez-Pinilla SM, Hardisson D, Cano A, Moreno-Bueno G, Palacios J (2008). Epithelial-mesenchymal transition in breast cancer relates to the basal-like phenotype. *Cancer Res* **68:** 989-97.

Sasaki CY, Lin H, Morin PJ, Longo DL (2000). Truncation of the extracellular region abrogrates cell contact but retains the growth-suppressive activity of E-cadherin. *Cancer Res* **60:** 7057-65.

Sasser AK, Mundy BL, Smith KM, Studebaker AW, Axel AE, Haidet AM *et al* (2007a). Human bone marrow stromal cells enhance breast cancer cell growth rates in a cell line-dependent manner when evaluated in 3D tumor environments. *Cancer Lett* **254:** 255-64.

Sasser AK, Sullivan NJ, Studebaker AW, Hendey LF, Axel AE, Hall BM (2007b). Interleukin-6 is a potent growth factor for ER-alpha-positive human breast cancer. *Faseb J* **21:** 3763-70.

Selander KS, Li L, Watson L, Merrell M, Dahmen H, Heinrich PC *et al* (2004). Inhibition of gp130 signaling in breast cancer blocks constitutive activation of Stat3 and inhibits in vivo malignancy. *Cancer Res* **64:** 6924-33.

Shankaran V, Ikeda H, Bruce AT, White JM, Swanson PE, Old LJ *et al* (2001). IFNgamma and lymphocytes prevent primary tumour development and shape tumour immunogenicity. *Nature* **410:** 1107-11.

Shoker BS, Jarvis C, Clarke RB, Anderson E, Hewlett J, Davies MP *et al* (1999). Estrogen receptor-positive proliferating cells in the normal and precancerous breast. *Am J Pathol* **155:** 1811-5.

Singh A, Purohit A, Ghilchik MW, Reed MJ (1999). The regulation of aromatase activity in breast fibroblasts: the role of interleukin-6 and prostaglandin E2. *Endocr Relat Cancer* **6:** 139-47.

Singh A, Purohit A, Wang DY, Duncan LJ, Ghilchik MW, Reed MJ (1995). IL-6sR: release from MCF-7 breast cancer cells and role in regulating peripheral oestrogen synthesis. *J Endocrinol* **147:** R9-12.

Sommers CL, Thompson EW, Torri JA, Kemler R, Gelmann EP, Byers SW (1991). Cell adhesion molecule uvomorulin expression in human breast cancer cell lines: relationship to morphology and invasive capacities. *Cell Growth Differ* **2:** 365-72.

Sorlie T, Perou CM, Tibshirani R, Aas T, Geisler S, Johnsen H *et al* (2001). Gene expression patterns of breast carcinomas distinguish tumor subclasses with clinical implications. *Proc Natl Acad Sci U S A* **98:** 10869-74.

Studebaker AW, Storci G, Werbeck JL, Sansone P, Sasser AK, Tavolari S *et al* (2008). Fibroblasts isolated from common sites of breast cancer metastasis enhance cancer cell growth rates and invasiveness in an interleukin-6-dependent manner. *Cancer Res* **68:** 9087-95.

Suematsu S, Matsuda T, Aozasa K, Akira S, Nakano N, Ohno S *et al* (1989). IgG1 plasmacytosis in interleukin 6 transgenic mice. *Proc Natl Acad Sci U S A* **86:** 7547-51.

Takeda K, Noguchi K, Shi W, Tanaka T, Matsumoto M, Yoshida N *et al* (1997). Targeted disruption of the mouse Stat3 gene leads to early embryonic lethality. *Proc Natl Acad Sci U S A* **94:** 3801-4.

Tarin D, Thompson EW, Newgreen DF (2005). The fallacy of epithelial mesenchymal transition in neoplasia. *Cancer Res* **65:** 5996-6000; discussion 6000-1.

Terui T, Okuyama R, Tagami H (2001). Molecular events occurring behind ultraviolet-induced skin inflammation. *Curr Opin Allergy Clin Immunol* **1:** 461-7.

Thiery JP (2002). Epithelial-mesenchymal transitions in tumour progression. *Nat Rev Cancer* **2:** 442-54.

Thiery JP, Sleeman JP (2006). Complex networks orchestrate epithelial-mesenchymal transitions. *Nat Rev Mol Cell Biol* **7:** 131-42.

Thomas-Ahner JM, Wulff BC, Tober KL, Kusewitt DF, Riggenbach JA, Oberyszyn TM (2007). Gender differences in UVB-induced skin carcinogenesis, inflammation, and DNA damage. *Cancer Res* **67:** 3468-74.

Thuault S, Valcourt U, Petersen M, Manfioletti G, Heldin CH, Moustakas A (2006). Transforming growth factor-beta employs HMGA2 to elicit epithelial-mesenchymal transition. *J Cell Biol* **174:** 175-83.

Turashvili G, Bouchal J, Burkadze G, Kolar Z (2005). Differentiation of tumours of ductal and lobular origin: I. Proteomics of invasive ductal and lobular breast carcinomas. *Biomed Pap Med Fac Univ Palacky Olomouc Czech Repub* **149:** 57-62.

van 't Veer LJ, Dai H, van de Vijver MJ, He YD, Hart AA, Mao M *et al* (2002). Gene expression profiling predicts clinical outcome of breast cancer. *Nature* **415:** 530-6.

van Dam M, Mullberg J, Schooltink H, Stoyan T, Brakenhoff JP, Graeve L *et al* (1993). Structure-function analysis of interleukin-6 utilizing human/murine chimeric molecules. Involvement of two separate domains in receptor binding. *J Biol Chem* **268:** 15285-90.

van de Vijver MJ, He YD, van't Veer LJ, Dai H, Hart AA, Voskuil DW *et al* (2002). A gene-expression signature as a predictor of survival in breast cancer. *N Engl J Med* **347:** 1999-2009.

van Steeg H, Kraemer KH (1999). Xeroderma pigmentosum and the role of UV-induced DNA damage in skin cancer. *Mol Med Today* **5:** 86-94.

Vannucchi AM, Bosi A, Glinz S, Pacini P, Linari S, Saccardi R *et al* (1998). Evaluation of breast tumour cell contamination in the bone marrow and leukapheresis collections by RT-PCR for cytokeratin-19 mRNA. *Br J Haematol* **103:** 610-7.

Veness MJ, Quinn DI, Ong CS, Keogh AM, Macdonald PS, Cooper SG *et al* (1999). Aggressive cutaneous malignancies following cardiothoracic transplantation: the Australian experience. *Cancer* **85:** 1758-64.

Waerner T, Alacakaptan M, Tamir I, Oberauer R, Gal A, Brabletz T *et al* (2006). ILEI: a cytokine essential for EMT, tumor formation, and late events in metastasis in epithelial cells. *Cancer Cell* **10:** 227-39.

Wang T, Niu G, Kortylewski M, Burdelya L, Shain K, Zhang S *et al* (2004). Regulation of the innate and adaptive immune responses by Stat-3 signaling in tumor cells. *Nat Med* **10:** 48-54.

Warren JL, Yabroff KR, Meekins A, Topor M, Lamont EB, Brown ML (2008). Evaluation of trends in the cost of initial cancer treatment. *J Natl Cancer Inst* **100:** 888-97.

Weigelt B, Bissell MJ (2008). Unraveling the microenvironmental influences on the normal mammary gland and breast cancer. *Semin Cancer Biol* **18:** 311-21.

Weigelt B, Peterse JL, van 't Veer LJ (2005). Breast cancer metastasis: markers and models. *Nat Rev Cancer* **5:** 591-602.

Weis WI, Nelson WJ (2006). Re-solving the cadherin-catenin-actin conundrum. *J Biol Chem* **281:** 35593-7.

Yang J, Weinberg RA (2008). Epithelial-mesenchymal transition: at the crossroads of development and tumor metastasis. *Dev Cell* **14:** 818-29.

Yoder BJ, Wilkinson EJ, Massoll NA (2007). Molecular and morphologic distinctions between infiltrating ductal and lobular carcinoma of the breast. *Breast J* **13:** 172-9.

Zhang GJ, Adachi I (1999). Serum interleukin-6 levels correlate to tumor progression and prognosis in metastatic breast carcinoma. *Anticancer Res* **19:** 1427-32.